AD_____

Award Number: W81XWH-09-1-0448

TITLE: Targeting Tim-1 to Circumvent Immune Tolerance in Prostate Cancer

PRINCIPAL INVESTIGATOR: Mohamed S. Arredouani, Ph.D.

CONTRACTING ORGANIZATION: Beth Israel Deaconess Medical Center, Boston, MA 02215

REPORT DATE: September 2012

TYPE OF REPORT: Revised Final

PREPARED FOR: U.S. Army Medical Research and Materiel Command
Fort Detrick, Maryland 21702-5012

DISTRIBUTION STATEMENT: Approved for Public Release;
Distribution Unlimited

REPORT DOCUMENTATION PAGE

Form Approved
OMB No. 0704-0188

1. REPORT DATE	2. REPORT TYPE	3. DATES COVERED
September 2012	Revised Final	15 June 2009 to 14 August 2012

4. TITLE AND SUBTITLE
Targeting TIM-1 to Circumvent Immune Tolerance in Prostate Cancer

5a. CONTRACT NUMBER

5b. GRANT NUMBER
W81XWH-09-1-0448

5c. PROGRAM ELEMENT NUMBER

6. AUTHOR(S)
Mohamed S. Arredouani

E-Mail: marredou@bidmc.harvard.edu

5d. PROJECT NUMBER

5e. TASK NUMBER

5f. WORK UNIT NUMBER

7. PERFORMING ORGANIZATION NAME(S) AND ADDRESS(ES)

Beth Israel Deaconess Medical Center
Boston, MA 02215

8. PERFORMING ORGANIZATION REPORT NUMBER

9. SPONSORING / MONITORING AGENCY NAME(S) AND ADDRESS(ES)

U.S. Army Medical Research and Materiel Command
Fort Detrick, Maryland 21702-5012

10. SPONSOR/MONITOR'S ACRONYM(S)

11. SPONSOR/MONITOR'S REPORT NUMBER(S)

12. DISTRIBUTION / AVAILABILITY STATEMENT
Approved for Public Release; Distribution Unlimited

13. SUPPLEMENTARY NOTES
This final report version is comprehensive of the progress over the entire length of the award and is supplemented with copies of published articles. It also cites a new manuscript in preparation.

14. ABSTRACT
Early-stage clinical testing raises the possibility that combinatorial approaches that augment tumor antigen-specific immune responses may accomplish significant tumor destruction without the induction of serious autoimmune disease. Accordingly, a rational and combinatorial manipulation of immune evasion pathways and their targets should aid in the development of safer and more effective vaccine strategies and immunotherapies for all stages of prostate cancer. In prostate cancer, a plausible combination that could be targeted towards patients who undergo androgen ablation, a therapeutic modality that is also known to enhance immune responses to prostate TAA, would include a vaccine in conjunction with biologic agents that are known to simultaneously augment antigen presentation by DCs and inhibit immunosuppressive cells such as regulatory T cells (Treg) or prolong the survival and enhance the vigor of tumor-specific lymphocytes. An example of such agents is the agonist antibody that targets TIM-1, a receptor expressed on lymphocytes and dendritic cells that enhances cytotoxic lymphocyte responses to tumor-associated antigens when used in combination with a vaccine. Here we explore the combination of androgen ablation and anti-TIM1 targeting as a strategy to ameliorate cancer-specific vaccine outcome in a mouse model of prostate cancer.

15. SUBJECT TERMS
Prostate Cancer; Immune tolerance; Immunotherapy; TIM-1 receptor; castration

16. SECURITY CLASSIFICATION OF:			17. LIMITATION OF ABSTRACT	18. NUMBER OF PAGES	19a. NAME OF RESPONSIBLE PERSON
a. REPORT	b. ABSTRACT	c. THIS PAGE			USAMRMC
U	U	U	UU	17	19b. TELEPHONE NUMBER *(include area code)*

TABLE OF CONTENTS

INTRODUCTION:

The survival benefit observed in prostate cancer (PCa) vaccine clinical trials of two formulations that delivered prostate-specific antigens (PAP delivered by autologous dendritic cells (DC) in Provenge and PSA delivered by a recombinant vaccinia virus (rVV) in PROSTVAC) (1, 2), suggests substantial potential for the next generation of therapeutic prostate cancer vaccines to alter paradigms of prostate cancer care and survivorship. These clinical trials provided clinical proof-of-principal that immunization with a single tumor-associated antigen (TAA) can generate an efficient anti-tumor response leading to increased survival. However, because of the negative immunoregulatory mechanisms in place, immune responses to vaccines have resulted in modest survival benefit (3), hindering the prospect of implementing immunotherapy as an efficient, cost effective alternative therapeutic modality for the treatment of PCa.

We and others have previously shown that in mice, androgen ablation prevents immune tolerance to tumor-specific antigens and enhances immunotherapy to PCa (4-7). Nevertheless, increased CD8+ T cell responses following castration and immunization is partially hampered by a parallel expansion of Treg (8). Expansion of Treg population and their suppressive activity can be prevented using an agonist antibody targeting the receptor TIM-1(9). This agonist antibody proved to be a powerful positive regulator of T cell function in wild type and prostate tumor-bearing TRAMP mice.

In the present project, we have explored the effect of androgen ablation and anti-TIM1 treatment on the outcome of vaccines targeting prostate tumors in different mouse models. Our data indicate that the enhancing effects of androgen ablation and anti-TIM1 mAb treatment take place under specific conditions influenced by tumor load, vaccine formulation, and combination of the two treatments in the same immunotherapy regimen. While castration convincingly ameliorates the outcome of a therapeutic vaccine in tumor-bearing mice, anti-TIM1 targeting wasn't necessary to observe the beneficial effect of the vaccine.

BODY:

Task 1: To investigate the role of manipulating TIM-1 pathway in overcoming prostate antigen-specific tolerance in the TRAMP mouse.

Task 1-a) **Using anti-TIM 1 monoclonal antibody, TIM-4:Ig fusion protein, and TIM-4(+) dendritic cells**: In this aim, we proposed to combine a vaccine targeting a model prostate-specific antigen (SV40 Tag) and an agonist anti-TIM1 monoclonal antibody to break immune tolerance to Tag in the TRAMP (TRansgenic Adenocarcinoma of Mouse Prostate) mouse model of prostate cancer in a similar approach that we have previously successfully used in wild type mice. The onset of immune tolerance to Tag in TRAMP mice takes place as soon as Tag is being produced (i.e. at about 12 weeks of age, the age of onset of puberty, when the prostate starts producing Probasin-driven Tag oncogene under the control of androgens). In this mouse model, the depth of tolerance increases with age and cancer progression and can be evidenced in both prostate-infiltrating lymphocytes, prostate-draining lymph nodes and spleen (2). Accordingly, using a TRAMP/Foxp3-GFP hybrid mouse, we have shown that the number of Tregs (i.e. CD4+Foxp3+) in the spleen and prostate-draining lymph nodes of male mice increases with age, an increase that is more substantial that the one observed in wild type control, tumor-free mice. Our preliminary work has concluded that concomitant administration of Tag antigen and agonist anti-TIM1 antibody to male C57BL/6 mice results in elevated numbers of Tag-specific cytotoxic lymphocytes (CTL) in the spleen and prostate-draining lymph nodes, while isotype-matched control antibody had no effect on the outcome of immunization. In these experiments, mice were immunized with either a recombinant Tag-expressing vaccinia virus (vac-mTag, 10 million pfu/mouse, i.v.) (3) or with the syngeneic Tag-transfected WT19 fibroblast cell line (4) (30-40 million/mouse, i.p.). Both agents have been shown to elicit detectable CTL responses to Tag in both spleen and draining lymph nodes. These responses were evidenced by Tag peptide-tetramer reactivity and the presence of IFN-γ-releasing CD8 T cells upon restimulation with the H2Db-restricted, Tag-derived Tag IV peptide in vitro. Following this set of experiments, which also included titration of the antibody, we opted for the use of 200 μg of anti-TIM1

antibody i.p. in subsequent work. To test the agonist anti-TIM1 antibody in TRAMP mice in a way that would allow us to correlate the outcome with the depth of immune tolerance, we used different ages of mice as these became available. The first age we tested was 12 weeks, and then we tested 20 and 26 weeks. From our experience, 12 weeks-old mice exhibit prostatic expression of Tag but show a relatively normal prostate, whereas older mice develop tumors of regular, round shape (20 weeks) and much bigger tumors that also affect the seminal vesicles (26 weeks). Mice of these two last groups were discarded when no tumor was found at time of dissection. Our data show that Tag-specific CTL responses elicited through immunization with WT19 cells are significantly higher in B6 control mice than in 12 weeks-old TRAMP mice (Figure 1A). This low response in TRAMP mice at this early age reflects the early onset of immune tolerance to prostatic T antigen.
Interestingly, this weak response is substantially strengthened by administering the anti-TIM1 antibody at time of immunization, although this does not lead to full recovery of the response (Figure 1A). The isotype control antibody did not have any effect. Similarly, a significant recovery of the CTL response is observed in the 15 week-old TRAMP mice (Figure 1B). However, the mice that exceeded 20 wks of age did not respond to anti-TIM1 treatment and exhibited a low CTL response (Figure 1C). This suggests that tumor burden (illustrated in Figure 1D where the whole GU tract is shown) might interfere with the effect of TIM-1 manipulation in the TRAMP mouse and might dictate how future experiments are designed to test the efficacy of combining vaccines and TIM-1 Ab in eradicating tumors. Because TIM-1 receptor on T cells interacts with TIM-4 on antigen presenting cells, we proposed to use TIM-4.Ig fusion protein and peptide-loaded TIM-4(+) dendritic cells as alternatives to the agonist anti-TIM1 antibody. However, these two alternatives have not been tested for a variety of reasons: 1) The antibody we have in hand is very efficient, readily available, and warrants further characterization before other alternatives are considered, 2) the TIM4.Ig fusion protein is still being produced and functionally tested in the laboratory of my mentor and collaborator Dr. Terry Strom at our institution, and 3) TIM4(+) dendritic cells represent less than 10% of spleen DCs and it would take over 10 spleens to sort enough DCs to immunize 1 mouse, and increasing DC numbers in the spleen using treatment with Flt3L- or GM-CSF-secreting cell lines seems to affect TIM4 expression. Similarly, bone marrow-derived DCs lack TIM-4 expression (Figure 3).

Task 1-b) Using TIM-1- deficient TRAMP mouse:
This task was intended to use the TIM1 deficient TRAMP mouse to demonstrate the specificity of the agonist antibody we are using as a tool to break tolerance to Tag and investigate the role of TIM1 in the onset of such tolerance in vivo.
TIM1 KO and TRAMP/TIM1 KO mice were immunized with T antigen producing WT19 cell line intraperitoneally. Four hours later, a single dose of agonist anti-TIM1 antibody or isotype control antibody was administered. T antigen-specific CTL response was monitored by IFN-g ELISPOT in response to Tag IV peptide in vitro using splenocytes from immunized mice. Our data show no differences between isotype and anti-TIM1-treated mice in both WT and TRAMP mice (**Figure 4**).

Additionally, we sought to provide evidence that the observed effects of the agonist anti-TIM1 antibody described above are mediated through TIM-1 receptor using a different approach. TRAMP mice were immunized with WT19 cells and administered equal doses of either the agonist anti-TIM1 mAb clone 1 described above or the antagonist mAb clone 2 (RMT1-4) or a combination of both. Following this protocol, Tag-specific CTL responses were significantly enhanced in the agonist anti-TIM1-treated group. The antagonist antibody alone did not affect CTL responses, but was able to reduce the effect mediated by the agonist antibody when these two were combined (Figure 2).

Task 2: To explore the role of manipulating TIM-1 pathway in overcoming human HLA-restricted tolerance in transgenic mouse models expressing human prostate TAA.

Task 2-a) Evaluation of immunogenicity and anti-tumor effects of the ERG and SIM2 peptides:

The CTL response to ERG- and SIM2-derived, HLA-A2.1-restricted peptides was tested in HHD (HLA-A2.1 transgenic) mice and was measurable by ELISPOT in spleens and prostate-draining lymph nodes, although weaker than what we have previously seen with SV40 T antigen or full-length PSA (6, 10-12). Treatment with

the agonist anti-TIM1 antibody at time of immunization resulted in a significant enhancement of the response for both peptides (**Figure 5**).

Task 2-b) Impact of developing prostate cancers on ERG- and SIM2-specific CTL tolerance:
As mentioned in last year's progress report, we took the decision to switch from the whole body $PTEN^{+/-}$ mouse to the TRAMP mouse to accomplish this task because of the hyper-activation of T lymphocytes in PTEN haplo-insufficient mice. This hyper-activation is a consequence of reduced suppression of PI3K.

For ERG peptide testing, Pb-ERG mice were crossed to HHD mice to generate the ERG/HHD hybrid. This hybrid was further crossed to TRAMP to generate the ERG/HHD/TRAMP mouse.
For SIM2 peptide testing, HHD/TRAMP mouse was generated. Only 25% of male HHD/TRAMP express SIM2 in prostate tumors as we have shown using RT-PCR, a limitation that will required a large number of mice. These SIM2-related experiments are underway, and testing of tumors for SIM2 expression status will be performed upon sacrifice of mice.

Double and triple hybrid mice were immunized with ERG- or SIM-2-derived, HLA-A2.1-restricted peptides. Splenocytes and prostate draining lymph node lymphocytes were tested for their ability to secrete IFN-γ in response to antigen-specific restimulation in vitro.
Probasin-driven expression of ERG in HHD mice clearly results in a reduced anti-ERG CTL response upon immunization with ERG157, ERG295 and ERG 412 peptides (**Figure 6**). However, a part of loss of response is recovered upon addition of the agonist anti-TIM1 antibody at time of immunization.

To test the effect of anti-TIM1 antibody in the context of a tumor-imposed immune tolerance, we generated the HHD/ERG/TRAMP mice. Generating this triple hybrid mouse takes a lot of time and we have been able to generate only a few animals so far. Immunization of HHD, HHD/ERG and HHD/ERG/TRAMP mice with an ERG-derived peptide shows that immune tolerance to this antigen is induced by prostatic expression in the absence of tumors, and that prostate tumors bring the level of tolerance even lower, although the response is till detectable (**Figure 7**). More triple hybrid mice are being generated to test the effect of anti-TIM1 antibody on tumor-induced immune tolerance.

Task 3: To exploit the combination of manipulating TIM-1 pathway and androgen ablation for ERG- and SIM2-targeted immunotherapy.

Data from previous published reports, including our own, have provided evidence for an enhancing effect of androgen ablation and anti-TIM1 treatment on antigen-specific cytotoxic lymphocyte responses. However, it was also reported that like humans, mice do not all respond to androgen ablation, and therefore there should be caution when it comes to using the mouse for androgen-regulated immune regulation studies.

Task 3-a) Androgen ablation and immune tolerance to ERG and SIM2:

To accomplish this task, we have used the humanized HLA-A2.1/pb-ERG (HHD/ERG) hybrid mouse to test whether androgen ablation results in elevated CTL response to prostate-specific antigen in the prostate draining lymph nodes.

Because we do not have a mouse expressing prostate-specific SIM2, we used the HHD/ERG mouse to evaluate responses to both SIM2 and ERG-derived, HLA-A2.1-restricted peptides. Androgen ablation was achieved through surgical castration and sham-castrated mice were used as controls.

Consistent with what we have reported in last year's report, HHD mice that do not express ERG in the prostate respond well to ERG295 immunization. This response is attenuated in HHD mice that exhibit ERG expression in the prostate, indicative of an ongoing peripheral immune tolerance. Interestingly, castration of male HHD/ERG mice did not restore the loss of CTL response to ERG (Figure 8A). This finding is in contrast to our

previous data showing that castration induces a significant augmentation of CTL responses to prostate specific antigen (PSA) in a HLA-A2.1/Pb-PSA mouse model (6). However, key differences between HHD/ERG and HLA-A2.1/PSA should be highlighted; 1) while PSA is not expressed in the mouse, ERG is expressed in low amounts in the endothelium, 2) while the HLA-A2.1/PSA also expressed mouse MHC-I, HHD/ERG only expresses human HLA-A2.1, and 3) in the past we have used a recombinant vaccinia-PSA vaccine administered intravenously while here we have used MHC-I peptides in IFA subcutaneously. These 3 major differences in the models we have utilized may explain the discrepancy in immunization outcome.

We also used the HHD/ERG mouse model to evaluate CTL responses to SIM2 immunization. This model can be very informative as it does not express SIM2 in the prostate, so SIM2 expression would escape to androgen ablation effect, providing a tool to study the effect of castration on immunization to androgen-independent antigens.

Interestingly, sham-castrated HHD responded to SIM2 peptide immunization, while sham-castrated HHD/ERG showed a much higher response. This high response lost its strength when castrated HHD also expressed ERG (Figure 8B). This outcome remains intriguing and implies a possible role of the transcription factor ERG in SIM2-induced CTL responses in the prostate-draining lymph nodes.

We sought an alternative immunotherapy model where we use the TRAMP-C2/GM-CSF as a cell-based vaccine that recapitulates the human GVAX formulation. One dose of this vaccine given 4 weeks post-castration showed a significant augmentation in specific CTL responses in both WT and TRAMP mice, indicating its capability of breaking immune tolerance to tumor antigens seen in sham-castrated TRAMP mice in this regimen (Figure 9). This model illustrates the power of androgen ablation in immune stimulation and corroborates our previous findings and those from other groups.

In an attempt to identify the mechanism behind this enhancing effect, we purified CD4 T cells from spleen and stimulated them with anti-CD3 and anti-CD28 antibodies, in the presence of IL-12 to skew T cell differentiation into the Th1 phenotype. This treatment induces STAT4 phosphorylation (Figure 10A), demonstrating an ongoing Th1 differentiation. However, this phosphorylation disappears upon addition of the androgen analog R1881 (Figure 10B). In a recent report (13), Morse and colleagues demonstrated that T lymphocytes infiltrates in rat's prostate following castration is predominantly Th1 at early stage, before differentiation shifts to other lineages such as the Th17 lineage.

The importance of this finding relies in the necessary helper role that CD4 T lymphocytes provide to cytotoxic T cells for optimal activation. The consequence of this CD4-targeted effect of androgens on CD8 T cells is highlighted in figure 10C, where the number of antigen specific CD8 T cells producing IFN-γ following restimulation in vitro is reduced in the presence of R1881 (Figure 10C).

Task 3-b) Combining TIM-1 manipulation and androgen ablation to overcome immune tolerance to ERG and SIM2:

The rationale behind this task was based upon our preliminary findings showing that 1) castration enhances CTL responses to a probasin-driven prostate specific antigen in the HLA-A2.1/PSA mouse model, and 2) agonist anti-TIM1 antibody augments CTL responses to a probasin-driven prostate specific antigen in the TRAMP mouse model.

In both mouse models, the target antigens are from human and viral (SV40 virus) origins and are expressed exclusively in the prostate gland, which provides complete prostate specificity of antigen expression and circumvents any immune tolerance that might be generated by extra-prostatic expression.

We have proposed to use a mouse model that emulates the human in that vaccine antigen targets are expressed in the prostate and in other tissues. This is an important consideration as none of the antigens targeted in ongoing clinical trials in various vaccine immunotherapy formulations is strictly prostate-specific. These include PSA, PAP, PSMA, PSCA, and others.

However, in line of our unexpected and surprising findings from Task 3a, we realize that we need to utilize an alternative vaccine formulation and mouse model to test our hypothesis. Therefore, we have used TRAMP mice as a model and a GM-CSF-expressing, TRAMP-derived epithelial cell line (TRAMP-C2/GM-CSF) as a cell-based vaccine that resembles GVAX (14). TRAMP-C2 cell line, although derived from the TRAMP mouse prostate, does not express T antigen.

We have tested two treatment regimens:

Single dose vaccine: Male TRAMP mice, around 20 weeks old, were surgically castrated or sham-castrated. They were immunized 4 weeks later with TRAMP-C2/GM-CSF. Mice were divided in groups that were given 200 μg of anti-TIM1 antibody or isotype control antibody at time of immunization, and then at 2 and 4 weeks.

In this setup, spleens from treated mice were restimulated in vitro with irradiated cell-based vaccine and flow cytometry was used to quantitate IFN-γ-releasing CTL. The data show that castration alone has a strong enhancing effect (over 6-fold increase), while anti-TIM1 mAb has a less important effect (2-fold increase). However, the enhancing effect that follows castration disappears when combined with anti-TIM1 mAb treatment (Figure 11)

Triple dose vaccine: Prime–boost immunization generates a high frequency, high-avidity $CD8^+$ cytotoxic T lymphocyte population and is the preferred, most efficient regimen in cancer immunotherapy trials. Male TRAMP mice, around 20 weeks old, were surgically castrated or sham-castrated. They were immunized 4 weeks later with TRAMP-C2/GM-CSF. Mice were divided in groups that were given 200 μg of anti-TIM1 antibody or isotype control antibody at time of immunization, and then at 2 and 4 weeks later.

Under this regimen, castration seems to dramatically reduce the CTL response. Anti-TIM1 treatment shows a slight enhancing effect when given to castrated mice, but surprisingly a strong suppressive effect when given to sham-castrated mice (Figure 12).

These differences may be explained by the nature of the immune response that operates in both regimens. The pool of memory T cells that is generated following the first injection can vary between treatments, and the time to the decline of the expanded T cells that respond to antigen can be different. Since we have not used the prime-boost regimen in our previous experiments, we lack the necessary data to explain this kind of discrepancy in outcome. Nevertheless, the immunotherapy treatment we implemented in the last year of this project warrants further investigation in vaccine regimens that closely resemble those previously tested and have proven efficient in men.

Interestingly, despite the higher response in sham-castrated mice (Figure 12), these animals did not have any apparent prostate tumors, but all had enlarged seminal vesicles. This might suggest some residual tumor that may have disappeared if mice were kept for a longer period of time. Mice treated with different combinations of castration and anti-TIM1 mAb had no tumors and no enlarged seminal vesicles. This resembles the survival benefit observed in a fraction of patients who took Provenge despite the barely measurable immune indicators to PAP antigen in their peripheral blood. Many more examples highlighting the lack of correlation between immune parameters and clinical outcome in cancer immunotherapy clinical trials are available in the literature, underscoring the urgency for identifying immune biomarkers for a more accurate evaluation of immunotherapy outcomes.

KEY RESEARCH ACCOMPLISHMENTS:

1) Demonstration that immune tolerance to the prostate tumor-associated antigen Tag in the TRAMP mouse can be overcome by a combination of immunization and anti-TIM1 manipulation.
2) Demonstration that the effect of anti-TIM1 antibody depends on prostate tumor burden.
3) Demonstration that the effect of the agonist anti-TIM1 antibody can be counteracted by antagonist anti-TIM1 antibodies.
4) We demonstrated that anti-TIM1 treatment of immunized HHD and ERG/HHD mice leads to overcoming immune tolerance to ERG-derived, HLA-A2.1-restricted epitopes. Immune tolerance was not totally circumvented using this treatment, even with higher doses of antibody.
5) We showed treatment of T antigen-immunized TIM1 KO mice and TRAMP/TIM1 KO mice with the agonist anti-TIM1 Ab does not result in enhanced CTL responses to Tag-restimulation in the ELISPOT assay.
6) We have been able to generate a few male HHD/ERG/TRAMP mice and their immunization shows that they exhibit a partial immune tolerance to prostatic ERG.
7) We have demonstrated an enhancing effect of castration and anti-TIM1 targeting on tumor-specific immune responses when applied separately.
8) We have identified a major difference to these treatments between single-dose and prime/boost vaccine formulations in TRAMP mice.
9) Castration leads to eradication of prostate tumors in TRAMP mice if combined with a prime-boost vaccine regimen.

REPORTABLE OUTCOMES:

Published articles: The following articles published by the PI report some findings that were used to support the hypothesis outlined in or generated through this project:

1) **Arredouani MS**, Tseng-Rogenski SS, Hollenbeck BK, Escara-Wilke J, Leander KR, Defeo-Jones D, Hwang C, Sanda MG. Androgen ablation augments human HLA2.1-restricted T cell responses to PSA self-antigen in transgenic mice. Prostate. 2010 Jun 15;70(9):1002-11.

2) **Arredouani MS**, Lu B, Bhasin M, Eljanne M, Yue W, Mosquera JM, Bubley GJ, Li V, Rubin MA, Libermann TA, Sanda MG. Identification of the transcription factor single-minded homologue 2 as a potential biomarker and immunotherapy target in prostate cancer. Clin Cancer Res. 2009 Sep 15;15(18):5794-802. [The financial support of the Department of Defense was acknowledged in this publication]

3) Lu B, Asara JM, Sanda MG, **Arredouani MS**. The role of the transcription factor SIM2 in prostate cancer. PLoS One. 2011;6(12):e28837. Epub 2011 Dec 9. [The financial support of the Department of Defense was acknowledged in this publication]

Articles in Preparation:

1) Arredouani et al. Circumventing immune tolerance to prostate tumor-associated antigens through manipulation of TIM-1 receptor.
2) Kissick et al. Targeting the transcription factor ERG for prostate cancer immunotherapy.
3) Kissick et al. Androgens regulate T helper 1 lymphocyte differentiation through STAT-1 and STAT-4 phosphorylation
4) Varghese et al. A novel iNKT cell-mediated vaccine maneuver induces potent long-lasting anti-tumor specific immunity via 'GVax' in an advanced prostate cancer model by boosting CD8+ T cell memory and function

Presentations/Abstracts. Parts of the data generated by this project were presented by the PI of this award at the following meetings:

1- Innovative Minds in Prostate Cancer Today (IMPaCT) conference. March 10, 2011. Orlando, FL. Targeting TIM-1 to Circumvent Immune Tolerance in Prostate Cancer. **Arredouani MS**, Ph.D. Yue W, M.S., Dunn L, B.S., Putheti P, Ph.D., Strom TB, M.D., Sanda MG, M.D. Beth Israel Deaconess Medical Center, Harvard Medical School, Boston, MA

2- Breaking immune tolerance to prostate-associated tumor antigens through TIM-1 receptor. M. **Simo Arredouani**, Haydn Kissick, Laura Dunn, Terry Strom, and Martin Sanda. J. Immunol. 2012; 188: p. 162.20. IMMUNOLOGY 2012, May 4-8, Boston, Massachusetts. Annual Meeting of The American Association of Immunologists

3- Immunogenic Peptides Derived from the Transcription Factor ERG as a Vaccine for Prostate Cancer. Haydn Kissick, Laura Dunn, Bin Lu, Martin Sanda, and M. **Simo Arredouani**. J. Immunol. 2012; 188: p. 162.17. IMMUNOLOGY 2012, May 4-8, Boston, Massachusetts. Annual Meeting of The American Association of Immunologists

Oral Presentations:

1- **Arredouani MS**. Targeting Tim-1 to circumvent immune tolerance to prostate tumor-associated antigens. 1st International Conference on Immune Tolerance. 2009, Boston, MA

2- **Arredouani MS**, Yue W, Lu B, Dunn L, Finke J, Asara J, Sanda MG, M.D. Molecular Profiling of T lymphocytes in Prostate Cancer. Multi-institutional Prostate Cancer Program Retreat, 2011, Ft-Lauderdale, FL.

3- **Arredouani MS**, Insights into the mechanisms of immune tolerance to prostate tumor antigens. DF/HCC Cancer Immunology Seminar Series, May 2011, Dana Farber Cancer Institute

4- **Arredouani MS**. Novel Interventions for Prostate Cancer Immunotherapy. PCF Young Investigator Forum, September 2011, Lake Tahoe, NV

5- **Arredouani MS**. Nanoparticle-Targeted Peptide Vaccines for Prostate Cancer: The Harvard – Hopkins – Carolina Consortium. PCF Prostate Immunotherapy Group Meeting, September 2011, Lake Tahoe, NV

Mouse models. The following mice were/are being generated for use in the remaining tasks of this project:
1) TRAMP/TIM1-/-: This hybrid mouse will allow us to ascertain that the effects we observe upon treatment with the anti-TIM1 antibody are mediated through TIM1 receptor. Additionally, it will be used as a valuable tool to study the role of TIM1 in prostate tumor-associated antigen-specific CTL responses and onset of immune tolerance in a more elaborate fashion.
2) Pb-ERG/HHD hybrid: This mouse will allow to develop humanized vaccine formulations and investigate immune tolerance to a prostate-specific, human antigen (ERG) in the context of HLA-A2.1.
3) TRAMP/ERG/HHD: to carry out ERG-targeted immunotherapy of prostate cancer using human ERG-derived, HLA-A2.1-restricted epitopes.
4) TRAMP/HHD: to carry out SIM2-targeted immunotherapy of prostate cancer using human SIM2-derived, HLA-A2.1-restricted epitopes.
5) PTEN(+/-): This mouse was obtained from our colleague Dr Pandolfi to use in combination with Pb-ERG (5) and HHD mice. However, we realized that a whole-body PTEN aplodeficiency is not suitable for vaccine development because of the exaggerated immune responses in this mouse following a hyperactivation of PI3kinase as a result of decreased PTEN suppression. We therefore opted for the TRAMP mouse as a model and generated the mouse described in #3.

CONCLUSION:

Our findings show that targeting TIM-1 receptor with an agonist monoclonal antibody results in circumventing immune tolerance to prostate tumor-associated antigens in prostate tumor-bearing mice and suggest that this strategy could be combined with vaccines to improve the outcome of prostate cancer immunotherapy. This is a novel strategy that differs from other interventions in the field in that it does not aim at blocking an inhibitory pathway (such as anti-CTLA4 antibodies) or deplete a regulatory cell component (such as Regulatory T lymphocytes). It rather interferes with differentiation and vigor of lymphocytes that results in an optimal balance of effector/regulatory cells that prevents the onset of immune tolerance.

We have shown the specificity of anti-TIM1 treatment through the use of TIM1 KO and TRAMP/TIM1 KO mice. Unlike C57BL/6 mice, these 2 genetically modified mice do not respond to antibody treatment, confirming the specificity of the antibody and discarding the possibility that the observed effects are merely a result of its interaction with TCR/CD3 complex (15).

The anti-tumor, immunostimulatory effects we have observed seem to vary depending on prostate-specificity of the targeted antigen, its sensitivity to androgens, tumor load, and the composition of the vaccine and the immunization regimen.

Our findings indicate an advantage for using androgen ablation over anti-TIM1 treatment in treating prostate cancer in mice and highlight the importance of mouse models and vaccine formulations in investigating the effects of androgen deprivation and TIM-1-targeted immunomodulation.

Androgen deprivation is now being tested in patients in conjunction with immunotherapy and is expected to provide a new platform for combinatorial therapies aiming at reinvigorating the immunotherapy option.

REFERENCES:

1. **Higano, C. S., P. F. Schellhammer, E. J. Small, P. A. Burch, J. Nemunaitis, L. Yuh, N. Provost, and M. W. Frohlich. 2009. Integrated data from 2 randomized, double-blind, placebo-controlled, phase 3 trials of active cellular immunotherapy with sipuleucel-T in advanced prostate cancer. *Cancer 115:3670*.**
2. **Kantoff, P. W., T. J. Schuetz, B. A. Blumenstein, L. M. Glode, D. L. Bilhartz, M. Wyand, K. Manson, D. L. Panicali, R. Laus, J. Schlom, W. L. Dahut, P. M. Arlen, J. L. Gulley, and W. R. Godfrey. 2010. Overall survival analysis of a phase II randomized controlled trial of a Poxviral-based PSA-targeted immunotherapy in metastatic castration-resistant prostate cancer. *J Clin Oncol 28:1099*.**
3. **Peggs, K. S., S. A. Quezada, and J. P. Allison. 2008. Cell intrinsic mechanisms of T-cell inhibition and application to cancer therapy. *Immunol Rev 224:141*.**
4. **Higgins, A. D., M. A. Mihalyo, and A. J. Adler. 2002. Effector CD4 cells are tolerized upon exposure to parenchymal self-antigen. *J Immunol 169:3622*.**
5. **Drake, C. G., A. D. Doody, M. A. Mihalyo, C. T. Huang, E. Kelleher, S. Ravi, E. L. Hipkiss, D. B. Flies, E. P. Kennedy, M. Long, P. W. McGary, L. Coryell, W. G. Nelson, D. M. Pardoll, and A. J. Adler. 2005. Androgen ablation mitigates tolerance to a prostate/prostate cancer-restricted antigen. *Cancer Cell 7:239*.**
6. **Arredouani, M. S., S. S. Tseng-Rogenski, B. K. Hollenbeck, J. Escara-Wilke, K. R. Leander, D. Defeo-Jones, C. Hwang, and M. G. Sanda. 2010. Androgen ablation augments human HLA2.1-restricted T cell responses to PSA self-antigen in transgenic mice. *Prostate 70:1002*.**
7. **Koh, Y. T., A. Gray, S. A. Higgins, B. Hubby, and W. M. Kast. 2009. Androgen ablation augments prostate cancer vaccine immunogenicity only when applied after immunization. *Prostate 69:571*.**
8. **Tang, S., M. L. Moore, J. M. Grayson, and P. Dubey. 2012. Increased CD8+ T-cell Function following Castration and Immunization Is Countered by Parallel Expansion of Regulatory T Cells. *Cancer Res 72:1975*.**
9. **Degauque, N., C. Mariat, J. Kenny, D. Zhang, W. Gao, M. D. Vu, S. Alexopoulos, M. Oukka, D. T. Umetsu, R. H. Dekruyff, V. Kuchroo, X. X. Zheng, and T. B. Strom. 2008. Immunostimulatory Tim-1-specific antibody deprograms Tregs and prevents transplant tolerance in mice. *J Clin Invest 118:735*.**
10. **Neeley, Y. C., M. S. Arredouani, B. Hollenbeck, M. H. Eng, M. A. Rubin, and M. G. Sanda. 2008. Partially circumventing peripheral tolerance for oncogene-specific prostate cancer immunotherapy. *Prostate 68:715*.**

11. **Tseng-Rogenski, S. S., M. S. Arredouani, J. F. Escara-Wilke, Y. C. Neeley, M. J. Imperiale, and M. G. Sanda. 2008. A safety-modified SV40 Tag developed for human cancer immunotherapy. *Drug Design, Development and Therapy 2:17*.**
12. **Tseng-Rogenski, S. S., M. S. Arredouani, Y. C. Neeley, B. Lu, A. M. Chinnaiyan, and M. G. Sanda. 2008. Fas-mediated T cell deletion potentiates tumor antigen-specific tolerance in a mouse model of prostate cancer. *Cancer Immunol Immunother*.**
13. **Morse, M. D., and D. G. McNeel. 2012. T cells localized to the androgen-deprived prostate are TH1 and TH17 biased. *Prostate 72:1239*.**
14. **Ward, J. E., and D. G. McNeel. 2007. GVAX: an allogeneic, whole-cell, GM-CSF-secreting cellular immunotherapy for the treatment of prostate cancer. *Expert Opin Biol Ther 7:1893*.**
15. **Binne, L. L., M. L. Scott, and P. D. Rennert. 2007. Human TIM-1 associates with the TCR complex and up-regulates T cell activation signals. *J Immunol 178:4342*.**

APPENDICES: None

SUPPORTING DATA: All figures and/or tables shall include legends and be clearly marked with figure/table numbers.

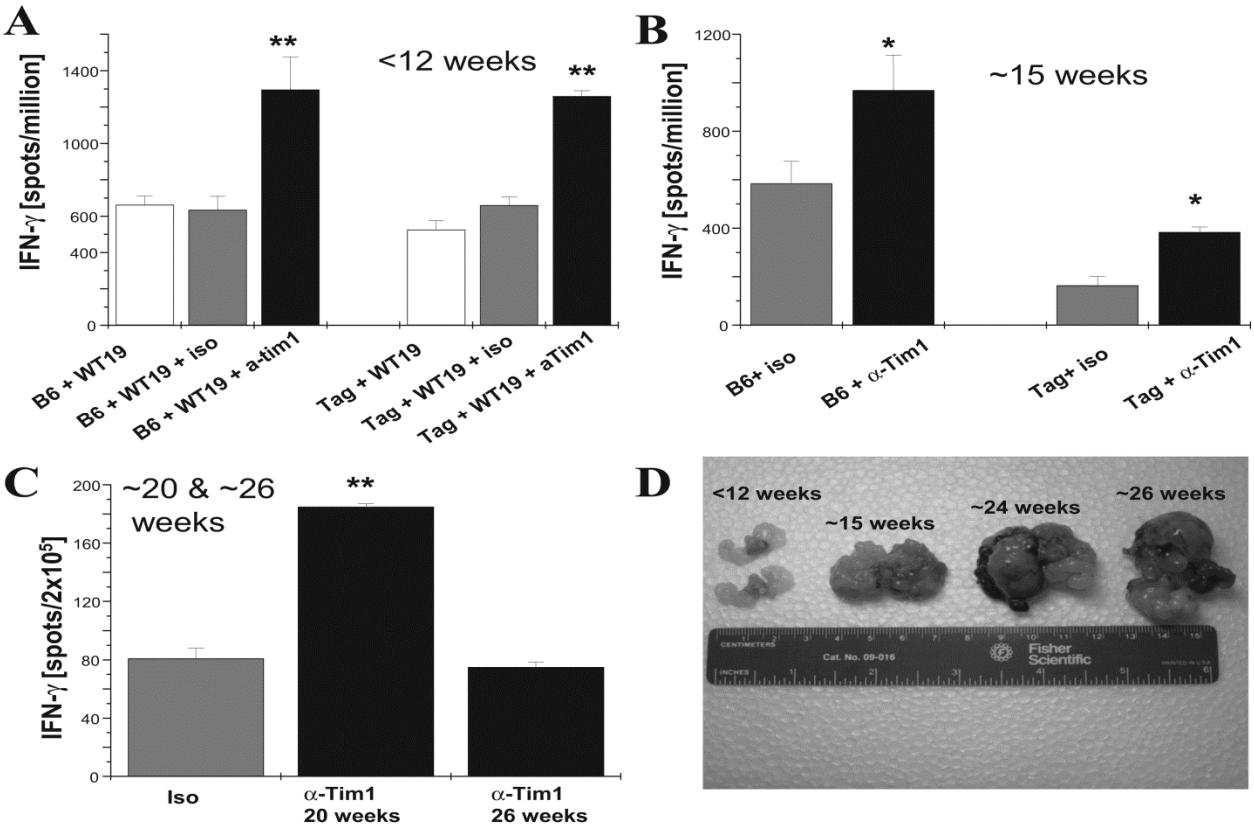

Figure 1: Agonist anti-TIM1 monoclonal antibody enhances CTL responses to prostate antigens. **A**. Male B57BL/6 and TRAMP mice under 12 weeks of age were immunized with the Tag expressing WT19 cell line i.p. and either 200 μg of anti-TIM1 mAb or its isotype control Ab. **B**. Mice around 15 weeks of age were submitted to the same treatments as in A. **C**. Mice aged 20 or 26 weeks old were treated as above. Tag-specific CTL responses in the spleen were evaluated in response to Tag IV MHC-I-restricted peptide restimulation suing an IFN-γ elispot assay. At least 6 mice were tested per group. *, P<.05; **, P<.01 for anti-TIM1 Ab vs. isotype control treatment. **D**. GU tract from male TRAMP mice of different ages are shown that illustrate prostate tumor load as described in the results.

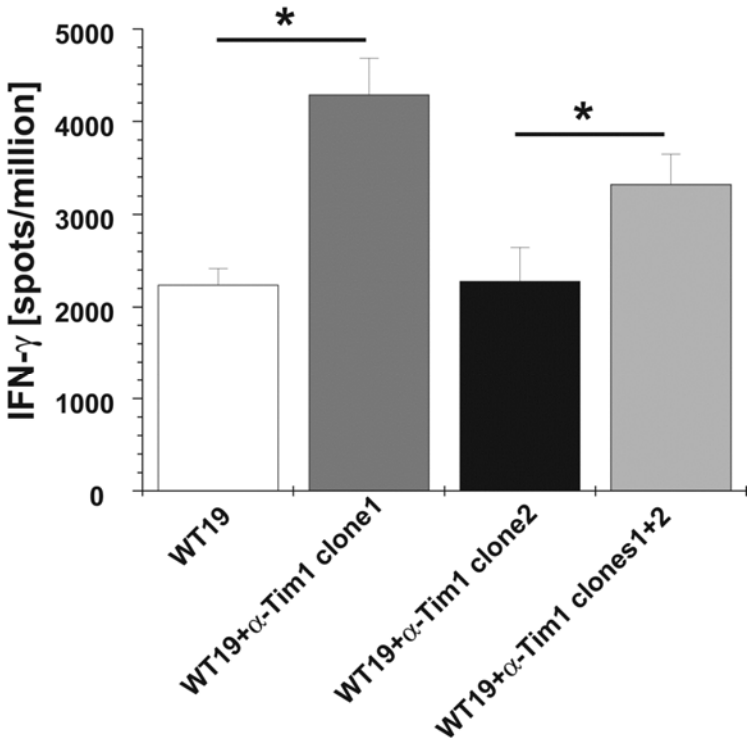

Figure 2: Agonist anti-TIM1 mAb acts specifically through TIM-1 receptor. Male B6 mice were immunized with WT19 cells and administered either 200ug of the agonist anti-TIM1 mAb (clone 1) or antagonist mAb (clone 2) or both. *, P<.05 between two treatments as shown. 4 mice were used per group.

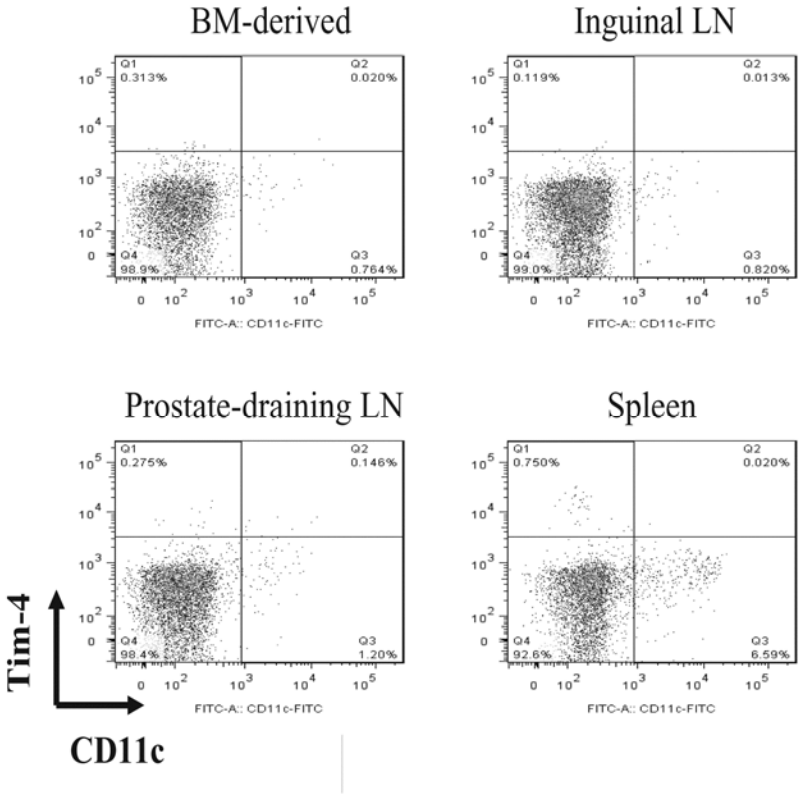

Figure 3: Low TIM4 expression on dendritic cells from various sources. Bone-marrow derived DCs were generated by treating bone marrow cells with a combination of IL-4 and GM-CFS for 1 week. Spleens and lymph nodes were prepared from a naïve mouse. Cells were stained for CD11c and TIM4 to highlight TIM4 expression on DCs.

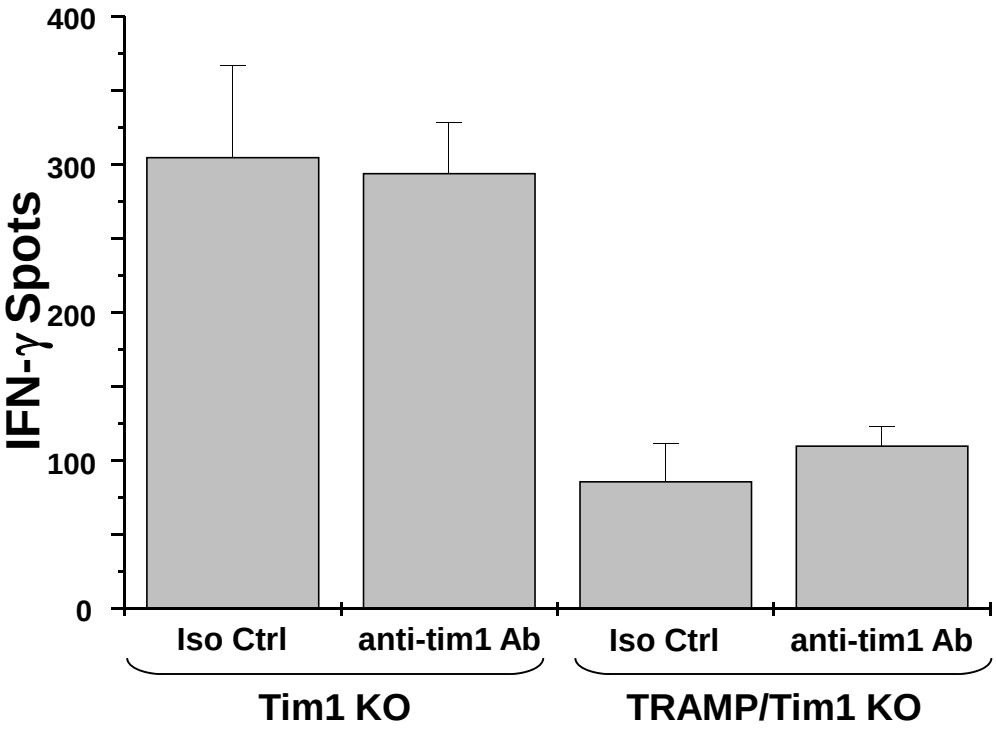

Figure 4: Agonist anti-Tim1 monoclonal antibody exerts its action through TIM-1. Male Tim1 KO and TRAMP/Tim1 KO mice were immunized with the Tag expressing WT19 cell line i.p. and either 200 μg of anti-Tim1 mAb or its isotype control Ab. Tag-specific CTL responses in the spleen were evaluated in response to Tag IV MHC-I-restricted peptide restimulation suing an IFN-γ elispot assay. At least 3 mice were tested per group.

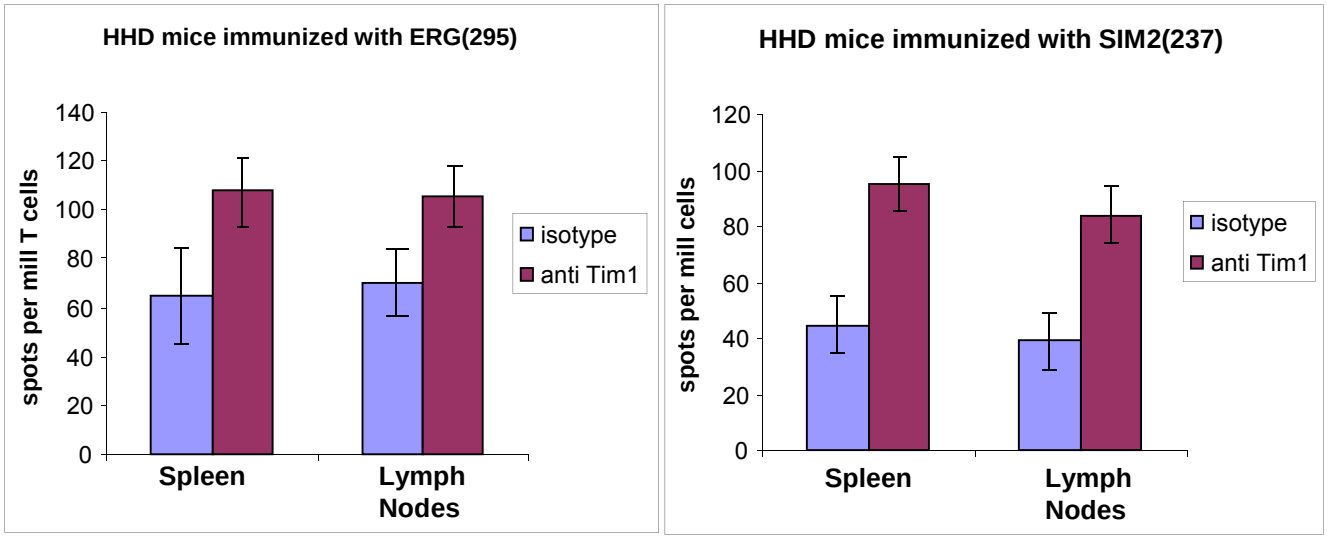

Figure 5: Agonist anti-Tim1 monoclonal antibody enhances CTL responses to human prostate tumor-associated antigens. Male HLA-A2.1 transgenic mice (HHD) were immunized with immunogenic peptides derived from human ERG or SIM2 together with the agonist anti-TIM1 antibody or its isotype control antibody. IFN-γ ELISPOT was performed 10 days post-immunization using splenocytes or prostate-draining lymph node cells.

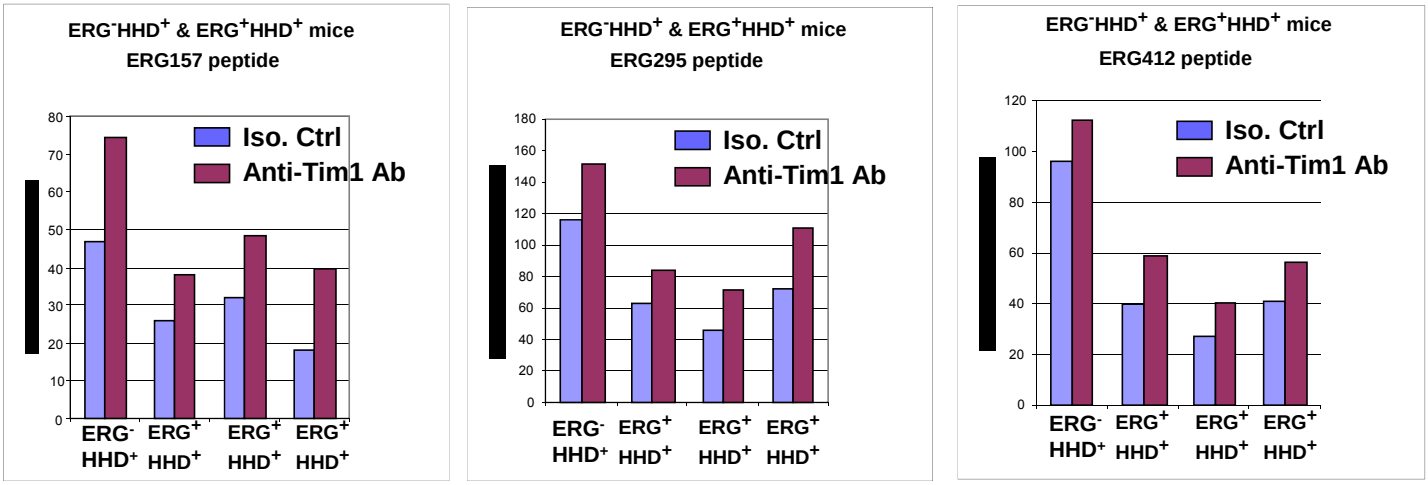

Figure 6: Agonist anti-Tim1 monoclonal antibody partially circumvents immune tolerance to human prostate tumor-associated antigens. Male HLA-A2.1 transgenic mice (HHD, homozygous) were crossed with Pb-ERG (Homozygous) mice. The offspring was either $ERG^{-}HHD^{+}$ & $ERG^{+}HHD^{+}$. Male offspring was immunized with one of the three immunogenic peptides derived from human ERG together with the agonist anti-TIM1 antibody or its isotype control antibody. IFN-γ ELISPOT was performed using splenocytes 10 days post-immunization.

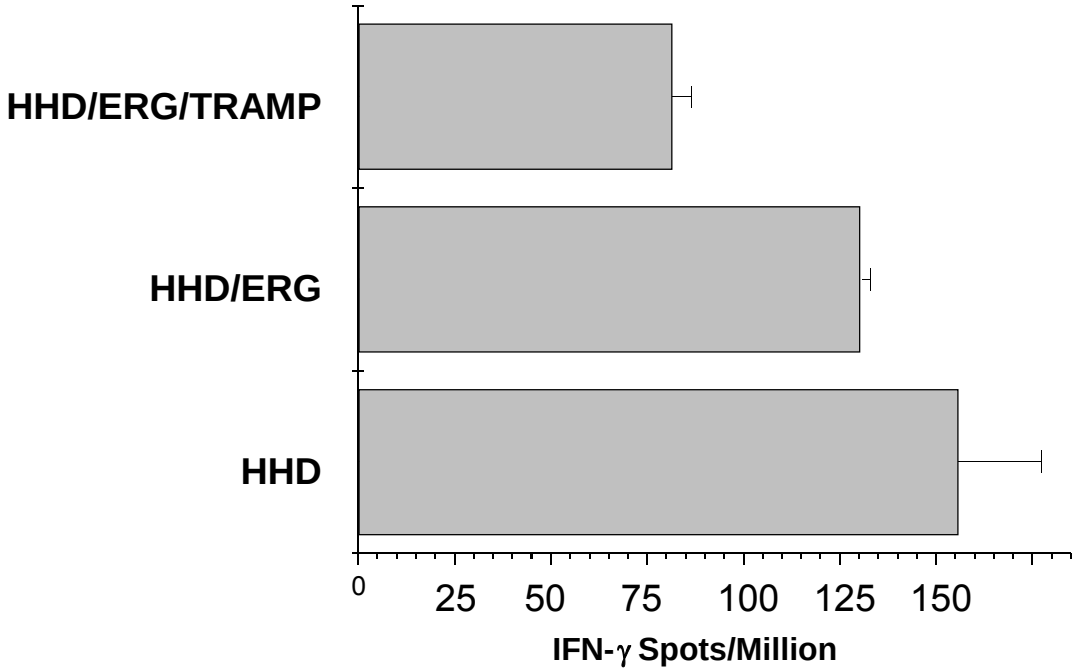

Figure 7: Prostate tumors reduce but do not fully abrogate CTL responses to human TAA. Male HHD, HHD/ERG or HHD/ERG/TRAMP were immunized with ERG295 peptide. IFN-γ ELISPOT was performed 10 days post-immunization using splenocytes.

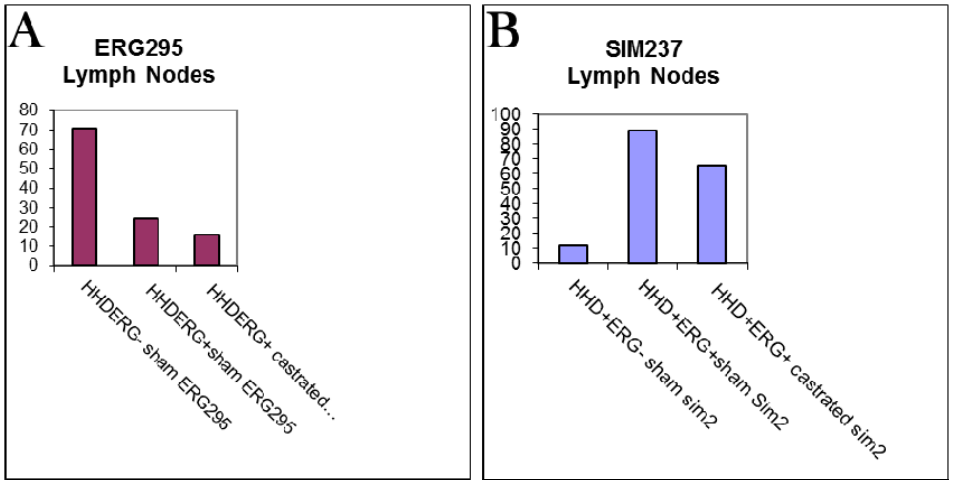

Figure 8: Effect of castration on SIM2 and ERG-specific, CTL responses. Male HHD/ERG- and HHD/ERG+ mice were surgically castrated and immunized with sim2- and ERG-derived HLA-A2.1-restricted peptides (peptides SIM237 and ERG295) 4 weeks later. IFN-γ ELISPOT was performed on prostate-draining lymph nodes 10 days post-immunization. Lymph nodes from 3 mice per group were pooled to obtain sufficient cells for the assay. Number of spots on the Y axis is per 10^5 cells.

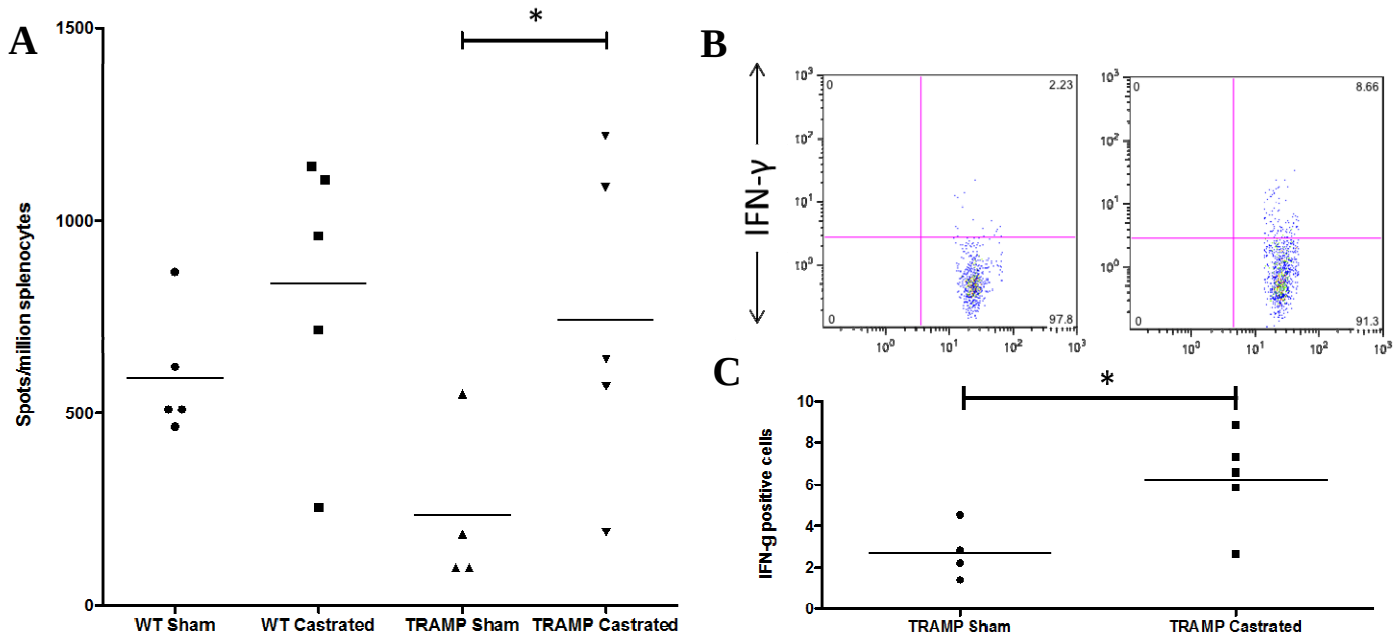

Figure 9: TRAMP-C2/GM-CSF vaccine, in combination with androgen deprivation, overcomes immune tolerance to prostate tumor antigens in wild healthy and prostate tumor-bearing mice. Sham-castrated and castrated C57BL/6 and TRAMP mice were administered one dose of the TRAMP-C2/GM-CSF vaccine. IFN-γ-producing CD8 T cells were evaluated with ELISPOT (A) and intracellular staining (B&C). * P<.05.

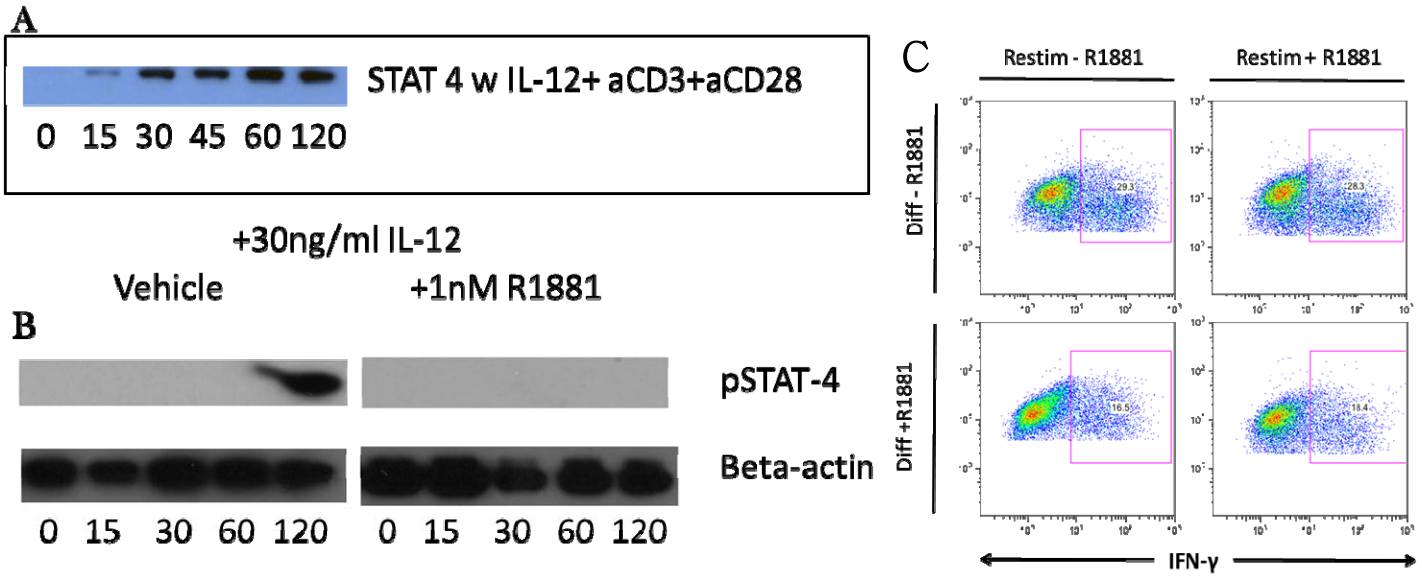

Figure 10: Androgens suppress Th1 differentiation through inhibition of STAT4 phosphorylation. (**A**) Pure CD4 T cells were obtained from spleen and incubated in vitro in the presence of anti-CD3, anti-CD28 and IL-12 to slew T cell differentiation towards the Th1 phenotype. (**B**) Pure CD4 T cells were treated in vitro as in (A) in the presence of vehicle or testosterone analog R1881. pSTAT was assayed by western blot over time (0 through 120 minutes). (**C**) Th1 differentiated CD4 T cells produce IFN-γ upon stimulation. This production is reduced when cells are cultured in the presence of androgen analog.

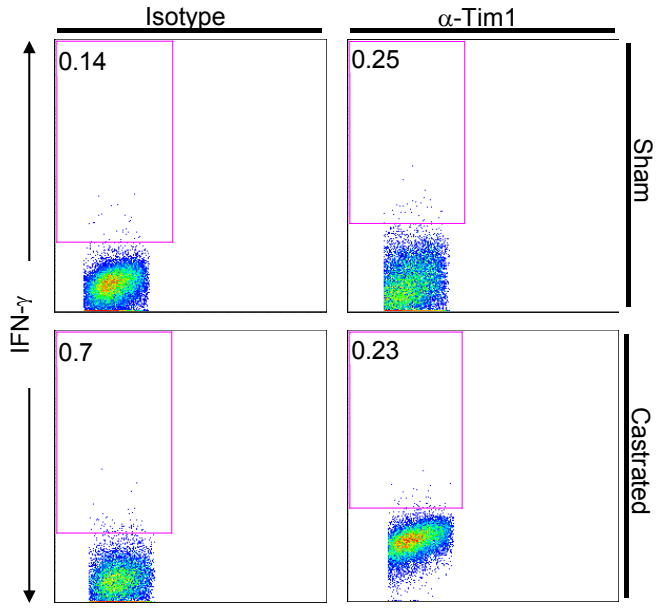

Figure 11: Castration and anti-TIM1 treatment exhibit immuno-enhancing effects of single-dose vaccine individually but not in combination. Sham-castrated and castrated 20 week-old male TRAMP mice were administered one dose of the TRAMP-C2/GM-CSF vaccine. IFN-g-producing CD8 T cells were evaluated with intracellular staining.

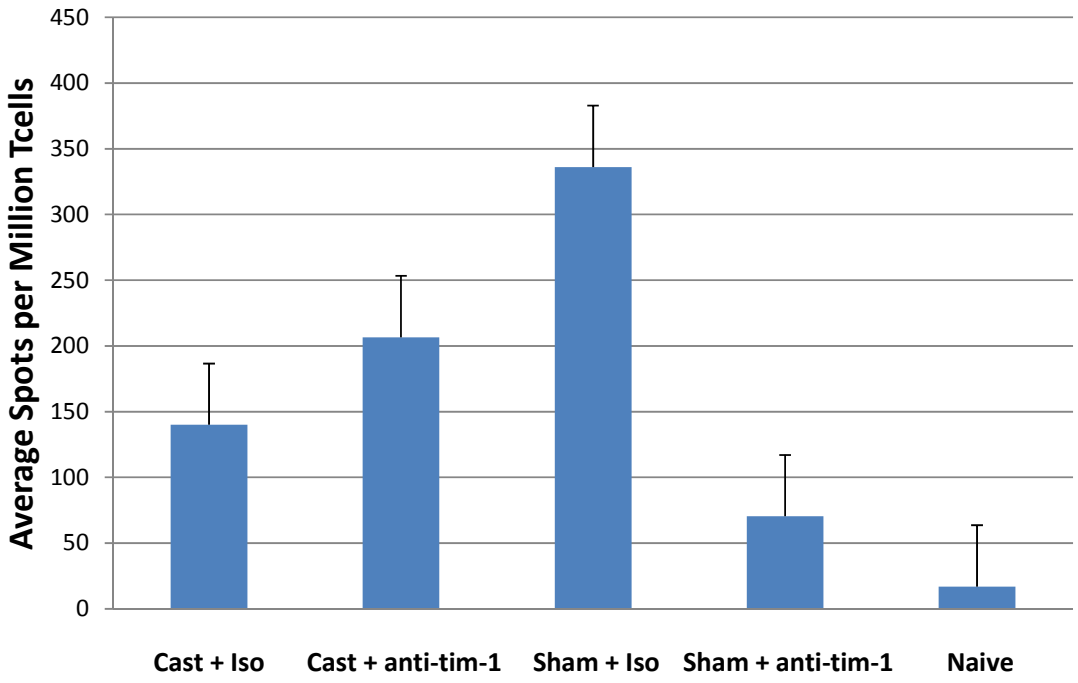

Figure 12: Castration and anti-TIM1 treatment immuno-modulating effects exhibit a different pattern in a triple-dose vaccine regimen. Sham-castrated and castrated 20-wk old male TRAMP mice were administered three doses (injections separated by 2 weeks) of the TRAMP-C2/GM-CSF vaccine. Isotype control or anti-TIM1 mAb were administered with each vaccine treatment. IFN-γ-producing CD8 T cells were evaluated with intracellular staining in spleens 2 months following the last injection.

Published in final edited form as:
Prostate. 2010 June 15; 70(9): 1002–1011. doi:10.1002/pros.21134.

Androgen ablation augments human HLA2.1-restricted T cell responses to PSA self antigen in transgenic mice

Mohamed S. Arredouani[1], **Stephanie S. Tseng-Rogenski**[2], **Brent K. Hollenbeck**[2], **June Escara-Wilke**[2], **Karen R. Leander**[3], **Deborah Defeo-Jones**[3], **Clara Hwang**, and **MartinG. Sanda**[1]

[1] Department of Surgery, Beth Israel Deaconess Medical Center, Harvard Medical School, Boston, MA

[2] Department of Urology & Department of Microbiology and Immunology, School of Medicine, University of Michigan, Ann Arbor, MI

[3] Merck Research Laboratories, West Point, PA

Abstract

Background—In recent years, there has been an increasing interest in targeting human prostate tumor-associated antigens (TAAs) **for** prostate cancer immunotherapy as an alternative to other therapeutic modalities. However, immunologic tolerance to TAA poses a significant obstacle to effective, TAA-targeted immunotherapy.

We sought to investigate whether androgen deprivation would result in circumventing immune tolerance to prostate TAA by impacting CD8 cell responses.

Methods—To this end, we generated a transgenic mouse that expresses the human prostate specific antigen (PSA) specifically in the prostate, and crossed it to the HLA-A2.1 transgenic mouse.

Results—Our PSA transgenic mouse showed restricted expression of PSA in the prostate and detectable circulating PSA levels. Additionally, PSA expression was androgen-dependent with reduced PSA expression in the prostate within one week of castration, and undetectable PSA by day 42 after castration as evaluated by ELISA. Castration of the PSA/A2.1 hybrid mouse prior to immunization with a PSA-expressing recombinant vaccinia virus resulted in a significant augmentation of PSA-specific cytotoxic lymphocytes.

Conclusions—This humanized hybrid mouse model provides a well defined system to gain additional insight into the mechanisms of immune tolerance to PSA and to test novel strategies aiming at circumventing immune tolerance to PSA and other TAA for targeted prostate cancer immunotherapy.

Keywords

Prostate cancer; immune tolerance; immunotherapy

INTRODUCTION

To date, clinical trials of PCa immunotherapy included immunization with defined antigenic preparations such as synthetic peptides (1-3), antigen- (4,5) or mRNA-loaded dendritic cells

Correspondence: Martin G. Sanda, 330 Brookline Ave., CLS-447, Boston, MA 02215, Phone 617-735-2101, Fax 617-735-2110, Fax 617-735-2110.

(6), manipulated tumor cells (7), or with plasmid DNA (8) or viral vectors engineered to express immunogenic genes (9). In particular, recombinant vaccinia virus expressing prostate specific antigen (PSA) was tested in clinical trials in combination with recombinant PSA-expressing fowlpox virus (10,11), demonstrating its ability to trigger a specific immune response (11) and an 8.5 month improvement in median overall survival in men with metastatic castration-resistant prostate cancer (10). However, the survival benefit remains modest, suggesting an opportunity and need for significant improvement of efficacy in PCa immunotherapy.

In 1999, a study reported combined immunization with androgen deprivation to modulate antigen expression as a means of circumventing tolerance to a prostate TAA-specific in the setting of a human PCa clinical trial that targeted PSA as a prototype PCa TAA (12). The scientific basis for combining androgen deprivation and PCa TAA-specific immunization was subsequently validated in mouse models that focused on MHC class II-mediated helper T cell responses (13,14). Androgen ablation results in a rapid involution of benign and neoplastic prostate tissue at both primary and metastatic sites, seemingly due to apoptosis of androgen-dependent epithelial cells (15-17). This treatment has been shown to induce infiltration of lymphocytes, macrophages and dendritic cells into the prostate and trigger inflammation (18). Such infiltration proved to be beneficial for PCa immunotherapy as it provides a synergistic help by increasing the number of tumor antigen-specific lymphocytes (13,19,20). Additional supporting evidence for this concept was provided by the demonstration that testosterone can be immunosuppressive by stimulating tumors to secrete TGF-β, a cytokine that promotes the expansion of Treg (21). Androgen deprivation has been shown to result in a decrease in expression of these genes in both patients undergoing androgen ablation therapy and in human PCa cell lines (22). In mice, androgen deprivation-induced TAA gene downregulation has been shown to circumvent immune tolerance and enhance CD4 T cell responses to prostate TAA (13). However, the effect of androgen deprivation on the generation of TAA-specific CD8 T cells has not been addressed before.

In this report, we describe the initial characterization of transgenic mice expressing the PSA transgene in an androgen-regulated and prostate-specific manner. To further refine current prostate cancer models, we developed a unique double-transgenic mouse model co-expressing PSA and HLA-A2.1 to facilitate the investigation of PSA-specific tolerance in the context of human MHC. Finally, we sought to determine whether castration of male mice prior to immunization to PSA improves class I MCH-restricted T cell responses to this clinically relevant target antigen.

MATERIALS AND METHODS

Peptides, proteins and viruses

Previously described HLA-A2.1-restricted, PSA-derived peptide PSA-3 (VISNDVCAQV) and its agonist PSA-3A (YISNDVCAQV) (23) and the H-2Kb restricted-, SV40 Tag-derived Tag-IV peptide (VVYDFLKC) (24,25) were purchased from the Macromolecular Resources Facility at Colorado State University (Ft. Collins, CO). Human PSA was purchased from Calbiochem (San Diego, CA). Vac-PSA was obtained from Therion Biologics Corporation (Cambridge, MA). Vac-mTag was generated in our laboratory (26-28).

Generation of transgenic rPB-PSA mice, construction of PSA transgenic map

Human prostate-specific antigen (PSA) prepro-cDNA (Accession M26663, NID g618463) was ligated to rat probasin (rPB) promoter cassette (GI:10000942 −426 to +28) (29) at the introduced BamH1 site. The rPB-PSA was ligated to a bovine growth hormone (bGH, GI:

2168498 1872 to 2028) terminator sequence at the BglII site. The final rPB-PSA transgene construct was microinjected into oocytes of foster mouse mothers and offspring were evaluated by PCR using PSA primers. The transgene transmission to the progeny of potential founder mice was verified by PCR and Southern blot. From among several candidate founders we have generated, the mouse expressing stably the highest levels of PSA as detected by ELISA was selected as the founder to propagate hybrid transgenic colonies.

The rPB-PSA transgenic map was constructed to confirm boundary sequences between the rat probasin promoter region, PSA open reading frame (ORF) and the bGH terminator. Primer sets located in the promoter-PSA and PSA-terminator flanking regions were designed and utilized to generate overlapping PCR fragments for complete DNA sequencing of the boundary regions.

Generation of PSA/HLA-A2.1 double transgenic mouse

Hybrid PSA and HLA-A2.1double transgenic mice (PSA/A2.1) were generated by cross-breeding PSA mice with HLA A2.1/H2K^b transgenic mice (Harlan Sprague Dawley, Indianapolis, IN). All double transgenic mice were heterozygous for each of their transgenes as confirmed by PCR.

Genotyping of PSA transgenic mice

Tail snippets from three-week old transgenic mice were collected and their DNA isolated. PCR was used to genotype transgenic progeny using the following PSA primers (InVitrogen): *PSA -FOR*: 5’ ACCATGTGGGTCCCGGTTG 3’and *PSA-REV*: 5 ’ TCAGGGGTTGGCCACGATG 3’.

DNA quality was tested with a β-globin PCR performed concurrently in each of the PSA reactions using the following primers: FOR: 5’ GCCAATCTGCTCACACAGGATA 3’ and REV: 5’ CATGCAGCTTGTCACAGTGGA 3’.

PCR reactions contained 200-300ng of genomic DNA template, 10mM Tris/HCL pH 8.3, 50mM KCl, 200μM dNTPs, 1μM each of forward and reverse primers, 1.25U Taq DNA polymerase (Applied Biosystems) and 1.5 mM $MgCl_2$ in a 25 μl final reaction volume. PSA-β -globin PCR was performed using PSA and globin primers in 25 μL reaction at 94°C, 3 minutes followed by 30 cycles of 94°C for 1 minute, 55°C for 1 minute, 72°C for 2 minutes, and final elongation at 72°C for 10 minutes. Samples were stored at 4°C until gel electrophoresis was performed using a 1% agarose gel in 1×TAE buffer.

Extraction of RNA and RT-PCR

Total RNA was isolated from the prostate and other tissues using the Nucleospin RNA II Kit (Clontech, Mountain View, CA). RT-PCR was performed using a reverse transcriptase kit (Promega, Madison, WI). PSA primers were as described above, and β-actin primers that were used for control reactions as follows: β-actin *Forward:* 5’ TGTGATGGTGGGAATGGGTCAG 3’and *Reverse:* 5’ TTTGATGTCACGCACGATTTCC 3’. A parallel RT-PCR reaction without reverse transcriptase served as a negative control. PCR products were visualized on a 1% agarose gel.

Castration of PSA transgenic mice

Mice were anesthetized with a ketamine-xylazine mixture (ratio 90 mg/kg ketamine to 4.5 mg/kg xylazine) administered *i.p.* A lower abdominal incision was made, the testicular blood supply isolated and ligated with electrocautery. The testes were removed and the vasa

cauterized. Mice were re-explored at various time intervals (e.g. 7, 14, 21, 28, and 42 days) for harvesting of tissues.

Quantitaion of PSA levels by ELISA

Tissues were homogenized by mincing with surgical blade, resuspend in equal volume of Buffer A (50mM Tris, KCl 1.15% pH 7.5) and Buffer C (10mM KPO_4, 0.25 mM Sucrose pH 7.4) (max volume of 500 ul), and passed through a 21G needle with 1ml of syringe. Cells were sonicated at 30% output (180 watt) for 10 sec pulse (three times). The lysate was centrifuged at 13,000 rpm for 10 minutes at room temperature. The protein concentration in the supernatant was calculated using the Bio-Rad protein assay kit (BioRad Laboratories, Hercules, CA). 120 μl of lysate containing 50 μg of protein was used for PSA ELISA. Serum PSA concentration was measured by AxSYM PSA assay (AxSym system, Abbott Diagnostics, Abbott Park, IL), a Microparticle Enzyme Immunoassay designed to quantitate PSA levels in human serum.

One hundred micrograms of total protein was placed in 250μl of clear Hanks balanced salt solution and samples were submitted to the University of Michigan clinical pathology laboratory for PSA ELISA. Samples consisting of purified PSA from human semen or protein from wild type C57BL/6 mice were submitted to serve as positive and negative controls, respectively.

Mouse whole blood processing and HLA A2.1/K^b FACS analysis

One hundred microliters of blood was obtained from each mouse via orbital puncture and placed in a heparinized microfuge tube. Blood was placed in 2ml lysis buffer (Mouse Erythrocyte Lysing Kit, R&D Systems Inc.) for 10 minutes at room temperature. Samples were centrifuged for 5 minutes at 250×g, the supernatant was discarded, and the pellets were washed with 2ml of 1×PBS. One million peripheral blood cells were incubated with 0.5 μg anti-mouse FcγR antibody (Mouse Fc Block, BD PharMingen) for 10 minutes at 4°C. 0.5 μg of FITC-conjugated anti-HLA A2 antibody (One Lambda, Inc., Canoga Park, CA) or isotype control was then added and the reaction mixture was incubated in a final volume of 20 μl at 4°C for 1 hour. Cells labeled with isotype control were used to assess background fluorescence, and 10,000 viable cells were analyzed in a FACScan microflourometer (Becton Dickinson, Sunnyvale, CA).

Immunization of castrated PSA/A2.1 transgenic mice

PSA/A2.1 mice were anesthetized with a ketamine-xylazine mixture (ratio 90 mg/kg ketamine to 4.5 mg/kg xylazine) administered *i.p.* A lower abdominal incision was made, the testicular blood supply isolated, and ligated with electrocautery. The testes were removed and the vasa cauterized. Four weeks post-castration, mice were immunized intravenously with 10^6 PFU of a recombinant vaccinia virus expressing either the entire sequence of PSA (vac-PSA) (30) or the modified SV40 T antigen (vac-mTag) we previously generated in our laboratory (26-28).

Generation of bone-marrow-derived dendritic cells

Dendritic cells (DC) were generated from bone marrow using IL-4 and GM-CSF (PeproTech, Rocky Hill, New Jersey), and purified on a metrizamide gradient. DC maturation was evaluated by measuring MHC Class II, CD11c, CD40, CD80 and CD86 surface expression. Peptides (final 20μg/ml) or proteins (50 μg /ml) were loaded on DC at 37°C for 4 hrs or overnight, respecitvely. Loaded DC were washed and used as antigen-presenting cells in the ELISPOT assay.

IFN-γ ELISPOT assay

MultiScreen 96-well plates were first coated with purified anti-mouse IFN-γ antibody (capture antibody) (4 μg/ml in 1X PBS; PharMingen) overnight at 4°C. Plates were blocked with PBS/1% BSA (PBS-BSA) at room temperature for 90 min and then washed 3 times with 1X PBS before seeding the cells. $CD8^+$ T cells were isolated from mice three weeks after immunization with 10^6 pfu/mouse vac-PSA or 10^7 vac-mTag. One million $CD8^+$ T cells were seeded into each well (E/S = 10) and incubated at 37°C/5% CO_2 for 24 hours with irradiated (5000 rads) peptide-or protein-loaded DC. Plates were washed 3 times with 1X PBS and then 4 times with 1X PBS/0.025% Tween-20 (PBS-TW20) before adding biotin rat anti-mouse IFN-γ antibody (2 μg/ml in PBS-BSA; PharMingen) overnight at 4°C. The plates were washed 4 times with PBS-TW20 and incubated with anti-biotin antibody (1:1000 dilution; Vector; Burtingame, CA) at room temperature for 90 min, followed by washing 4 times with PBS. Plates were then developed with NBT/BCIP before subjecting to an ELISPOT reader (Cellular Technology Laboratories, Ltd.; Cleveland, OH) to count spots.

RESULTS

Prostate-specific, androgen-dependent expression of PSA in a transgenic mouse

The rat probasin gene promoter has been demonstrated to be both developmentally and hormonally regulated in the mouse and demonstrates a high ability to direct transgene expression specifically to the prostate tissue (31). The promoter has been previously utilized to generate transgenic mice that express viral (29) and human oncogenes (32,33) in the prostate to study prostate cancer development. We adopted a similar strategy to generate a transgenic mouse that exhibits prostate-specific expression of human PSA. To this end, an expression cassette containing human PSA cDNA, the rat probasin promoter, and the bovine growth hormone terminator sequence (Figure 1A) served to generate transgenic founders. The founder that produced progeny that had stable and high levels of PSA expression was selected to propagate the colony.

To address the specificity of the PSA expression, we isolated RNA from prostate, testis, seminal vesicle, spleen, pancreas, liver, lung, and nodal tissue from multiple progeny. Using RT-PCR, we confirmed that the presence of RNA transcript for PSA was restricted to the prostate tissue (Figure 1B). In line with this finding, analysis of protein extracts from these tissues by ELISA detected PSA in the prostate but not in any of the other tissues (Figure 2A).

To test androgen-responsiveness of the PSA transgene, mice were castrated and sacrificed at various time points, and the presence of PSA mRNA was tested by RT-PCR. As shown in figure2B, expression of the transgene decreased in a time-dependent fashion after castration. Only a minimal expression was present at day 28 post-castration, and no transcripts were detected at day 42.

Generation of a PSA/HLA-A2.1 hybrid mouse

To generate a hybrid mouse that expresses both human HLA-A2.1 and PSA, PSA and HLA A2.1/K^b transgenic mice were crossed and the progeny tested by PCR of genomic DNA (**data not shown**). Progeny that possessed copies of both transgenes (data not shown) were further tested for HLA-A2.1 expression by flow cytometry. These double positive mice demonstrated expression of the HLA A2.1/K^b chimeric receptor on peripheral blood lymphocytes as demonstrated by FACS analysis. Some of these mice were sacrificed and protein extracts from mouse prostate tissue contained high levels of PSA as demonstrated by ELISA (data not shown).

Androgen deprivation augments CD8 T cell responses to prostate TAA

Consistent with the known immunosuppressive effects of androgens, castration of prostate tumor-bearing mice has been shown to enhance antigen-specific CD4 T cell responses to a model prostate TAA (13). We therefore sought to determine whether CD8 responses are affected by androgen deprivation using the PSA/A2.1 as a model and PSA or PSA-derived peptides as immunogens. Male A2.1 and female PSA/A2.1 mice were used as controls.

Mice were immunized with recombinant vaccinia virus constructs that express either PSA (vac-PSA) or SV40 Tag (vac-mTag). Splenocytes from immunized mice were re-stimulated in vitro with peptide- or full protein-loaded dendritic cells and IFN-γ-releasing CD8 T cells were quantitated by ELISPOT and tetramer staining. Our data show that splenocytes from sham-castrated male, castrated male, and female PSA/A2.1 mice immunized with vac-mTag responded in a similar fashion to restimulation with Tag-IV, while no response was observed with splenocytes from vac-PSA immunized mice. A similar response to Tag IV was obtained in control vac-mTag-immunized A2.1 mice, indicating a complete absence of tolerance to exogenous antigen in these mice (Figure 3A). Immunization with vac-PSA resulted in a strong and specific response in A2.1 mice upon re-stimulation with full PSA-loaded DC. However, a very weak response was observed in PSA/A2.1. Castrated mice responded better ($P<.001$), although this response was still significantly lower than male A2.1 and female PSA/A2.1 mice ($P<.001$) (Figure 3B). Splenocytes from vac-PSA-immunized mice showed a much lower number of IFN-γ-releasing, PSA-specific CD8 T cells upon re-stimulation with DC loaded with the peptides PSA3A (Figure 3C) and PSA3 (Figure 3D). Such a weak response to PSA peptides as compared to full PSA protein is possibly due to the contribution of H2-Db to the response to potential H2-Db-restricted, PSA-derived epitopes in this mouse model. Sham-castrated male PSA/A2.1 showed no response, while castrated mice showed a weak response. Due to the overall signal to noise window for ELISPOT evaluation of A2.1-restricted PSA peptide responses (females vac-mTag controls showed low but significant activity of PSA peptides, Figure 3C & 3D), we turned to tetramer assay to ascertain detection of A2.1-restricted, PSA-specific CTL. To this aim, we labeled in vitro-restimulated splenocytes with a PSA-3A-A2.1 tetramer and used flow cytometry to determine the fraction of CD8(+) T cells that bound the tetramer. Consistent with the ELISPOT data, tetramer staining revealed elevated amounts of PSA-specific CD8 T cells in spleens of immunized non-transgenic mice. These amounts were significantly lower (comparable to background level as seen in vac-mTag-immunized mice) in PSA transgenic mice, reflecting a deep immune tolerance to PSA. Splenocytes from castrated immunized male PSA/A2.1 mice exhibited significantly higher numbers of tetramer-positive CD8 cells than did their non-castrated counterparts. The effect of castration was similar to the one observed in A2.1-PSA females, but still lower than in A2.1 male mice (Figure 4).

DISCUSSION

A large body of evidence suggests the feasibility of PSA-based vaccines for prostate cancer (2,3,12,34-41). However, because PSA is a self antigen, these vaccines face the challenge of immune tolerance to PSA and are yet to demonstrate clinical efficacy. Hence, immunotherapy for PCa will most likely consist of combined approaches that simultaneously target tumors through TAA and interfere with tolerizing mechanisms that hinder immunity to tumors. These mechanisms include innate and adaptive immune responses, activation/inhibition of co-stimulatory/inhibitory molecules (e.g. CTLA-4), elimination of regulatory/suppressive cells (e.g. regulatory T cells - Treg) and soluble factors, and manipulation of hormonal pathways. So far, interference with the inhibitory co-stimulatory signals mediated by CTLA-4 using monoclonal antibodies has provided the most promising results, although a myriad of adverse autoimmune responses generated by

this strategy still represent a sizeable obstacle to its implementation in clinic (reviewed in ref.(42)).

In prostate cancer, androgen deprivation is a therapeutic modality that aims at depriving the prostate from testosterone to suppress its growth. Interestingly, this deprivation also results in strengthening immunity to tumors as shown in mice (13) and humans (12). The mechanisms whereby androgen deprivation affects immunity to tumors are poorly understood, partly due to the lack of appropriate mouse models.

Although the impact of androgen deprivation on prostate tumor immunity has been addressed in previous work, these failed to look at the extent to which CTL responses to a human prostate TAA are affected in vivo in humanized mice.

In this work, we describe a transgenic mouse that expresses human PSA specifically in the prostate. Tissue specific expression was demonstrated at both RNA and protein levels. We additionally show that expression of PSA in this mouse is regulated by androgens, confirming an optimal performance of the rat probasin promoter in this setting. This is evidenced by a time-dependent decrease of PSA levels in castrated male mice. At day 42 post-castration, no PSA was detected.

We crossed the PSA transgenic mouse with HLA-A2.1/Kb transgenic mouse. The resulting male offspring offers a valuable tool that allows investigation of immune tolerance to a human prostate antigen in a way that closely emulates human biology.

As expected, immunization of this hybrid mouse to a non-self antigen (SV40 Tag) resulted in a strong CTL response, whereas only a very weak response was generated towards a self antigen (PSA). In contrast, castration of male mice 4 weeks prior to immunization resulted in a significant augmentation of CTL response to PSA, while it did not affect the response to SV40 Tag. Interestingly, female hybrid mice showed a stronger response to PSA than did their castrated male counterparts.

Although interference of castration with immune tolerance to prostate specific antigens has been reported in two previous studies (13,14), these studies either focused on CD4 responses (13) or did not show any effect of castration when applied before immunization (14). In the latter study, a prime-boost immunization protocol was applied and immune responses following primary immunization were not evaluated.

Overall, our present work describes a PSA/A2.1 transgenic mouse that might represent an attractive animal model to investigate immune tolerance to human prostate TAA and for preclinical development and refinement of PSA-targeted vaccines. It also provides compelling evidence supporting the use of androgen deprivation as a modality to circumvent immune tolerance to prostate TAA.

Acknowledgments

We thank Priyanka Priyadarsiny, PhD and Robert Vessella, PhD for their help with this work.

This work is supported by grants NIH P50 DK065313-1 (M Sanda, PI) and NIH R01 CA8241901-A1 (M Sanda, PI)

References

1. Vieweg J, Dannull J. Technology Insight: vaccine therapy for prostate cancer. Nat Clin Pract Urol. 2005; 2:44–51. [PubMed: 16474576]

2. Noguchi M, Kobayashi K, Suetsugu N, Tomiyasu K, Suekane S, Yamada A, Itoh K, Noda S. Induction of cellular and humoral immune responses to tumor cells and peptides in HLA-A24 positive hormone-refractory prostate cancer patients by peptide vaccination. Prostate. 2003; 57:80–92. [PubMed: 12886526]

3. Hildenbrand B, Sauer B, Kalis O, Stoll C, Freudenberg MA, Niedermann G, Giesler JM, Juttner E, Peters JH, Haring B, Leo R, Unger C, Azemar M. Immunotherapy of patients with hormone-refractory prostate carcinoma pre-treated with interferon-gamma and vaccinated with autologous PSA-peptide loaded dendritic cells--a pilot study. Prostate. 2007; 67:500–508. [PubMed: 17262804]

4. Pandha HS, John RJ, Hutchinson J, James N, Whelan M, Corbishley C, Dalgleish AG. Dendritic cell immunotherapy for urological cancers using cryopreserved allogeneic tumour lysate-pulsed cells: a phase I/II study. BJU Int. 2004; 94:412–418. [PubMed: 15291878]

5. Small EJ, Schellhammer PF, Higano CS, Redfern CH, Nemunaitis JJ, Valone FH, Verjee SS, Jones LA, Hershberg RM. Placebo-controlled phase III trial of immunologic therapy with sipuleucel-T (APC8015) in patients with metastatic, asymptomatic hormone refractory prostate cancer. J Clin Oncol. 2006; 24:3089–3094. [PubMed: 16809734]

6. Gilboa E, Vieweg J. Cancer immunotherapy with mRNA-transfected dendritic cells. Immunol Rev. 2004; 199:251–263. [PubMed: 15233739]

7. Simons JW, Mikhak B, Chang JF, DeMarzo AM, Carducci MA, Lim M, Weber CE, Baccala AA, Goemann MA, Clift SM, Ando DG, Levitsky HI, Cohen LK, Sanda MG, Mulligan RC, Partin AW, Carter HB, Piantadosi S, Marshall FF, Nelson WG. Induction of immunity to prostate cancer antigens: results of a clinical trial of vaccination with irradiated autologous prostate tumor cells engineered to secrete granulocyte-macrophage colony-stimulating factor using ex vivo gene transfer. Cancer Res. 1999; 59:5160–5168. [PubMed: 10537292]

8. Pavlenko M, Roos AK, Lundqvist A, Palmborg A, Miller AM, Ozenci V, Bergman B, Egevad L, Hellstrom M, Kiessling R, Masucci G, Wersall P, Nilsson S, Pisa P. A phase I trial of DNA vaccination with a plasmid expressing prostate-specific antigen in patients with hormone-refractory prostate cancer. Br J Cancer. 2004; 91:688–694. [PubMed: 15280930]

9. Eder JP, Kantoff PW, Roper K, Xu GX, Bubley GJ, Boyden J, Gritz L, Mazzara G, Oh WK, Arlen P, Tsang KY, Panicali D, Schlom J, Kufe DW. A phase I trial of a recombinant vaccinia virus expressing prostate-specific antigen in advanced prostate cancer. Clin Cancer Res. 2000; 6:1632–1638. [PubMed: 10815880]

10. Kantoff PW, Schuetz T, Blumenstein BA, Glode MM, Bilhartz D, Gulley J, Schlom J, Laus R, Godfrey W. Overall survival (OS) analysis of a phase II randomized controlled trial (RCT) of a poxviral-based PSA targeted immunotherapy in metastatic castration-resistant prostate cancer (mCRPC). J Clin Oncol. 2009; 27 abstr 5013.

11. Kaufman HL, Wang W, Manola J, DiPaola RS, Ko YJ, Sweeney C, Whiteside TL, Schlom J, Wilding G, Weiner LM. Phase II randomized study of vaccine treatment of advanced prostate cancer (E7897): a trial of the Eastern Cooperative Oncology Group. J Clin Oncol. 2004; 22:2122–2132. [PubMed: 15169798]

12. Sanda MG, Smith DC, Charles LG, Hwang C, Pienta KJ, Schlom J, Milenic D, Panicali D, Montie JE. Recombinant vaccinia-PSA (PROSTVAC) can induce a prostate-specific immune response in androgen-modulated human prostate cancer. Urology. 1999; 53:260–266. [PubMed: 9933036]

13. Drake CG, Doody AD, Mihalyo MA, Huang CT, Kelleher E, Ravi S, Hipkiss EL, Flies DB, Kennedy EP, Long M, McGary PW, Coryell L, Nelson WG, Pardoll DM, Adler AJ. Androgen ablation mitigates tolerance to a prostate/prostate cancer-restricted antigen. Cancer Cell. 2005; 7:239–249. [PubMed: 15766662]

14. Koh YT, Gray A, Higgins SA, Hubby B, Kast WM. Androgen ablation augments prostate cancer vaccine immunogenicity only when applied after immunization. Prostate. 2009

15. Eng MH, Charles LG, Ross BD, Chrisp CE, Pienta KJ, Greenberg NM, Hsu CX, Sanda MG. Early castration reduces prostatic carcinogenesis in transgenic mice. Urology. 1999; 54:1112–1119. [PubMed: 10604719]

16. Isaacs JT, Furuya Y, Berges R. The role of androgen in the regulation of programmed cell death/apoptosis in normal and malignant prostatic tissue. Semin Cancer Biol. 1994; 5:391–400. [PubMed: 7849267]

17. Feldman BJ, Feldman D. The development of androgen-independent prostate cancer. Nat Rev Cancer. 2001; 1:34–45. [PubMed: 11900250]

18. Mercader M, Bodner BK, Moser MT, Kwon PS, Park ES, Manecke RG, Ellis TM, Wojcik EM, Yang D, Flanigan RC, Waters WB, Kast WM, Kwon ED. T cell infiltration of the prostate induced by androgen withdrawal in patients with prostate cancer. Proc Natl Acad Sci U S A. 2001; 98:14565–14570. [PubMed: 11734652]

19. Kwon ED, Hurwitz AA, Foster BA, Madias C, Feldhaus AL, Greenberg NM, Burg MB, Allison JP. Manipulation of T cell costimulatory and inhibitory signals for immunotherapy of prostate cancer. Proc Natl Acad Sci U S A. 1997; 94:8099–8103. [PubMed: 9223321]

20. Roden AC, Moser MT, Tri SD, Mercader M, Kuntz SM, Dong H, Hurwitz AA, McKean DJ, Celis E, Leibovich BC, Allison JP, Kwon ED. Augmentation of T cell levels and responses induced by androgen deprivation. J Immunol. 2004; 173:6098–6108. [PubMed: 15528346]

21. Coles AJ, Thompson S, Cox AL, Curran S, Gurnell EM, Chatterjee VK. Dehydroepiandrosterone replacement in patients with Addison's disease has a bimodal effect on regulatory (CD4+CD25hi and CD4+FoxP3+) T cells. Eur J Immunol. 2005; 35:3694–3703. [PubMed: 16252254]

22. Holzbeierlein J, Lal P, LaTulippe E, Smith A, Satagopan J, Zhang L, Ryan C, Smith S, Scher H, Scardino P, Reuter V, Gerald WL. Gene expression analysis of human prostate carcinoma during hormonal therapy identifies androgen-responsive genes and mechanisms of therapy resistance. Am J Pathol. 2004; 164:217–227. [PubMed: 14695335]

23. Terasawa H, Tsang KY, Gulley J, Arlen P, Schlom J. Identification and characterization of a human agonist cytotoxic T-lymphocyte epitope of human prostate-specific antigen. Clin Cancer Res. 2002; 8:41–53. [PubMed: 11801539]

24. Mylin LM, Deckhut AM, Bonneau RH, Kierstead TD, Tevethia MJ, Simmons DT, Tevethi SS. Cytotoxic T lymphocyte escape variants, induced mutations, and synthetic peptides define a dominant H-2Kb-restricted determinant in simian virus 40 tumor antigen. Virology. 1995; 208:159–172. [PubMed: 11831696]

25. Mylin LM, Bonneau RH, Lippolis JD, Tevethia SS. Hierarchy among multiple H-2b-restricted cytotoxic T-lymphocyte epitopes within simian virus 40 T antigen. J Virol. 1995; 69:6665–6677. [PubMed: 7474076]

26. Tseng-Rogenski SS, Arredouani MS, Escara-Wilke JF, Neeley YC, Imperiale MJ, Sanda MG. A safety-modified SV40 Tag developed for human cancer immunotherapy. Drug Design, Development and Therapy. 2008; 2:17–24.

27. Tseng-Rogenski SS, Arredouani MS, Neeley YC, Lu B, Chinnaiyan AM, Sanda MG. Fas-mediated T cell deletion potentiates tumor antigen-specific tolerance in a mouse model of prostate cancer. Cancer Immunol Immunother. 2008

28. Xie YC, Hwang C, Overwijk W, Zeng Z, Eng MH, Mule JJ, Imperiale MJ, Restifo NP, Sanda MG. Induction of tumor antigen-specific immunity in vivo by a novel vaccinia vector encoding safety-modified simian virus 40 T antigen. Journal of the National Cancer Institute. 1999; 91:169–175. [PubMed: 9923859]

29. Greenberg NM, DeMayo F, Finegold MJ, Medina D, Tilley WD, Aspinall JO, Cunha GR, Donjacour AA, Matusik RJ, Rosen JM. Prostate cancer in a transgenic mouse. Proceedings of the National Academy of Sciences of the United States of America. 1995; 92:3439–3443. [PubMed: 7724580]

30. Hodge JW, Schlom J, Donohue SJ, Tomaszewski JE, Wheeler CW, Levine BS, Gritz L, Panicali D, Kantor JA. A recombinant vaccinia virus expressing human prostate-specific antigen (PSA): safety and immunogenicity in a non-human primate. Int J Cancer. 1995; 63:231–237. [PubMed: 7591210]

31. Greenberg NM, DeMayo FJ, Sheppard PC, Barrios R, Lebovitz R, Finegold M, Angelopoulou R, Dodd JG, Duckworth ML, Rosen JM, et al. The rat probasin gene promoter directs hormonally and developmentally regulated expression of a heterologous gene specifically to the prostate in transgenic mice. Mol Endocrinol. 1994; 8:230–239. [PubMed: 8170479]

32. Tomlins SA, Laxman B, Varambally S, Cao X, Yu J, Helgeson BE, Cao Q, Prensner JR, Rubin MA, Shah RB, Mehra R, Chinnaiyan AM. Role of the TMPRSS2-ERG gene fusion in prostate cancer. Neoplasia. 2008; 10:177–188. [PubMed: 18283340]

33. Carver BS, Tran J, Chen Z, Varmeh S, Carracedo-Perez A, Alimonti A, Nardella C, Gopalan A, Scardino PT, Cordon-Cardo C, Gerald w. Pandolfi PP. ETS genetic rearrangements are progression events in prostate tumorigenesis. Nature (submitted). 2008
34. Kim JJ, Trivedi NN, Wilson DM, Mahalingam S, Morrison L, Tsai A, Chattergoon MA, Dang K, Patel M, Ahn L, Boyer JD, Chalian AA, Schoemaker H, Kieber-Emmons T, Agadjanyan MA, Weiner DB. Molecular and immunological analysis of genetic prostate specific antigen (PSA) vaccine. Oncogene. 1998; 17:3125–3135. [PubMed: 9872328]
35. Correale P, Walmsley K, Nieroda C, Zaremba S, Zhu M, Schlom J, Tsang KY. In vitro generation of human cytotoxic T lymphocytes specific for peptides derived from prostate-specific antigen. J Natl Cancer Inst. 1997; 89:293–300. [PubMed: 9048833]
36. Barrou B, Benoit G, Ouldkaci M, Cussenot O, Salcedo M, Agrawal S, Massicard S, Bercovici N, Ericson ML, Thiounn N. Vaccination of prostatectomized prostate cancer patients in biochemical relapse, with autologous dendritic cells pulsed with recombinant human PSA. Cancer Immunol Immunother. 2004; 53:453–460. [PubMed: 14760510]
37. Arlen PM, Gulley JL, Parker C, Skarupa L, Pazdur M, Panicali D, Beetham P, Tsang KY, Grosenbach DW, Feldman J, Steinberg SM, Jones E, Chen C, Marte J, Schlom J, Dahut W. A randomized phase II study of concurrent docetaxel plus vaccine versus vaccine alone in metastatic androgen-independent prostate cancer. Clin Cancer Res. 2006; 12:1260–1269. [PubMed: 16489082]
38. Heiser A, Coleman D, Dannull J, Yancey D, Maurice MA, Lallas CD, Dahm P, Niedzwiecki D, Gilboa E, Vieweg J. Autologous dendritic cells transfected with prostate-specific antigen RNA stimulate CTL responses against metastatic prostate tumors. J Clin Invest. 2002; 109:409–417. [PubMed: 11828001]
39. Marshall DJ, San Mateo LR, Rudnick KA, McCarthy SG, Harris MC, McCauley C, Schantz A, Geng D, Cawood P, Snyder LA. Induction of Th1-type immunity and tumor protection with a prostate-specific antigen DNA vaccine. Cancer Immunol Immunother. 2005; 54:1082–1094. [PubMed: 16047142]
40. Roos AK, Pavlenko M, Charo J, Egevad L, Pisa P. Induction of PSA-specific CTLs and anti-tumor immunity by a genetic prostate cancer vaccine. Prostate. 2005; 62:217–223. [PubMed: 15389792]
41. Wallecha A, Maciag PC, Rivera S, Paterson Y, Shahabi V. Construction and characterization of an attenuated Listeria monocytogenes strain for clinical use in cancer immunotherapy. Clin Vaccine Immunol. 2009; 16:96–103. [PubMed: 19020110]
42. Langer LF, Clay TM, Morse MA. Update on anti-CTLA-4 antibodies in clinical trials. Expert Opin Biol Ther. 2007; 7:1245–1256. [PubMed: 17696822]

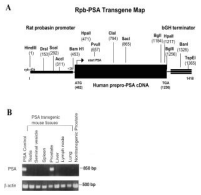

Figure 1. Generation of Rat probasin-regulated PSA transgenic mice

(A) schematic map of the rpb-PSA transgene shows unique restriction enzyme sites. The transgene map was generated by sequencing PCR products using primer pairs that span the boundaries between the rat probasin (rpb) promoter, the PSA prepro-cDNA and the bovine growth hormone (bGH) terminator. Restriction map was generated using the BCM Search Launcher WebCutter Search Utility**. (B)** PSA expression in rpb-PSA transgenic mice was confirmed by RT-PCR. RNAs isolated from various tissues show prostate-specific transcription. RT-PCR was performed in the presence or absence (not shown) of Reverse Transcriptase. The amplification of actin transcripts was used as internal control. Only samples isolated from prostate tissues displayed significant amplification of PSA transcripts by RT-PCR.

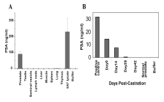

Figure 2. Androgen-regulated, prostate-specific expression of PSA

(A) Prostate lysates from three different mice (P719, P722, P748) showed significant PSA levels as compared to lysates from other tissues/organs or prostate from non-transgenic mice. Tissue PSA levels were determined using PSA-specific ELISA. Data shown as Mean ± SD from 3 animals. **(B)** Expression of the PSA transgene is androgen dependent and tissue levels of the protein decrease with time following surgical castration. PSA mice exhibit high levels of PSA expression and are similar to PSA positive controls. Following castration, prostate levels of PSA fall and at 28 days are similar to non-transgenic mouse prostates. One representative mouse is shown.

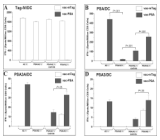

Figure 3. Castration of male PSA/A2.1 mice augments PSA-specific cellular immune responses

Castrated male mice were immunized with either vac-mTag or vac-PSA and antigen-specific CD8 responses were evaluated by ELISPOT and tetramer staining. Non-castrated male mice and female mice were used as controls. For splenocyte restimulation in vitro, bone marrow-derived DC were loaded with either H-2Kb restricted**-,** SV40 Tag-derived epitope IV (Tag-IV/DC) (**A**), with PSA (PSA/DC) (**B**) or with HLA-A2.1-restricted, PSA-derived epitopes (PSA3A/DC) (**C**) and (PSA3/DC) (**D**). IFN-γ-releasing CD8 T cells were revealed using an ELISPOT assay. Data shown as Mean ± SD, representative of one experiment with from 3 animals/group.

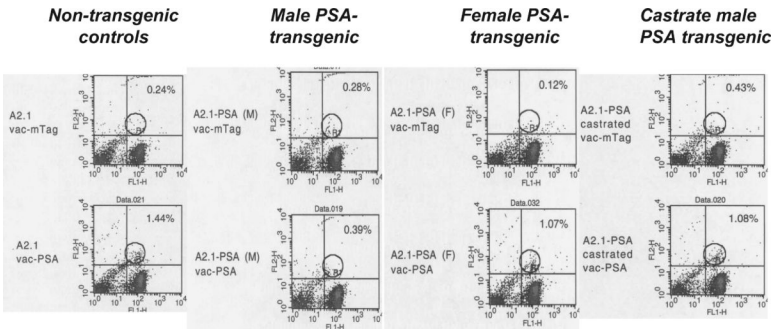

Figure 4. Castration of male PSA/A2.1 mice augments PSA-specific cellular immune responses

PSA-3A-tetramer staining was performed on splenocytes from the same mice as described under Figure **3** to demonstrate the effect of castration on the elevation of **PSA**-specific CTL responses. Representative plots corresponding to mice within the same experiment are shown here.

Clinical Cancer Research

Identification of the Transcription Factor Single-Minded Homologue 2 as a Potential Biomarker and Immunotherapy Target in Prostate Cancer

Mohamed S. Arredouani, Bin Lu, Manoj Bhasin, et al.

Clin Cancer Res 2009;15:5794-5802. Published OnlineFirst September 8, 2009.

Published OnlineFirst September 8, 2009; DOI:10.1158/1078-0432.CCR-09-0911

Identification of the Transcription Factor Single-Minded Homologue 2 as a Potential Biomarker and Immunotherapy Target in Prostate Cancer

Mohamed S. Arredouani,[1] Bin Lu,[1] Manoj Bhasin,[2] Miriam Eljanne,[1] Wen Yue,[1] Juan-Miguel Mosquera,[4] Glenn J. Bubley,[3] Vivian Li,[1] Mark A. Rubin,[4] Towia A. Libermann,[2] and Martin G. Sanda[1]

Abstract

Purpose: Identification of novel biomarkers and immunotherapy targets for prostate cancer (PCa) is crucial to better diagnosis and therapy. We sought to identify novel PCa tumor-associated antigens (TAA) that are expressed in PCa, absent in nonprostate human tissue, and immunogenic for immune responses restricted by human HLA.

Experimental Design and Results: Using microarray analysis of normal and cancerous human prostate tissues, we identified 1,063 genes overexpressed in PCa. After validating 195 transcripts in publicly available array data sets, we interrogated expression of these TAAs in normal human tissues to identify genes that are not expressed at detectable levels in normal, nonprostate adult human tissue. We identified 23 PCa TAA candidates. Real-time PCR confirmed that 15 of these genes were overexpressed in PCa ($P < 0.05$ for each). The most frequently overexpressed gene, *single-minded homologue 2* (*SIM2*), was selected for further evaluation as a potential target for immunotherapy. ELISA assay revealed that a fraction of PCa patients exhibited immune responsiveness to SIM2 as evidenced by the presence of autoantibodies to SIM2 in their sera. We next showed binding of putative HLA-A2.1–restricted SIM2 epitopes to human A2.1, and immunization of transgenic HLA-A2.1 mice showed induction of SIM2-specific CTL responses *in vivo*.

Conclusions: Our findings that SIM2 is selectively expressed in PCa, that human HLA-A2.1–restricted SIM2 epitopes induce specific T cells *in vivo*, and that anti-SIM2 antibodies are detectable in PCa patients' sera implicate SIM2 as a PCa-associated antigen that is a suitable potential target for PCa immunotherapy. (Clin Cancer Res 2009;15(18):5794–802)

Gene expression profiling of prostate cancer (PCa) has proven effective in identifying genes and molecular pathways associated with PCa. Profiling of RNA transcripts has been widely used to dissect molecular aspects of tumor cell biology as well as to project disease outcome that can be of high prognostic value (1–5). For example, the determination by several such array studies that ERG is commonly overexpressed in PCa led to identification of novel gene arrangements between TMPRSS2 and ETS transcription factors in PCa (6). Identifying PCa-associated genes (those with higher levels in PCa than benign prostate) that are concurrently not expressed at abundant levels in normal human adult extraprostatic tissues would potentially identify PCa tumor-associated antigens (TAA) with greater specificity as therapy targets than that of cancer-associated genes identified without consideration of their extraprostatic expression patterns. However, prior genome-wide expression array studies to identify genes that are overexpressed in PCa have usually focused on interrogating

Authors' Affiliations: [1]Division of Urology, Department of Surgery, [2]Genomics Center, and [3]Department of Medicine, Beth Israel Deaconess Medical Center, Harvard Medical School, Boston, Massachusetts and [4]Department of Pathology and Laboratory Medicine, Weill Cornell Medical College, New York, New York

Received 4/10/09; revised 5/18/09; accepted 5/19/09; published OnlineFirst 9/8/09.

Grant support: NIH-National Cancer Institute Early Detection Research Network grant UO1-CA113913 (M.G. Sanda), National Cancer Institute Prostate Specialized Program of Research Excellence Career Development Award (M.S. Arredouani), Prostate Cancer Foundation Young Investigator Award (M.S. Arredouani), and Hershey Family Foundation Prostate Cancer Tissue Bank. Department of Defense New Investigator Award W81XWH-09-1-0448 (M.S. Arredouani), Department of Defense Prostate Cancer Training Award W81XWH-09-1-0626 (B. Lu).

The costs of publication of this article were defrayed in part by the payment of page charges. This article must therefore be hereby marked *advertisement* in accordance with 18 U.S.C. Section 1734 solely to indicate this fact.

Note: Supplementary data for this article are available at Clinical Cancer Research Online (http://clincancerres.aacrjournals.org/).

M.S. Arredouani and B. Lu contributed equally to this work.

Requests for reprints: Martin G. Sanda, Division of Urology, Department of Surgery, Beth Israel Deaconess Medical Center, Harvard Medical School, 330 Brookline Avenue, Rabb 440, Boston, MA 02215. Phone: 617-735-2100; Fax: 617-735-2110; E-mail: msanda@bidmc.harvard.edu.

doi:10.1158/1078-0432.CCR-09-0911

Published OnlineFirst September 8, 2009; DOI:10.1158/1078-0432.CCR-09-0911

Translational Relevance

We sought to identify novel targets for prostate cancer (PCa) detection and therapy. Toward this objective, we used fresh-frozen prostatectomy specimens to generate new PCa gene expression arrays and interrogated the expressed gene profile against gene expression of normal human adult tissue *in silico* to identify genes expressed in PCa but not in nonprostatic normal human tissues. This novel strategy identified 15 genes that are abundant in PCa and not in other adult human male tissue. Proof of principle that these are rational targets for PCa detection or therapy was shown for the transcription factor single-minded homologue 2 (SIM2), for which we showed that some PCa patients have intrinsic immune response as evidenced by autoantibodies to SIM2 in patient sera and that human HLA-A2.1–restricted, cytotoxic T-cell responses can be induced against SIM2 epitopes *in vivo* in HLA-A2.1 transgenic mice. Our findings identify peptide epitopes of SIM2 that may serve as PCa immunotherapy targets in future clinical trials.

relative levels of gene expression in cancerous prostate tissue compared with normal prostate tissue, and the relationship of prostatic gene expression to expression of such genes in adult tissues outside of the prostate has previously only been explored with genes expressed in normal prostate and not PCa (7).

One approach for translating newly discovered TAAs to a new direction for cancer therapy is to interrogate newly discovered TAA sequences for immunogenic peptide sequences that are predicted to bind human class I MHC and that are therefore putative targets for T-cell–mediated immunotherapy (8). However, such a strategy for identifying putative targets for PCa immunotherapy has not yet been linked directly to the interrogation of prostate TAAs discovered through concurrent interrogation of cancer and normal human tissue expression arrays. Instead, recent clinical trials of PCa immunotherapy have targeted PCa TAAs that had been identified before the era of genome-wide gene expression profiling. Limitations of this "first generation" of prostate TAA targets for immunotherapy have included limited cancer specificity of the target [as in prostate-specific antigen (PSA)] or limited tissue specificity [as with prostate-specific membrane antigen (PSMA) or prostate stem cell antigen (PSCA)], but despite these limitations, reduction of tumor activity has been observed in several PCa immunotherapy studies, and modest survival benefit was noted in two such trials (9, 10). The targeting of immunogenic peptides in PCa TAA identified from genome-wide expression profiling is an untested but promising direction for improving on the early foundations of PCa immunotherapy.

We sought to identify such immunogenic peptide targets (for immunotherapy) first by interrogating new PCa and normal prostate expression arrays against existing human expression arrays to identify PCa-specific TAA, then by ascertaining the immunogenicity of the TAA target through detecting autoantibody responses in PCa patients, next by evaluating binding to human HLA-A2.1 of potentially immunogenic peptide sequences from the lead TAA, and finally by ascertaining the ability of these epitopes to induce cellular immune responses in HLA-A2.1 transgenic mice.

Materials and Methods

Animals

The HHD mice were received from Dr. Francois Lemonnier (Unite d'Immunite Cellulaire Antivirale, Institut Pasteur, Paris, France). These mice are $\beta_2m^{-/-}$, $D^{b-/-}$ double knockout and express an HLA-A*0201 monochain composed of a chimeric heavy chain ($\alpha1$ and $\alpha2$ domains of HLA-A*0201 allele and the $\alpha3$ and intracellular domains of D^b allele) linked by its NH_2 terminus to the COOH terminus of the human β_2m by a 15–amino acid peptide arm (11). Mice were housed in pathogen-free conditions, and all experimental procedures involving animals were approved by the Institutional Animal Care and Use Committee at Beth Israel Deaconess Medical Center.

Cell lines

The human TAP-deficient T2 cell line was purchased from the American Type Culture Collection and cultured as per the American Type Culture Collection's protocol.

Peptides

All peptides used in this study were purchased from the Biopolymers Laboratory at Harvard Medical School. Peptides were >90% pure and high-performance liquid chromatography tested. Peptides were dissolved in DMSO and stored in aliquots at -20°C until use.

Sample selection and RNA purification. Radical prostatectomy tissue samples were obtained from the Hershey Foundation Prostate Cancer Serum and Tumor Bank at our institution. Morphologic diagnosis was done by a pathologist. OCT blocks containing >30% of PCa tissue (with Gleason score of 6 or 7) were selected for RNA purification. A biopsy punch was used to select the PCa tissues from the OCT sample blocks. Benign or PCa tissues were homogenized using a TissueLyser (Qiagen) at 28 Hz for 5 min. Total RNA was isolated using Trizol reagent. RNA was quantified by NanoDrop ND-1000 spectrophotometer, and quality was evaluated with Agilent RNA 6000 NanoChip and the 2100 Bioanalyzer, with 28S/18S ratios and RIN determined by 2100 Expert software.

Gene expression microarrays and analysis

Total RNA (250 ng) was amplified using Ambion MessageAmp II mRNA Amplification kit. Biotin-UTP was incorporated during the overnight *in vitro* transcription step according to the manufacturer's protocol. Gene expression was assessed using Affymetrix GeneChip U133 array (Plus 2.0 chip) consisting of >52,000 transcripts from whole human genome transcripts. cRNA (15 μg) was fragmented and hybridized to arrays according to the manufacturer's protocols. The quality of scanned array images was determined based on background values, percent present calls, scaling factors, and 3′-5′ ratio of β-actin and glyceraldehyde-3-phosphate dehydrogenase (GAPDH) using the BioConductor R packages. The signal value for each transcript was summarized using perfect matched only–based signal modeling algorithm described in dchip. The perfect matched only–based modeling algorithm yields less number of false positives compared with the perfect matched-mismatched model. In this way, the signal value corresponds to the absolute level of expression of a transcript (12). These normalized and modeled signal values for each transcript were used for further high-level bioinformatic analysis. During the calculation of model-based expression signal values, array and probe outliers are interrogated and image spikes are treated as signal outliers. The outlier detection was carried out using dchip outlier detection algorithm. A chip is considered as an outlier if the probe, single, or array outlier percentage exceeds a default threshold of 5%. When comparing two groups of samples to identify genes enriched in a given phenotype, if 90% lower confidence bound (LCB) of the fold change

Published OnlineFirst September 8, 2009; DOI:10.1158/1078-0432.CCR-09-0911

Table 1. Validation of 15 novel prostate TAAs by qRT-PCR

Gene accession number	Gene name	Primer sequences (5′→3′)	*P* (*t* test)
AMACR (NM_014324)	α-Methylacyl-CoA racemase	F: ttatgtgtgcactgggcatt R: tggggttctattgctccaac	0.0196
BICD1 (NM_001714)	Bicaudal D homologue 1	F: aggcaaacttggaaagagca R: gtaggaagcccctgaagtcc	0.035
C10orf137 (NM_015608)	Chromosome 10 open reading frame 137	F: agacccagttgtgcatttcc R: ttttaacgggattggagtgc	0.013
CDC2L6 (NM_015076)	Cell division cycle 2–like 6	F: agaacagcacccagaccaac R: acaggtccacctgagtttgc	0.0065
ICA1 (NM_022307)	Islet cell autoantigen 1	F: tctcctgcctacatcccatc R: tccagagctcactggaaggt	0.0138
KIAA1661 (AB051448)	KIAA1661 protein	F: cgctcagttagggcagtttc R: tgggaccaaaggcatagaag	0.05
MAP7 (NM_003980)	Microtubule-associated protein 7	F: gtgtttggcacacaggacac R: aaaacatgtgcaccctctcc	0.03
MYO6 (NM_004999)	Myosin VI	F: aatcactggctcacatgcag R: agtgtgcccaccttaaccag	0.01
OR51E2 (NM_030774)	Olfactory receptor, family 51, subfamily E, member 2	F: tacgaacggttctgcaactg R: aggcagcagcaggtagatgt	0.005
PAICS (NM_006452)	Phosphoribosylaminoimidazole carboxylase	F: ctggggagttcaggatgtgt R: cagcctgcttcaaggaaatc	0.003
PCSK6 (NM_002570)	Proprotein convertase subtilisin/kexin type 6	F: gccaaacctgtgtaggcatt R: gggttctctccagctcacag	0.0045
PVT1 (NR_003367)	Pvt1 oncogene (nonprotein coding)	F: ggaggctgaggagttcactg R: ggggcagagatgaaatcgta	0.01
RGS10 (NM_002925)	Regulator of G protein signaling 10	F: tctcggctcaacgagaagat R: cagtttgagcatcaggcaaa	0.02
SGEF (NM_015595)	Src homology 3 domain-containing guanine nucleotide exchange factor	F: agagaatgggacgcttgcta R: tggcaagcttaaaggcaagt	0.0082
SIM2 (NM_005069)	Single-minded homologue 2	F: cttccctctggactctcacg R: aggctgtgcctagcagtgtt	0.004

NOTE: qRT-PCR validation of mRNA expression levels of individual genes (AMACR, BICD1, C10orf137, CDC2L6, ICA1, KIAA1661, MAP7, MYO6, OR51E2, PAICS, PCSK6, PVT1, RGS10, SGEF, and SIM2) was done using the Taqman gene expression assay. From a total of 23 genes tested, only the 15 genes that were significantly overexpressed ($P < 0.05$) in 7 PCa compared with 8 normal prostate specimens are shown. Statistical analysis showed that these genes are overexpressed in PCa over normal prostate tissue.

between the two groups was above 1.2, the corresponding gene was considered to be differentially expressed. LCB is a stringent estimate of fold change and is the better ranking statistic. It has been suggested that a criterion of selecting genes that have a LCB above 1.2 most likely corresponds to genes with an "actual" fold change of at least 2 in gene expression (13).

Analysis of the Stanford prostate data. The raw gene expression data from 62 PCa and 41 normal prostate published by Lapointe et al. (3) were obtained from the BRB-Array archived data sets. The preprocessed data were normalized using the Z transformation (M1, ONCOMINE: a cancer microarray database and integrated data-mining platform). The differentially expressed genes were identified based on fold change (>0.5) and Q value of <0.05. The analysis identified 510 genes that are differentially expressed.

Biomarker analysis. To prioritize the biomarker and immunotherapy targets, we need to identify the genes that are not ubiquitously expressed in all normal tissues. The gene expression data for the various human normal tissues were obtained from gene expression atlas of the Genomics Institute of the Novartis Research Foundation.[5] Using this database, MAS5 normalized expression data along with present (P), absent (A), and marginal (M) calls for each transcript were obtained. Based on present and absent calls for each transcript, a priority value is calculated (Eq. A). The gene that is absent in all tissues was given highest priority (rank 1), and the gene that is present in all of tissues is given a least priority. In other words, number of present and absent calls in different tissues was used to find out the genes having restrictive expression level. To further extend the list of genes, we have also obtained a list of prostate-specific genes by analyzing the Novartis gene expression data (1). The genes that are annotated absent based on MAS5 calls in all the normal tissues except prostate were considered as prostate-specific genes.

$$\text{Priority value} = X^{j}_{i}\,(\text{Pp} + \text{A} + \text{M})$$

where Pp is present calls in prostate tissues and i to j are rest of normal tissues except prostate

Quantitative real-time PCR

Validation of overexpression of the selected prostate TAAs in seven PCa tumor and eight control tissue specimens was done by quantitative real-time PCR (qRT-PCR). High-quality RNA samples (50 ng; RIN > 6.0 by Agilent 2100 Bioanalyzer) were reverse transcribed to first-strand cDNA and 1 μL cDNA was used for each well RT-PCR. Samples were done in triplicates. SYBR Green PCR Master Mix (Applied Biosystems) was used for two-step RT-PCR analysis on SA Biosciences 7900HT Prism instrument. PCR primer sequences for targeted genes are shown in Table 1. The sequences for GAPDH are 5′-TGCACCACCAACTGCTTAGC-3′ (forward) and 5′-GGCATGGACTGTGGTCATGAG-3′ (reverse). Expression value of the targeted gene in a given sample was normalized to the corresponding expression of GAPDH. The $2^{-\Delta\Delta Ct}$ method was used to calculate relative expression of the targeted genes (14).

[5] http://symatlas.gnf.org

Published OnlineFirst September 8, 2009; DOI:10.1158/1078-0432.CCR-09-0911

Detection of autoantibodies to single-minded homologue 2 in sera from PCa patients

Patients and sera. Serum samples were collected at Harvard University and University of Michigan patient accrual sites. All patients were over the age of 40 y and were seen at the clinic because of PSA value exceeding 2.5 ng/mL, abnormal digital rectal exam, rising PSA, or lower PSA with risk factors such as family history. The study also includes men who have had previous biopsies that have not been positive for cancer. After enrollment and blood collection, all patients get a prostate biopsy to determine the presence or absence of cancer.

Cloning and in vitro *cell-free expression of single-minded homologue 2.* Full-length human single-minded homologue 2 (SIM2) cDNA in a pCR-BLUNT2-topo plasmid was amplified using two rounds of PCR. The PCR product was cloned into pDONR plasmid to produce entry clones of each cDNA. Entry clones (130 ng) were used to produce expression clones using pCITE-glutathione *S*-transferase (GST) expression vector (130 ng), LR clonase II enzyme mix (2 μL), and TE with a total volume of 10 μL. The SIM2 protein was produced as GST recombinant proteins with GST at the COOH terminus. A GST control vector from which only GST is expressed served as a negative control for serum antibody binding. The Kozak sequence was introduced into the original pDEST15 5′ of GST so that it can be used in the mammalian cell-free system.

Detection of serum autoanti-SIM2 antibodies by ELISA. GST precoated ELISA plates (GE Biosciences) were blocked overnight with 5% milk and 0.2% Tween 20. The SIM2 protein was expressed using rabbit reticulocyte lysate cell-free expression system (Promega) according to the manufacturer's instructions. The expressed protein was transferred to the ELISA plate and bound overnight at 4°C. The plates were washed and incubated with serum diluted 1:300 in blocking buffer for 1 h followed by incubation for 1 h with horseradish peroxidase–linked anti-human antibodies. The substrate (100 μL; SuperSignal ELISA Femto Maximum Sensitivity Substrate, Pierce) was added to each well, and the luminescence signal was read using Victor3 ELISA reader. Each serum sample was screened in duplicates. The plate also included a secondary antibody negative control and a GST control.

Prediction of HLA-A2.1–restricted epitopes from SIM2

To predict potential nonamer epitopes that bind HLA-A*0201, the most frequent haplotype in Caucasians, SIM2 protein sequence (SIM2_HUMAN, Q14190) was processed using BIMAS[6] and SYFPEITHI[7] as well as MHCPred,[8] RankPep,[9] NetMHC,[10] PREDEP,[11] ProPred-I,[12] and MAPPP.[13] Only epitopes that were predicted by most algorithms were selected for further testing.

Measurement of peptide/HLA-A*0201 binding and stability

MHC stabilization assay using T2 cells was used to assess binding of peptides to the HLA-A2.1 complex. Briefly, T2 cells were cultured for 6 h in serum-free Iscove's modified Dulbecco's medium (American Type Culture Collection) before the addition of candidate peptides at a concentration of 50 μg/250 × 10^3 cells/mL and further overnight incubation at 37°C. Cells were washed and surface HLA-A2.1 molecules were stained with FITC mouse anti-human HLA-A2 monoclonal antibody (mAb; clone BB7.2, mouse IgG2b κ; BD Pharmingen) for 1 h at 4°C. Cells were then washed thrice with PBS and analyzed by flow cytometry. A negative control (15) peptide (NEG) and the Flu matrix peptide M1 binder peptide (16) served as controls. The relative binding affinity of a given peptide was calculated as $MFI_{(peptide)}/MFI_{(negative\ peptide)}$. Only relative binding affinities of 1.5 or higher were considered for further testing.

T2 cells were incubated overnight with 50 μg/mL of each candidate peptide at 37°C in serum-free Iscove's modified Dulbecco's medium. Cells were then incubated with brefeldin A (Sigma) at 10 μg/mL for 1 h, washed, and incubated at 37°C for 0, 2, 4, or 6 h in the presence of brefeldin A (50 ng/mL). Cells were then stained with BB7.2 mAb. For each time point, peptide-induced HLA-A*0201 expression was calculated as follows: mean fluorescence of peptide-loaded T2 cells - mean fluorescence of negative peptide-loaded T2 cells. The rate of dissociation is reflected by the loss of A2.1 expression over time.

Generation of SIM2-specific CTL in HHD mice

Ten- to 12-wk-old male HHD mice were injected s.c. at the basis of the tail with 100 μg of each candidate peptide emulsified in 50 μL of incomplete Freund's adjuvant and 50 μL PBS in the presence of 150 μg of the I-A^b–restricted $HBVcore_{128-140}$ T helper epitope (TPPAYRPPNAPIL; ref. 17). Ten to 12 d after immunization, spleens were harvested and splenocytes were tested for peptide-induced specific release of IFN-γ by enzyme-linked immunospot (ELISPOT).

ELISPOT assay

Ninety-six–well Millipore Immobilon-P plates were coated with 100 μL/well mouse IFN-γ–specific capture mAb (AN18; Mabtech, Inc.) at a concentration of 10 μg/mL in PBS overnight at 4°C. Wells were washed with PBS and saturated with RPMI 1640/10% FCS for 1 h at 37°C. A total of 2.5 × 10^5 splenocytes were seeded in each well in four replicates, and 5 × 10^4 peptide-loaded (10 μg peptide/mL, for 2 h at 37°C) splenocytes pretreated with 50 μg/mL mitomycin C for 1 h were added to each well. Plates were incubated for 1 to 2 d at 37°C in 5% CO_2, washed five times with PBS, and then incubated with 1 μg/mL of biotinylated rat anti-mouse IFN-γ mAb (R4-6A2; Mabtech) for 24 h at 4°C or at room temperature for 2 h. The wells were washed and 100 μL of diluted alkaline phosphatase–conjugated streptavidin were added for 1 h at room temperature.

Spots were developed by adding peroxidase substrates (5-bromo-4,3-indolyl phosphate and nitroblue tetrazolium) and counted using the ELR04 AID EliSpot Reader System (Autoimmun Diagnostika GmbH).

Statistical analysis

Gene expression array data were analyzed as described in Materials and Methods. Group differences for gene expression (RT-PCR), autoantibody (ELISA), and IFN-γ (ELISPOT) data were analyzed using the Student's *t* test. *P* values of ≤0.05 were considered significant.

Results

Identification of novel prostate TAAs using gene expression profiling. In an effort to identify novel putative PCa TAAs with expression specificity for PCa over normal prostate or normal nonprostate tissue, we did a genome-wide gene expression analysis of a PCa and normal prostate microarray generated in our laboratory; validated the candidate TAAs in an external, published PCa tissue array data set; and then excluded those with detectable expression in nonprostatic adult tissues (Fig. 1). First, we used the Affymetrix U133 array (Plus 2.0 chip) to evaluate gene expression in cancer and normal fresh-frozen prostate tissue specimens from our tissue repository. The class comparison analysis based on LCB(1.2) and mean difference in absolute intensity of >40 identified 1,063 genes overexpressed in PCa compared with normal prostate. The heat map of top 100 genes is shown in Fig. 1A. Examples of the top 100 genes include *AMACR*, *ERG*, *MMP26*, *THBS4*, and *FOXD1* (Supplementary Table S1). Next, we validated the 1,063 putative TAA and conducted a comprehensive

[6] http://www-bimas.cit.nih.gov/molbio/hla_bind/
[7] http://www.syfpeithi.de/
[8] http://www.jenner.ac.uk/MHCPred/
[9] http://bio.dfci.harvard.edu/Tools/rankpep.html
[10] http://www.cbs.dtu.dk/services/NetMHC/
[11] http://margalit.huji.ac.il/Teppred/mhc-bind/index.html
[12] http://www.imtech.res.in/raghava/propred1/
[13] http://www.mpiib-berlin.mpg.de/MAPPP/binding.html

Published OnlineFirst September 8, 2009; DOI:10.1158/1078-0432.CCR-09-0911

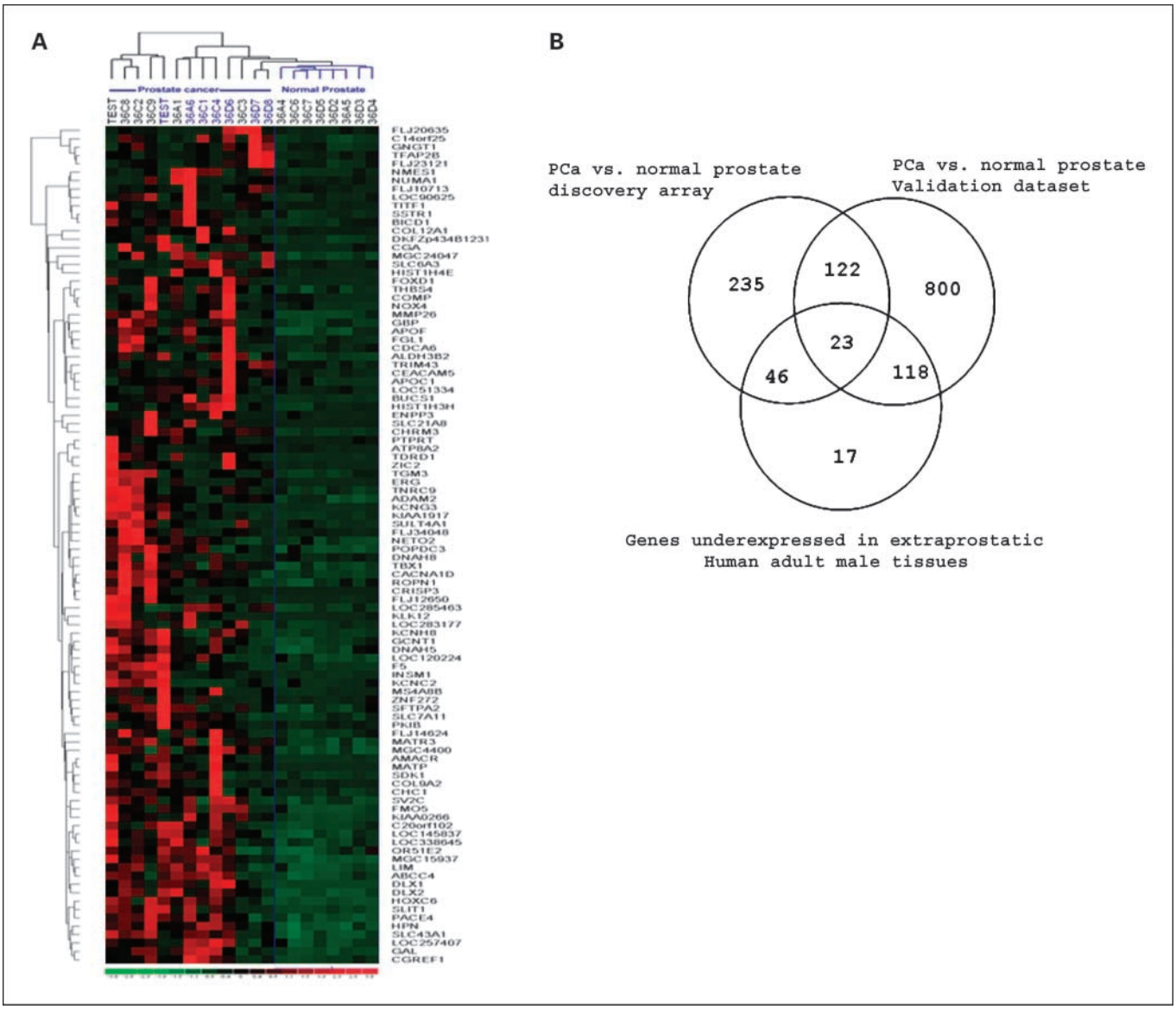

Fig. 1. Identification of novel putative prostate TAAs by gene expression profiling. *A,* hierarchical clustering analysis of 14 PCa tumor samples and 8 normal prostate samples. Top 100 genes that are overexpressed in PCa compared with normal. *B,* Venn diagram highlighting the genes overexpressed in PCa in our data set and in the Stanford data set and those underexpressed in extraprostatic human adult male tissues as deduced from the Novartis gene expression atlas.

analysis of microarray data from a previously published data set, which included 41 normal and 62 neoplastic prostate tissues (3). We looked at the genes that are significantly overexpressed in PCa for their potential to be used as biomarkers or targets for immunotherapy. A list of 426 PCa up-regulated genes was obtained based on the fold change (>0.5) and false discovery rate value of <0.05 after preprocessing and normalizing data (Z transformation). Validation of genes that were overexpressed in PCa in our data set by comparison with the Stanford PCa array data set implicated 195 transcripts with concordant overexpression between the array data sets. To identify PCa TAA with the greatest specificity for PCa, we then sought to exclude, by *in silico* analysis, those genes that are detectable in nonprostate normal human adult male tissues. For this purpose, gene expression data for various human tissues were obtained from the two studies conducted by Su et al. (18) and Ge et al. (19), and genes that were annotated absent based on MAS5 calls in all the normal tissues except prostate were considered as prostate-specific genes. The comprehensive analysis led the identification of 26 transcripts that are overexpressed in the PCa and are highly tissue restricted (Fig. 1B). These transcripts correspond to 23 genes (listed in Supplementary Table S2) that include *SIM2*. The analysis also identified 17 more genes that are present in the prostate and absent in the rest of the normal tissues (Supplementary Table S3).

We then did qRT-PCR targeting each of the 23 candidate antigens and confirmed that 15 (AMACR, BICD1, C10orf137, CDC2L6, ICA1, KIAA1661, MAP7, MYO6, OR51E2, PAICS, PCSK6, PVT1, RGS10, SGEF, and SIM2) were overexpressed in PCa (Table 1; Supplementary Fig. S1). Frequency of overexpression in PCa for these antigens ranged from 57% to 86%. From among these 15 PCa-specific antigens that were validated by

Published OnlineFirst September 8, 2009; DOI:10.1158/1078-0432.CCR-09-0911

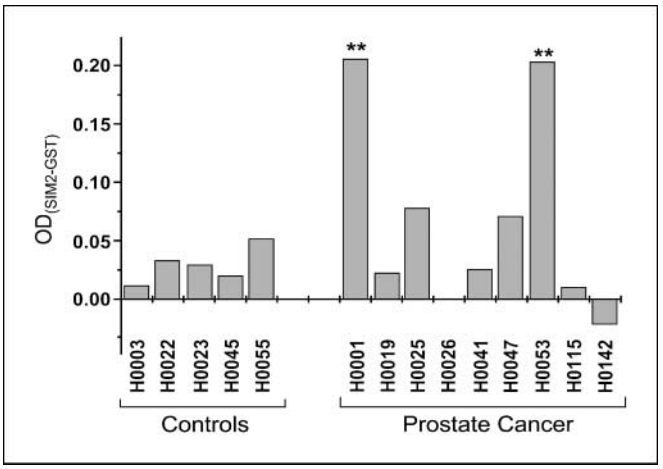

Fig. 2. SIM2 elicits spontaneous humoral responses in PCa patients. Sera from nine PCa patients and five healthy donors were subjected to an *in vitro*, cell-free protein expression–based ELISA to detect autoantibodies to SIM2. SIM2 was expressed as a GST-tagged protein and an anti–GST-coated plate was used in the assay. Serum antibodies that bound to immobilized SIM2 were detected using a labeled anti-human antibody. In each assay, wells containing a GST-expressing vector were used as a negative control. Signals obtained from GST wells were subtracted from those obtained from wells that contained GST-SIM2. Three experiments were done, with triplicate wells for each serum sample per experiment. Statistics were done in triplicate, and antibody amounts are plotted as the difference of absorbance (*OD*) signals produced by GST-SIM2 and GST alone. Columns, mean; **, $P < 0.01$.

qRT-PCR, we selected the gene that was most consistently absent in normal prostate and had the highest frequency of expression in PCa (Supplementary Fig. S1), *SIM2*, which we found overexpressed in 6 of 7 cancers we tested but not in benign prostate tissue, for further study as a potential PCa-associated antigen and target for immunotherapy. This selection of SIM2 is also supported by a previous work that reported up-regulation of SIM2 expression in PCa (20).

SIM2 induces spontaneous humoral responses in PCa patients. There is accumulating evidence suggesting that the immune system is able to mount aberrant immune responses against self-antigens expressed by tumor cells in various cancers (21, 22). The presence of autoantibodies against specific self-antigens has been found to correlate with clinical responses to immunotherapy in human cancer (23, 24). On this basis, antigens triggering autoantibodies may be suitable targets for active immunotherapy treatment strategies. Numerous tumor antigens that are currently targeted for therapy have been identified through detection of the patient's own anti-TAA antibodies (25, 26) or T cells (22, 27). To test whether sera from healthy individuals and PCa patients harbor antibodies to SIM2, we used an ELISA system with *in vitro* expressed GST-tagged SIM2 for capture. This ELISA is single-antigen adaptation of the nucleic acid programmable protein array, which consists of cDNA vectors coupled with a capture antibody, and could be advantageous over traditional protein arrays in that proteins do not have to be purified. Significant levels of autoantibody from patient sera with specific binding to SIM2 ($P < 0.01$) were detected in two of five evaluated PCa samples. In contrast, autoantibodies to SIM2 were not detectable in any of the nine control patients' sera (Fig. 2).

Identification of SIM2-derived, HLA-A2.1–restricted CTL epitopes. Prompted by the stringent specific expression of SIM2 in healthy adult tissues, its overexpression in PCa, and its ability to induce humoral responses in PCa patients, we sought to identify potential HLA-A2.1–restricted, SIM2-derived epitopes that could be used as vaccines to generate SIM2-specific cytotoxic lymphocytes directed against prostate tumors.

To predict potential SIM2-derived, HLA-A*0201–binding epitopes, SIM2 full protein sequence was screened using the eight algorithms. Out of all possible nonamer motifs, 15 epitopes that had the highest cumulative prediction scores were selected for further evaluation *in vitro* and *in vivo* (Table 2).

After predictions were done, we ascertained epitope homology between mouse and human to ensure that we are testing tolerant motifs relevant in both hosts. A BLAST sequence analysis revealed that these five human immunogenic epitopes are 100% identical to their corresponding murine orthologs and are not present in any other known protein sequences in humans or mice, with the exception of SIM2(241), which is also present in SIM1.

Binding to HLA-A2.1 molecules was assessed using T2 assembly assay, which is based on the ability to stabilize MHC class I molecules from the T2 cell line by the addition of suitable peptides. This peptide-HLA binding screen revealed nine SIM2 peptides that were able to stabilize HLA-A2.1 molecules, resulting in increased detection of surface A2.1 molecules with a specific mAb (Fig. 3A). Peptide-HLA dissociation rate correlated with time and showed weak stabilizing epitopes (epitopes 84, 199, 237, and 430) and strong stabilizing epitopes (epitopes 87, 205, 241, and 244). However, epitopes with a high dissociation rate (weak stabilizers) still showed a slight binding that was above the nonbinding control epitope even after 8 hours of incubation.

These nine binding epitopes were then tested for their capacity to elicit *in vivo* CTL responses in transgenic HHD mice. Mice were immunized with a mixture of candidate epitopes and a

Table 2. Identification of SIM2-derived HLA-A2.1–binding epitopes

Epitope	Sequence	SYFPEITHI score	Binding (FI)
SIM2(25)	KLLPLPSAI	25	3.22
SIM2(84)	LLQTLDGFV	23	1.88
SIM2(87)	TLDGFVFVV	27	5.43
SIM2(167)	VLAKRNAGL	26	0.82
SIM2(174)	GLTCSGYKV	23	1.1
SIM2(199)	SLYDSCYQI	23	4.39
SIM2(205)	YQIVGLVAV	23	3.82
SIM2(237)	SLDLKLIFL	27	1.7
SIM2(241)	KLIFLDSRV	23	2
SIM2(244)	FLDSRVTEV	27	4.75
SIM2(339)	ELQLSLEQV	21	1.28
SIM2(430)	LLYTPSYSL	27	2.61
SIM2(527)	GSGLLVGKV	18	0.82
SIM2(530)	LLVGKVGGL	30	0.97
SIM2(558)	SRFGQTCPL	17	0.88
flu-M1	GILGFVFTL	30	3.17
NEG	IAGNSAYEY	9	1

NOTE: Prediction algorithms were used to predict SIM2-derived, HLA-A2.1–binding epitopes. Also shown are peptide scores predicted by the algorithm SYFPEITHI. Binding of predicted peptides to HLA-A2.1 was assessed using the assembly assay on T2 cells *in vitro*. Of the 15 peptides we tested, 9 showed binding ability compared with a nonbinding peptide (NEG).

Published OnlineFirst September 8, 2009; DOI:10.1158/1078-0432.CCR-09-0911

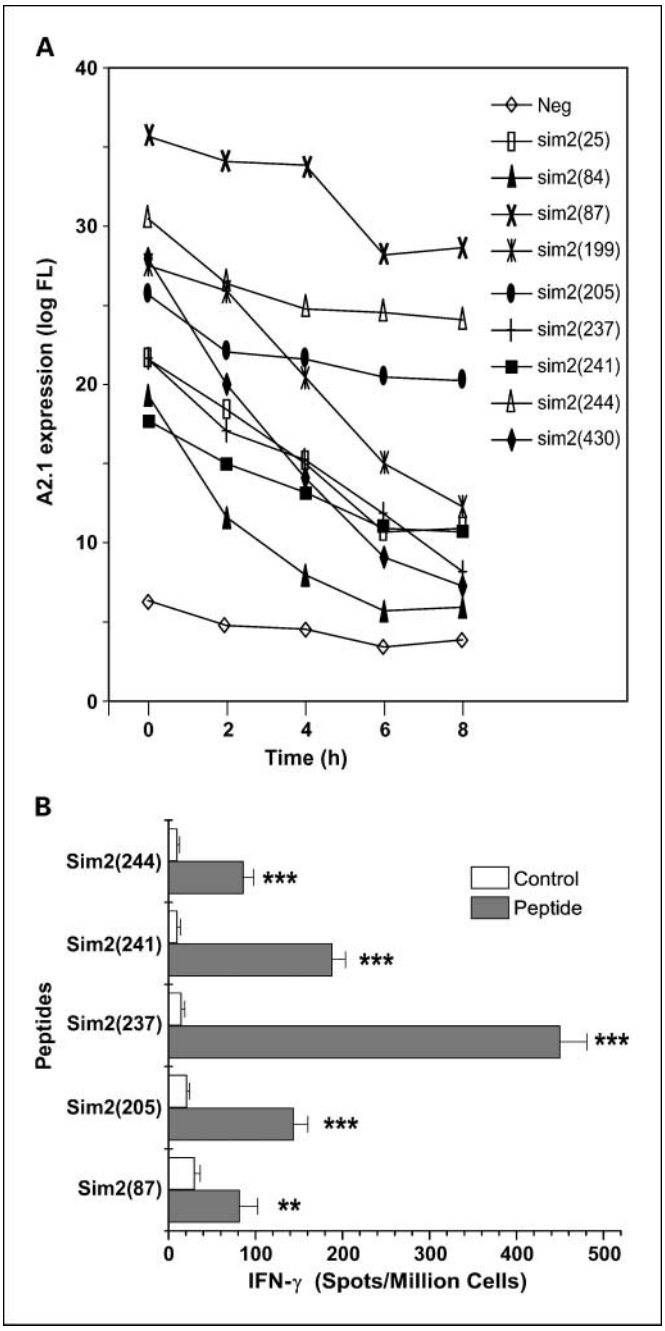

Fig. 3. SIM2 harbors HLA-A2.1–restricted immunogenic epitopes. *A,* the binding to and rate of dissociation of peptides from HLA-A2.1 was determined by monitoring the decrease in HLA-A2.1 expression over time after incubation with binder peptides. *B,* immunization of A2.1 transgenic HHD mice with the nine binding peptides revealed five immunogenic SIM2 peptides as shown by an IFN-γ ELISPOT assay. **, $P < 0.01$; ***, $P < 0.001$.

helper MHC II–restricted peptide, and splenocytes were restimulated 12 days later *in vitro* with peptide-loaded APC and subjected to an IFN-γ ELISPOT assay (Fig. 3B).

We found that *in vitro* restimulation with SIM2(87) (TLDGFVFVV), SIM2(205) (YQIVGLVAV), SIM2(237) (SLDLKLIFL), SIM2(241) (KLIFLDSRV), and SIM2 (244) (FLDSRVTEV) induced significantly [$P < 0.01$ for SIM2(87) and $P < 0.001$ for other epitopes] higher numbers of splenocytes to release IFN-γ in a peptide-specific manner in an ELISPOT assay (Fig. 3B). This provides evidence that tolerance to SIM2 is circumvented through immunization of mice to these epitopes because SIM2 (and SIM1) is also expressed in other nonprostatic tissues in mice. Interestingly, SIM2(25) and SIM2(199) were not immunogenic despite their ability to strongly bind to A2.1.

Discussion

Previous genome-wide expression profiling studies for PCa aimed at identifying genes that are overexpressed in prostate tumors regardless of their levels of gene expression in normal prostate and other adult tissues. The relationship of prostatic gene expression to expression of such genes in nonprostatic tissues has previously only been addressed in normal prostate and not PCa (7).

In the present study, we undertook a multistep strategy that combined gene expression profiling of malignant and benign human prostate tissues and *in silico* analysis of microarray data sets to identify novel prostate TAA. Our analysis focused on antigens that are overexpressed in PCa but are not or are weakly expressed in nonprostatic healthy adult male tissues. This innovative approach is undertaken to minimize the possibility of unwanted collateral autoimmune responses against nonprostate normal tissues and to optimize the possibility of attenuating autoantigen tolerance by prostatic manipulation (e.g., hormonal or ablative). This strategy has led to the identification of 23 potential TAA, among which 15 were validated by qRT-PCR. Whereas 4 of these TAAs [AMACR (28), MYO6 (29), OR51E2 (PSGR; ref. 30), and SIM2 (20)] have been previously reported to be associated with PCa, the remaining 11 (BICD1, C10orf137, CDC2L6, ICA1, KIAA1661, MAP7, PAICS, PCSK6, PVT1, RGS10, and SGEF) have not. These 11 novel TAAs represent a significant addition to the prostate TAA repertoire and warrant further investigation of their implication in PCa cancer biology.

Interestingly, our data revealed the presence of anti-SIM2 autoantibodies in sera from a fraction of PCa patients. It is well documented that PCa patients' immune system can mount antibody responses to prostate TAA (26) as well as to ubiquitous antigens such as the androgen receptor (31) and cellular proteins p90 and p62 (32). The presence of antibodies to TAA in PCa patients' sera is indicative of a humoral immune response against these TAA and results from a well-orchestrated response where an antigen-specific CD4 response is indispensable. This same CD4 response is a prerequisite for the immune system to mount a proper CTL response to a given antigen. In fact, previous studies have shown a close correlation between serum antibodies to TAA and both CD4 and CD8 T-cell responses *in vivo* (33, 34). Therefore, we assumed that a SIM2-derived, MHC I–restricted, peptide-based vaccine would lead to an optimal response in PCa patients.

SIM2 is a member of the basic helix-loop-helix per-Arnt-Sim (bHLH-PAS) family of transcription factors (35). It is mainly known as a contributing factor to Down's syndrome (36). SIM2 expression persists through adulthood in muscle and kidney (37) where its function remains to be elucidated. A prior *in silico* approach using the Cancer Genome Anatomy Project database of the National Cancer Institute identified SIM2 as associated with colon cancer, pancreatic cancer, and PCa, whereas absent in the corresponding normal tissues (38). Both spliced

Published OnlineFirst September 8, 2009; DOI:10.1158/1078-0432.CCR-09-0911

isoforms of SIM2 transcript, SIM2-long and SIM2-short, have been reported to be overexpressed in cancer (38). However, a biological role of SIM2 in cancer has not emerged yet, as it has been attributed suppressive and oncogenic properties that depend on the type of cancer (39, 40).

Vaccines designed to eradicate tumors by triggering immune responses against TAAs represent a tempting therapeutic modality. However, developing successful vaccines is hampered by the lack of highly specific tumor-derived antigens, immune tolerance, and undesired autoimmune responses.

Peptide-based cancer vaccines were among the first defined vaccines showing both protective and therapeutic efficacy in animal models and currently represent the majority of clinical trials of cancer immunotherapy (41, 42). This is attributed to the well-recognized requirement of T lymphocytes, especially CTLs, for the eradication of solid tumors as they represent the primary effector cells involved in tumor-specific immunity. Peptide-based vaccines offer considerable advantages over other vaccine formulations, namely, the absence of infectious material, the easy characterization and purification, the absence of risk of restored virulence or genetic integration, possibility of sequence modification, better storage, and lower cost (reviewed in ref. 41). In PCa, several TAA-derived, HLA-restricted, peptide-based vaccines have been tested clinically (reviewed in ref. 43). Hence, peptides derived from multiple TAAs were administered to hormone-refractory PCa patients and induced increased numbers of specific CD8 T cells (44). Similarly, promising clinical trials were done that tested a vaccine formulation based on dendritic cells loaded with peptides derived from PSMA (45, 46), from hTERT (47), or from a combination of two or more TAAs (PSA, PSMA, survivin, prostein, and trpp8, PAP, and PSCA; refs. 48–50).

Because both SIM2-long and SIM2-short isoforms are expressed in PCa tumors, we processed both protein sequences using various algorithms to predict potential HLA-A2.1–binding nonamer epitopes. Interestingly, all epitopes that were predicted with high scores are common to both isoforms, suggesting that these epitopes could theoretically be used as targets on prostate tumors regardless of the type of isoform they express. We used a panel of 8 prediction algorithms that culminated in a selection of 15 candidate epitopes, among which 9 showed significant binding to A2.1 molecules in the T2 cell assay and 5 of these induced specific *in vivo* CD8 responses in A2.1 transgenic HHD mice as evidenced by their ability to trigger IFN-γ release by CD8 T cells on restimulation. Although prior studies have shown that SIM2 expression can be detected by RT-PCR in some normal tissues such as normal adult kidney, the level of SIM2 expression in such noncancer tissues is apparently low enough such that tolerance to SIM2 can be readily overcome via immunization with class I MHC–restricted SIM2 peptides as we have shown here and below the level of detection of microarray platforms that have been used to catalogue normal human tissue gene expression (18, 19). Accordingly, human trials would need to carefully monitor subjects for possible nephritis or other autoimmune responses. Whether the other 14 putative prostatic TAAs have lower levels of normal tissue expression than SIM2 will require validation assays other than the microarray platform results (18, 19) that we interrogated to identify genes having low or absent expression in nonprostate adult tissue.

Collectively, our data showing overexpression of SIM2 in malignant prostate tissue, combined to the identification of humoral responses to SIM2 in PCa patients' sera and the ability of SIM2-derived peptides to induce HLA-A2.1–restricted cellular immune responses in humanized A2.1 transgenic mice, implicate SIM2 as a potential novel TAA target for PCa immunotherapy.

Disclosure of Potential Conflicts of Interest

M. Sanda received a commercial research grant from Beckman-Coulter.

References

1. Dhanasekaran SM, Barrette TR, Ghosh D, et al. Delineation of prognostic biomarkers in prostate cancer. Nature 2001;412:822–6.
2. Yu YP, Landsittel D, Jing L, et al. Gene expression alterations in prostate cancer predicting tumor aggression and preceding development of malignancy. J Clin Oncol 2004;22:2790–9.
3. Lapointe J, Li C, Higgins JP, et al. Gene expression profiling identifies clinically relevant subtypes of prostate cancer. Proc Natl Acad Sci U S A 2004; 101:811–6.
4. Holzbeierlein J, Lal P, LaTulippe E, et al. Gene expression analysis of human prostate carcinoma during hormonal therapy identifies androgen-responsive genes and mechanisms of therapy resistance. Am J Pathol 2004;164: 217–27.
5. Welsh JB, Sapinoso LM, Su AI, et al. Analysis of gene expression identifies candidate markers and pharmacological targets in prostate cancer. Cancer Res 2001;61:5974–8.
6. Tomlins SA, Rhodes DR, Perner S, et al. Recurrent fusion of TMPRSS2 and ETS transcription factor genes in prostate cancer. Science 2005; 310:644–8.
7. Lin B, Ferguson C, White JT, et al. Prostate-localized and androgen-regulated expression of the membrane-bound serine protease TMPRSS2. Cancer Res 1999;59:4180–4.
8. Stevanovic S. Identification of tumour-associated T-cell epitopes for vaccine development. Nat Rev Cancer 2002;2:514–20.
9. Kaufman HL, Wang W, Manola J, et al. Phase II randomized study of vaccine treatment of advanced prostate cancer (E7897): a trial of the Eastern Cooperative Oncology Group. J Clin Oncol 2004;22:2122–32.
10. Small EJ, Schellhammer PF, Higano CS, et al. Placebo-controlled phase III trial of immunologic therapy with sipuleucel-T (APC8015) in patients with metastatic, asymptomatic hormone refractory prostate cancer. J Clin Oncol 2006; 24:3089–94.
11. Pascolo S, Bervas N, Ure JM, Smith AG, Lemonnier FA, Perarnau B. HLA-A2.1-restricted education and cytolytic activity of CD8(+) T lymphocytes from β2 microglobulin (β2m) HLA-A2.1 monochain transgenic H-2Db β2m double knockout mice. J Exp Med 1997;185:2043–51.
12. Li C, Wong WH. Model-based analysis of oligonucleotide arrays: expression index computation and outlier detection. Proc Natl Acad Sci U S A 2001;98:31–6.
13. Ramalho-Santos M, Yoon S, Matsuzaki Y, Mulligan RC, Melton DA. "Stemness": transcriptional profiling of embryonic and adult stem cells. Science 2002;298:597–600.
14. Haram KM, Peltier HJ, Lu B, et al. Gene expression profile of mouse prostate tumors reveals dysregulations in major biological processes and identifies potential murine targets for preclinical development of human prostate cancer therapy. Prostate 2008;68:1517–30.
15. Bhasin M, Singh H, Raghava GP. MHCBN: a comprehensive database of MHC binding and non-binding peptides. Bioinformatics 2003; 19:665–6.
16. Micheletti F, Monini P, Fortini C, et al. Identification of cytotoxic T lymphocyte epitopes of human herpesvirus 8. Immunology 2002;106:395–403.
17. Firat H, Garcia-Pons F, Tourdot S, et al. H-2 class I knockout, HLA-A2.1-transgenic mice: a versatile animal model for preclinical evaluation of antitumor immunotherapeutic strategies. Eur J Immunol 1999;29:3112–21.
18. Su AI, Wiltshire T, Batalov S, et al. A gene atlas of the mouse and human protein-encoding transcriptomes. Proc Natl Acad Sci U S A 2004;101: 6062–7.
19. Ge X, Yamamoto S, Tsutsumi S, et al. Interpreting expression profiles of cancers by genome-wide survey of breadth of expression in normal tissues. Genomics 2005;86:127–41.
20. Halvorsen OJ, Rostad K, Oyan AM, et al. Increased expression of SIM2-s protein is a novel marker of aggressive prostate cancer. Clin Cancer Res 2007;13:892–7.

Published OnlineFirst September 8, 2009; DOI:10.1158/1078-0432.CCR-09-0911

21. Koziol JA, Zhang JY, Casiano CA, et al. Recursive partitioning as an approach to selection of immune markers for tumor diagnosis. Clin Cancer Res 2003;9:5120–6.

22. Tan EM. Autoantibodies as reporters identifying aberrant cellular mechanisms in tumorigenesis. J Clin Invest 2001;108:1411–5.

23. Sittler T, Zhou J, Park J, et al. Concerted potent humoral immune responses to autoantigens are associated with tumor destruction and favorable clinical outcomes without autoimmunity. Clin Cancer Res 2008;14:3896–905.

24. Homma S, Sagawa Y, Ito M, Ohno T, Toda G. Cancer immunotherapy using dendritic/tumour-fusion vaccine induces elevation of serum anti-nuclear antibody with better clinical responses. Clin Exp Immunol 2006;144:41–7.

25. Miller JC, Zhou H, Kwekel J, et al. Antibody microarray profiling of human prostate cancer sera: antibody screening and identification of potential biomarkers. Proteomics 2003;3:56–63.

26. Wang X, Yu J, Sreekumar A, et al. Autoantibody signatures in prostate cancer. N Engl J Med 2005;353:1224–35.

27. Lee SY, Obata Y, Yoshida M, et al. Immunomic analysis of human sarcoma. Proc Natl Acad Sci U S A 2003;100:2651–6.

28. Rhodes DR, Barrette TR, Rubin MA, Ghosh D, Chinnaiyan AM. Meta-analysis of microarrays: interstudy validation of gene expression profiles reveals pathway dysregulation in prostate cancer. Cancer Res 2002;62:4427–33.

29. Wei S, Dunn TA, Isaacs WB, De Marzo AM, Luo J. GOLPH2 and MYO6: putative prostate cancer markers localized to the Golgi apparatus. Prostate 2008;68:1387–95.

30. Xu LL, Stackhouse BG, Florence K, et al. PSGR, a novel prostate-specific gene with homology to a G protein-coupled receptor, is overexpressed in prostate cancer. Cancer Res 2000;60:6568–72.

31. Olson BM, McNeel DG. Antibody and T-cell responses specific for the androgen receptor in patients with prostate cancer. Prostate 2007;67:1729–39.

32. Shi FD, Zhang JY, Liu D, et al. Preferential humoral immune response in prostate cancer to cellular proteins p90 and p62 in a panel of tumor-associated antigens. Prostate 2005;63:252–8.

33. Jager E, Gnjatic S, Nagata Y, et al. Induction of primary NY-ESO-1 immunity: $CD8^+$ T lymphocyte and antibody responses in peptide-vaccinated patients with NY-ESO-1^+ cancers. Proc Natl Acad Sci U S A 2000;97:12198–203.

34. Jager E, Nagata Y, Gnjatic S, et al. Monitoring CD8 T cell responses to NY-ESO-1: correlation of humoral and cellular immune responses. Proc Natl Acad Sci U S A 2000;97:4760–5.

35. Moffett P, Pelletier J. Different transcriptional properties of mSim-1 and mSim-2. FEBS Lett 2000;466:80–6.

36. Ema M, Ikegami S, Hosoya T, et al. Mild impairment of learning and memory in mice overexpressing the mSim2 gene located on chromosome 16: an animal model of Down's syndrome. Hum Mol Genet 1999;8:1409–15.

37. Woods S, Farrall A, Procko C, Whitelaw ML. The bHLH/Per-Arnt-Sim transcription factor SIM2 regulates muscle transcript myomesin2 via a novel, non-canonical E-box sequence. Nucleic Acids Res 2008;36:3716–27.

38. Deyoung MP, Scheurle D, Damania H, Zylberberg C, Narayanan R. Down's syndrome-associated single minded gene as a novel tumor marker. Anticancer Res 2002;22:3149–57.

39. Kwak HI, Gustafson T, Metz RP, Laffin B, Schedin P, Porter WW. Inhibition of breast cancer growth and invasion by single-minded 2s. Carcinogenesis 2007;28:259–66.

40. Aleman MJ, DeYoung MP, Tress M, Keating P, Perry GW, Narayanan R. Inhibition of single minded 2 gene expression mediates tumor-selective apoptosis and differentiation in human colon cancer cells. Proc Natl Acad Sci U S A 2005;102:12765–70.

41. Purcell AW, McCluskey J, Rossjohn J. More than one reason to rethink the use of peptides in vaccine design. Nat Rev Drug Discov 2007;6:404–14.

42. Kanodia S, Kast WM. Peptide-based vaccines for cancer: realizing their potential. Expert Rev Vaccines 2008;7:1533–45.

43. Kiessling A, Fussel S, Wehner R, et al. Advances in specific immunotherapy for prostate cancer. Eur Urol 2008;53:694–708.

44. Noguchi M, Itoh K, Yao A, et al. Immunological evaluation of individualized peptide vaccination with a low dose of estramustine for HLA-$A24^+$ HRPC patients. Prostate 2005;63:1–12.

45. Murphy G, Tjoa B, Ragde H, Kenny G, Boynton A. Phase I clinical trial: T-cell therapy for prostate cancer using autologous dendritic cells pulsed with HLA-A0201-specific peptides from prostate-specific membrane antigen. Prostate 1996;29:371–80.

46. Tjoa BA, Murphy GP. Progress in active specific immunotherapy of prostate cancer. Semin Surg Oncol 2000;18:80–7.

47. Vonderheide RH, Domchek SM, Schultze JL, et al. Vaccination of cancer patients against telomerase induces functional antitumor $CD8^+$ T lymphocytes. Clin Cancer Res 2004;10:828–39.

48. Fuessel S, Meye A, Schmitz M, et al. Vaccination of hormone-refractory prostate cancer patients with peptide cocktail-loaded dendritic cells: results of a phase I clinical trial. Prostate 2006;66:811–21.

49. Waeckerle-Men Y, Uetz-von Allmen E, Fopp M, et al. Dendritic cell-based multi-epitope immunotherapy of hormone-refractory prostate carcinoma. Cancer Immunol Immunother 2006;55:1524–33.

50. Thomas-Kaskel AK, Zeiser R, Jochim R, et al. Vaccination of advanced prostate cancer patients with PSCA and PSA peptide-loaded dendritic cells induces DTH responses that correlate with superior overall survival. Int J Cancer 2006;119:2428–34.

OPEN ACCESS Freely available online

PLoS one

The Role of the Transcription Factor SIM2 in Prostate Cancer

Bin Lu[1], John M. Asara[2], Martin G. Sanda[1]*, Mohamed S. Arredouani[1]*

1 Department of Surgery, Beth Israel Deaconess Medical Center, Harvard Medical School, Boston, Massachusetts, United States of America, **2** Department of Medicine, Beth Israel Deaconess Medical Center, Harvard Medical School, Boston, Massachusetts, United States of America

Abstract

Background: Recent reports have suggested a possible involvement of Single-minded homolog 2 (SIM2) in human solid cancers, including prostate cancer. However, the exact role of SIM2 in cancer in general, and in prostate cancer in particular, remains largely unknown. This study was designed to elucidate the role of SIM2 in prostate cancer using a shRNA-based approach in the PC3 prostate cancer cell line.

Methods: Lentiviral shRNAs were used to inhibit SIM2 gene and protein levels in PC3 cells. Quantitative RT-PCR and branched DNA were performed to evaluate transcript expression. SIM2 protein expression level was measured by western blot. Profiling of gene expression spanning the whole genome, as well as polar metabolomics of several major metabolic pathways was performed to identify major pathway dysregulations.

Results: SIM2 gene and protein products were significantly downregulated by lenti-shRNA in PC3 cell line. This low expression of SIM2 affected gene expression profile, revealing significant changes in major signaling pathways, networks and functions. In addition, major metabolic pathways were affected.

Conclusion: Taken together, our results suggest an involvement of SIM2 in key traits of prostate tumor cell biology and might underlie a contribution of this transcription factor to prostate cancer onset and progression.

Citation: Lu B, Asara JM, Sanda MG, Arredouani MS (2011) The Role of the Transcription Factor SIM2 in Prostate Cancer. PLoS ONE 6(12): e28837. doi:10.1371/journal.pone.0028837

Editor: Klaus Roemer, University of Saarland Medical School, Germany

Received August 26, 2011; **Accepted** November 16, 2011; **Published** December 9, 2011

Funding: This work is supported by NIH-NCI Early Detection Research Network grant UO1-CA11391 (M. Sanda), Department of Defense Prostate Cancer Training Award W81XWH-09-1-0626 (B. Lu), and Prostate Cancer Foundation Young Investigator Award (M.S. Arredouani). The funders had no role in study design, data collection and analysis, decision to publish, or preparation of the manuscript.

Competing Interests: The authors have declared that no competing interests exist.

* E-mail: marredou@bidmc.harvard.edu (MSA); msanda@bidmc.harvard.edu (MGS)

Introduction

Single-minded homolog 2 (SIM2) gene is located on the human chromosome 21q22.2 and is a member of the basic helix-loop-helix PAS [per-Arnt-Sim] (bHLH-PAS) family of transcription factors [1,2]. SIM2 was originally thought to contribute to Down's syndrome (DS) [3]. As a transcription factor (TF), murine SIM2 (mSIM2) mediates gene expression through CNS midline enhancer (CME) element with its dimerization partner ARNT via ARNT carboxy-terminus [4]. The transcription factor c-myb regulates SIM2 transcription in glioblastoma cells, and a nuclear localization signal (NLS) mediates nuclear localization of SIM2 [5].

A prior *in silico* bioinformatics approach using the Cancer Genome Anatomy Project (CGAP) database of the National Cancer Institute (NCI) identified SIM2 as associated with colon, pancreas and prostate carcinomas, while absent in the corresponding normal tissues [6]. Two different spliced isoforms of SIM2 transcript, SIM2-long (SIM2-l) and SIM2-short (SIM2-s), have been reported while their differential function in humans are not known yet [1]. SIM2-s was specifically expressed in early stages of colon cancer. Antisense inhibition of SIM2-s expression by antisense oligos caused growth inhibition and apoptosis in colon cancer cell line RKO and tumor growth in nude mice and also in pancreatic cancer cell line CAPAN-1 [7,8]. Apoptosis was induced by SIM2-s inhibition in the RKO colon cancer cell line [9]. SIM2-s was also found to have tumor suppressive activity in breast cancer [10]. The invasion potential of glioblastoma was decreased significantly by SIM2s inhibition, consistent with a decrease in the expression of matrix metalloproteinase 2 at both mRNA and protein levels [11].

We have previously reported SIM2 as a potential biomarker and immunotherapy target for human prostate cancer [12]. Although SIM2-s expression (as measured by immunohistochemistry of prostatectomy specimens) has been associated with aggressive histopathology in prostate cancer, and overexpressing ectopic SIM2s enhanced survival in certain conditions in PC3AR+ cells [13,14], the functional role of SIM2 gene in prostate cancer cell is largely unknown.

In this study we sought to elucidate the functional role of SIM2 in PCa using a gene silencing approach and characterization of molecular and functional changes by both gene expression profiling and metabolomic profiling.

Materials and Methods

Cell lines

The human PC3, LNCaP, VCaP and DU145 cell lines were purchased from the American Type Culture Collection (ATCC,

Manassas, VA) and cultured as per ATCC's protocol. Benign PrEC cells, as described in Berger R et al, 2004, were kindly provided by Dr. W. Hahn at Dana-Farber Cancer Institute, Boston, MA.

Transduction Particles

The pLKO.1-puro control lentiviral transduction particles, MISSION luciferase shRNA control lentiviral transduction particles and MISSION SIM2 shRNA lentiviral transduction particles were used to infect PC3 cell line (Sigma-Aldrich, Saint Louis, MO).

Sample selection, RNA purification and reverse transcription

Ten benign and fourteen tumor radical prostatectomy tissue samples were obtained and total RNAs were processed as described in our previous work [12]. Cell line total RNA was isolated using TRIzol reagent (Invitrogen Corporation, Carlsbad, CA) according to the manufacturer's instructions. Purified RNA was quantified by NanoDrop ND-1000 Spectrophotometer (NanoDrop, Wilmington, DE). 500 ng of each cell total RNA was reverse transcribed into cDNA using oligo dT and superscript III reverse transcriptase (Invitrogen Corporation, Carlsbad, CA) under the manufacturer's instructions.

Gene expression microarrays and analysis

250 ng total RNA was amplified using Ambion's MessageAmp II mRNA Amplification kit. Biotin-UTP was incorporated during the overnight in vitro transcription step according to the manufacturer's protocol. Gene expression was assessed using Affymetrix's (Santa Clara, CA) GeneChip U133 array (Plus 2.0 chip) arrays representing the whole human genome transcripts. 15 μg cRNA was fragmented and hybridized to arrays' according to the manufacturer's protocols as described previously [15]. The quality of scanned arrays images were determined on the basis of background values, percent present calls, scaling factors, and 3′-5′ ratio of β-actin and GAPDH using the BioConductor R packages. The signal value for each transcript was summarized using PM-only based signal modeling algorithm described in dchip. The PM only based modeling based algorithm yields less number of false positives as compared to the PM-MM model. In this way, the signal value corresponds to the absolute level of expression of a transcript [16]. These normalized and modeled signal values for each transcript were used for further high level bioinformatics analysis. During the calculation of model based expression signal values, array and probe outliers are interrogated and images spike are treated as signal outliers. The outlier detection was carried out using dchip outlier detection algorithm. A chip is considered as an outlier if the probe, single or array outlier percentage exceeds a default threshold of 5%. When comparing two groups of samples to identify genes enriched in a given phenotype, if 90% lower confidence bound (LCB) of the fold change (FC) between the two groups was above 1.2, the corresponding gene was considered to be differentially expressed. LCB is a stringent estimate of FC and has been shown to be the better ranking statistic [17] It has been suggested that a criterion of selecting genes that have a LCB above 1.2 most likely corresponds to genes with an "actual" fold change of at least 2 in gene expression [18]. Data were extracted from CEL files and normalized using RMAexpress (http://rmaexpress.bmbolstad.com/). Data were analyzed using MeV software (http://www.tm4.org/mev/).

Cell signaling pathway analysis

The Ingenuity Pathways Analysis (Ingenuity Systems®, http://www.ingenuity.com) applications were used to generate networks and assess statistically relevant biofunctions, canonical pathways and networks associated with the differentially expressed gene profiles extracted from the transcriptome data.

Branched DNA and quantitative Real-Time PCR (qRT-PCR)

Branched DNA was performed to evaluate the SIM2s and SIM2L gene expression in the human prostate total RNA samples and normalized by 2 control genes ALSA1 and HPRT (QuantiGene 2.0 Reagent System, Affymetrix Inc, Fremont, CA). For quantitative RT-PCR, 1 μl cDNA was used for each well RT-PCR reactions. Samples were performed in triplicates. Taqman universal PCR Master Mix (Applied Biosystems, Foster City, CA) was used for two-step real-time RT-PCR analysis on Applied Biosystems 7900HT Prism instrument. Taqman real time PCR primers for GAPDH (4310884E) and SIM2L (hs00231925_m1) were purchased from Applied Biosystems (Foster City, CA). Taqman real time PCR primers for SIM2s were designed by our group and purchased from Biosearch Technologies (Novato, CA). SIM2s forward primer: 5′-gtgccaagct acgaaggtg-3′; SIM2s reverse primer: 5′-acttagaagcagaaagagggcaag-3′; probe: TCAGGTCTGCTCGTGGGGAAGGTG. Expression value of SIM2s or SIM2L in a given sample was normalized to the corresponding expression of GAPDH. The $2^{-\Delta\Delta Ct}$ method was used to calculate relative expression of SIM2 gene as described previously [19,20].

Lentiviral transduction and stable cell line selection

1.6 X 10^4 PC3 cells were plated in 96 well plate and incubated for 20 hours. Medium was removed and 110 ul of fresh medium containing hexadimethrine bromide to a final concentration of 8 ug/ml were added. Lentiviral particles were added to appropriate wells at 5 MOI (multiplicity of Infection) and incubated overnight. Fresh medium was then added and cells cultured for 2 days, followed by a 10–12 days culture with puromycin (2 ng/ml) added every 3 days.

Transient transduction was achieved over a 3-day incubation.

Western blot

Cells were washed twice with PBS twice before they were harvested by scraping. Cell lysates were prepared in cell lysis buffer (50 mmol/L Tris-HCl pH 8.0, 20 mM EDTA, 1% SDS, and 100 mM NaCl) containing an enzyme inhibitor mixture tablet (Roche Molecular Biochemicals, Indianapolis, IN) and PMSF (Sigma-Aldrich, Saint Louis, MO). Protein concentration was determined using BCA protein assay kit (Thermo Scientific, Rockford, IL). A total of 20–50 μg of protein extract was fractionated by SDS-PAGE and transferred to a polyvinylidene difluoride membrane (Immobilon-P; Millipore). The membrane was blocked with TBS-T (0.1% Tween 20 in PBS) containing 3% dry milk and incubated with SIM2s primary antibody (Santa Cruz, sc-8715, isoform NM_009586) overnight at 4°C. After three washes with TBS-T, the membrane was incubated with HRP-conjugated secondary Ab for 1 h and then washed with 0.05% Tween 20 in PBS. The immune complexes were detected by ECL methods (Thermo Scientific, Rockford, IL).

Metabolite profiling using Targeted Liquid-Chromatography Tandem Mass Spectrometry (LC/MS/MS)

10^6 cells exponentially growing in basal media with dialyzed serum were harvested in 3 mL 80% v/v HPLC grade methanol at dry ice temperatures. Fresh media was added 24 hours and 2 hours prior to the extraction. Insoluble material in lysates was

Table 1. Clinical information and SIM2 gene expression of 10 normal and 14 tumor prostatectomy evaluated by branched DNA technique.*

Case number	Tumor = 1 normal = 0	Gleason score	PSA level (ng/ml)	Sim2s mRNA expression **	Sim2L mRNA expression **	Sim2s/Sim2L ratio
315	0	N/A	7.6	0.0025	0.0024	1.041667
318	0	N/A	8.4	0.0057	0.008	0.7125
322	0	N/A	6.5	0.0182	0.0197	0.923858
334	0	N/A	5	0.0368	0.0645	0.570543
91	0	N/A	5	0.0215	0.0321	0.669782
20	0	N/A	7.2	0.01	0.0233	0.429185
149	0	N/A	7.1	0.0045	0.0057	0.789474
516	0	N/A	13.5	0.029	0.0379	0.765172
524	0	N/A	11.5	0.0338	0.0805	0.419876
544	0	N/A	7.8	0.0241	0.1094	0.220293
411	1	3+4 = 7	0.4	0.1449	0.2734	0.529993
417	1	3+4 = 7	4.2	0.2041	0.2281	0.894783
471	1	3+4 = 7	26.7	0.0414	0.0375	1.104
474	1	3+3 = 6	5.2	0.1711	0.2817	0.607384
478	1	3+4 = 7	4.4	0.0543	0.0921	0.589577
482	1	3+4 = 7	8.3	0.0513	0.1066	0.481238
523	1	3+4 = 7	8.7	0.2476	0.3987	0.621018
539	1	3+3 = 6	0.7	0.1956	0.5371	0.364178
545	1	3+3 = 6	3	0.1005	0.1996	0.503507
547	1	3+3 = 6	0.4	0.0824	0.134	0.614925
548	1	4+3 = 7	5.8	0.0606	0.1403	0.431932
303	1	N/A	6.4	0.0631	0.1084	0.582103
14	1	N/A	1.6	0.1812	0.2005	0.903741
125	1	4+3 = 7	18	0.0333	0.0494	0.674089

*Prostatectomy samples were from Hershey Tissue Bank at Beth Israel Deaconess Medical Center, Boston.
**mRNA expression values were normalized by ALSA1 and HPRT genes by branched DNA technique.
doi:10.1371/journal.pone.0028837.t001

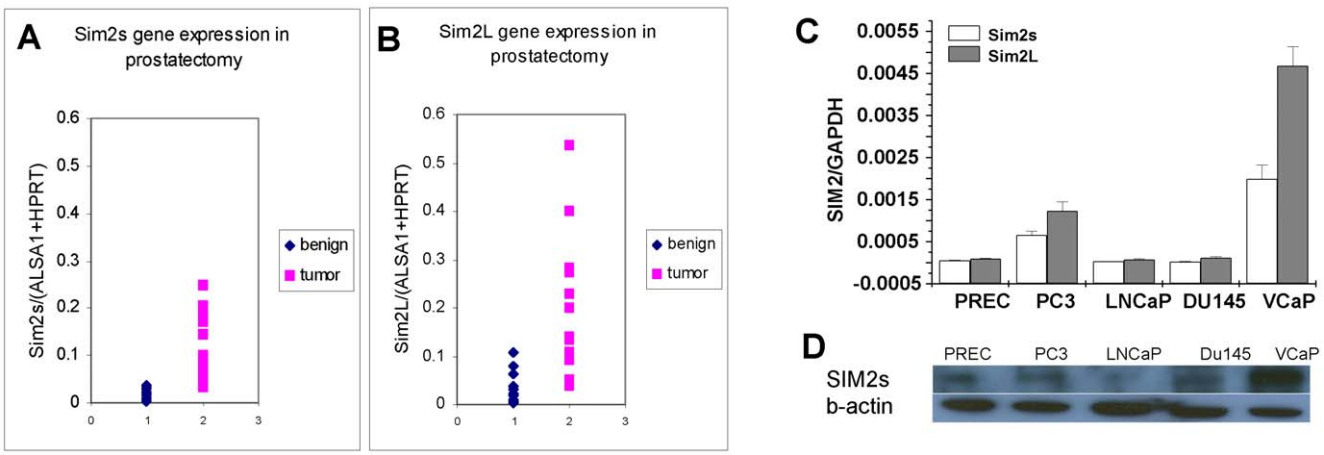

Figure 1. SIM2 expression in human prostatectomy, prostate normal and cancer cell lines. Quantitative Expression of SIM2 short isoform (A) and SIM2 long isoform (B) were evaluated by branched DNA technique in 10 normal and 14 human cancer prostatectomy specimens. Data were quantified using ALSA1 and HPRT as the normalizers. (C) Quantification of SIM2 short and long isoforms' expression in human prostate normal and cancer cell lines by real time RT-PCR. Data were quantified by the $\Delta\Delta C_T$ method and normalized to GAPDH. Column in white represents SIM2 short isoform and column in gray represents SIM2 long isoform. (D) Western blot were performed in prostate normal and cancer cell lines for SIM2s.
doi:10.1371/journal.pone.0028837.g001

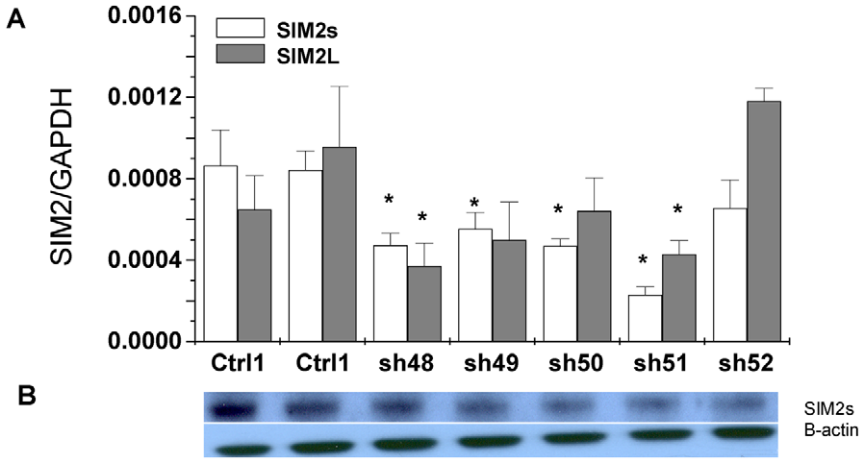

Figure 2. SIM2 expression in PC3 cells is downregulated by shRNA. Real time RT-PCR was performed in triplicates (A) and protein expression was evaluated by western blot (B). Control 1: Luciferase shRNA vector, Control 2: PLKO vector. sh48, sh49, sh50, sh50, sh51 and sh52: vectors expressing shRNAs targeting SIM2 gene at different sites. Column with ''*'' represents significant downregulation of SIM2 gene expression by shRNA comparing to both of control 1 and control 2 ($P < 0.05$).
doi:10.1371/journal.pone.0028837.g002

centrifuged at 4000 RPM for 15 minutes and the resulting supernatant (metabolite content) was evaporated using a refrigerated SpeedVac to a pellet. Samples were re-suspended using 20μL HPLC grade water for mass spectrometry analysis. 10μL were injected and analyzed using a 5500 QTRAP triple quadrupole mass spectrometer (AB/Sciex) coupled to a Prominence UFLC HPLC system (Shimadzu) via selected reaction monitoring (SRM) of a total of 255 endogenous water soluble metabolites for steady-

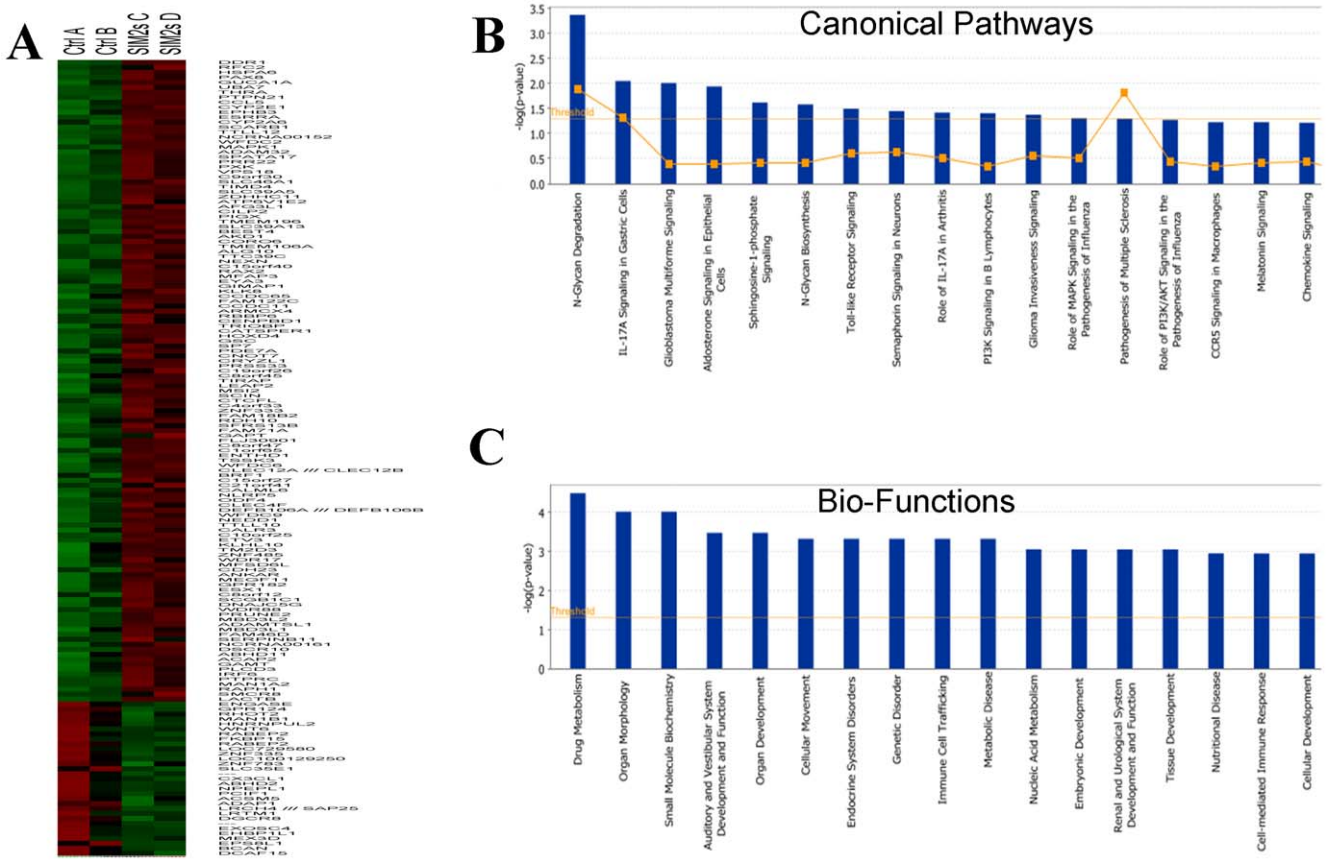

Figure 3. Heat map and cell signaling analysis for the dysregulated genes in SIM2^{low} comparing to control PC3 cells. A. Control A: PC3 luciferase shRNA; Control B: PC3 PLKO vector; SIM2 C: SIM2 sh48; SIM2 D: SIM2 sh51. Gene expressions were either up or down greater than 2 fold in the SIM2^{low} were listed. B. Top dysregulated signaling pathways in SIM2^{low} PC3 cells. C. Top dysregulated cell functions in SIM2^{low} PC3 cells.
doi:10.1371/journal.pone.0028837.g003

state analyses of samples. Some metabolites were targeted in both positive and negative ion mode for a total of 298 SRM transitions. ESI voltage was +4900V in positive ion mode and –4500V in negative ion mode. The dwell time was 5 ms per SRM transition and the total cycle time was 2.09 seconds. Approximately 8–10 data points were acquired per detected metabolite. Samples were delivered to the MS via normal phase chromatography using a 2.0 mm i.d x 15 cm Luna NH2 HILIC column (Phenomenex) at 285 µL/min. Gradients were run starting from 85% buffer B (HPLC grade acetonitrile) to 42% B from 0–5 minutes; 42% B to 0% B from 5–16 minutes; 0% B was held from 16–24 minutes; 0% B to 85% B from 24–25 minutes; 85% B was held for 7 minutes to re-equilibrate the column. Buffer A was comprised of 20 mM ammonium hydroxide/20 mM ammonium acetate (pH = 9.0) in 95:5 water:acetonitrile. Peak areas from the total ion current for each metabolite SRM transition were integrated using Multi-Quant v1.1 software (AB/Sciex).

Measurements were performed in triplicates and data were normalized per cell number. Only metabolites that were determined in all 6 samples were kept and analyzed using MetaboAnalyst [21,22].

Statistical analysis

Gene expression array data were analyzed as described under Materials and Methods. Based upon our earlier work [12], we tested for SIM2 upregulation in tumors versus controls with a one-sided t-test and compared against a p-value threshold of 0.05.

Quantitative Real-Time PCR (qRT-PCR). Validation of differentially expressed genes was performed by qRT-PCR. 200 ng of high quality RNA samples were reverse transcribed to first strand cDNA and 1 µl cDNA was used for each well RT-PCR reaction. Samples were performed in triplicates. SYBR Green PCR Master Mix (Applied Biosystems, Foster City, CA) was used for two-step real-time RT-PCR analysis on Applied Biosystems 7900HT Prism instrument. PCR primers' sequences for targeted genes are shown in Table S3. The sequences for GAPDH: GAPDH-F (5′-TGCACCACCAACTGCTTAGC -3′) and GAPDH-R (5′-GGCATGGACTGTGGTCATGAG -3′). Expression value of the targeted gene in a given sample was normalized to the corresponding expression of GAPDH. The $2^{-\Delta\Delta Ct}$ method was used to calculate relative expression of the targeted genes.

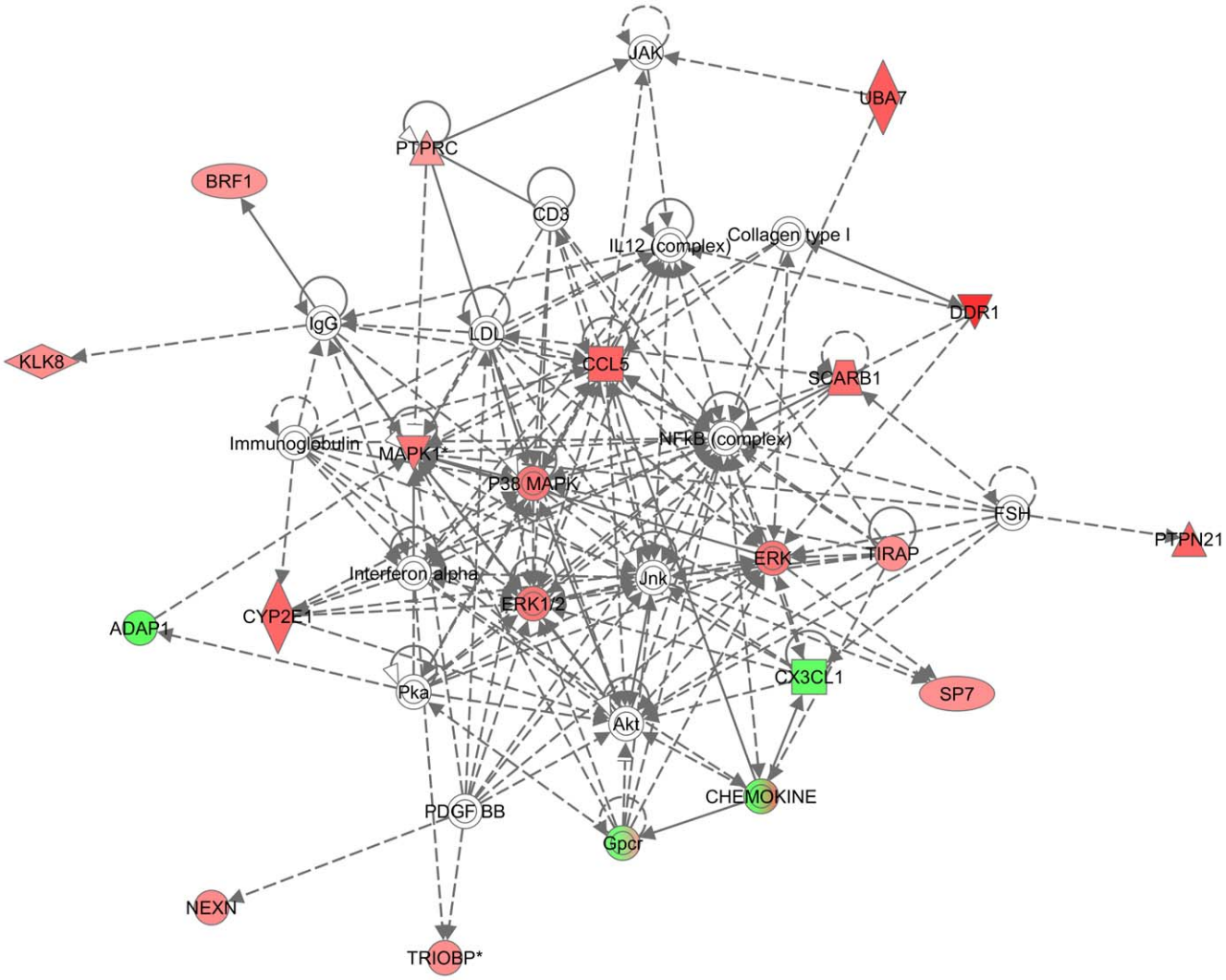

Figure 4. Top one network dysregulated in SIM2^{low}. This network contained 16 focus genes with a score of 29. Different shapes of the node represent different groups of the focus genes. The intensity of the node color indicated the degree of the up (red) and down (green) gene expression level. The top functions of this network are cellular movement, immune cell trafficking, organismal injury and abnormalities.
doi:10.1371/journal.pone.0028837.g004

Results

SIM2 gene is differentially expressed in prostate normal and cancer prostatectomy and cell lines

We have evaluated SIM2 gene expression in a total of 24 normal and tumor prostatectomy samples shown in table 1. Because SIM2 gene exists in two isoforms, SIM2 short (SIM2s) and SIM2 long (SIM2L), we confirmed the expression of both isoforms in RNA extracted from prostatectomy using branched DNA technique (Fig. 1A & 1B). SIM2s and SIM2L showed significant overexpression in tumor samples when compared to benign samples, with $p < 0.000003$ and $p < 0.00005$, respectively. However, the ratio of SIM2s to SIM2L expression was no difference between benign and tumor (table 1, T-test with $p = 0.85$). The SIM2s and SIM2L expression were 7.03 and 6.95 times higher respectively in the tumors comparing the means of the two groups after a log adjustment to assure normality and constant variance within each group. Expression of SIM2s and SIM2L was also evaluated in four human prostate cancer cell lines, PC3, LNCaP, DU145 and VCaP, and in the normal prostate epithelial cell line PrEC. Both SIM2s and SIM2L isoforms were highly expressed in VCaP cells, while there was a moderate expression level in PC3 cells and very low expression in DU145, LNCaP, and PrEC cells (Fig. 1C). Because there are only a few available antibodies to SIM2, we have only been able to clearly identify the short isoform of SIM2 (SIM2s) in cellular protein extracts by western blot. This scarcity of antibodies complicated our task of studying the function of SIM2 long isoform. The SIM2s protein expression level was consistent with its gene expression in prostate normal and cancer cell lines. (Fig. 1D).

Silencing SIM2 expression in PC3 cells

To achieve the highest downregulation of SIM2 expression using lentiviral shRNA, we have selected the PC3 cell line as a model. PC3 cells were transduced with five different SIM2 shRNA expression vectors, four of which (shRNA48, shRNA49, shRNA50 and shRNA51) showed significant inhibitory effect compared to control shRNAs. Over 80% silencing of gene expression was achieved using shRNA51 (Fig. 2A&B). Two control cell lines were generated using either a vector stably expressing shRNA targeting luciferase or an empty vector. A similar inhibitory pattern was observed for SIM2L gene expression in these stably infected PC3 cell lines. Similarly, efficient transient silencing of SIM2S and SIM2L was achieved in PC3 (Figure S1).

Impact of SIM2 silencing on gene expression profile in PC3 cells

Despite its suspected role in cancer, very little is known about the contribution of the transcription factor SIM2 to the regulation

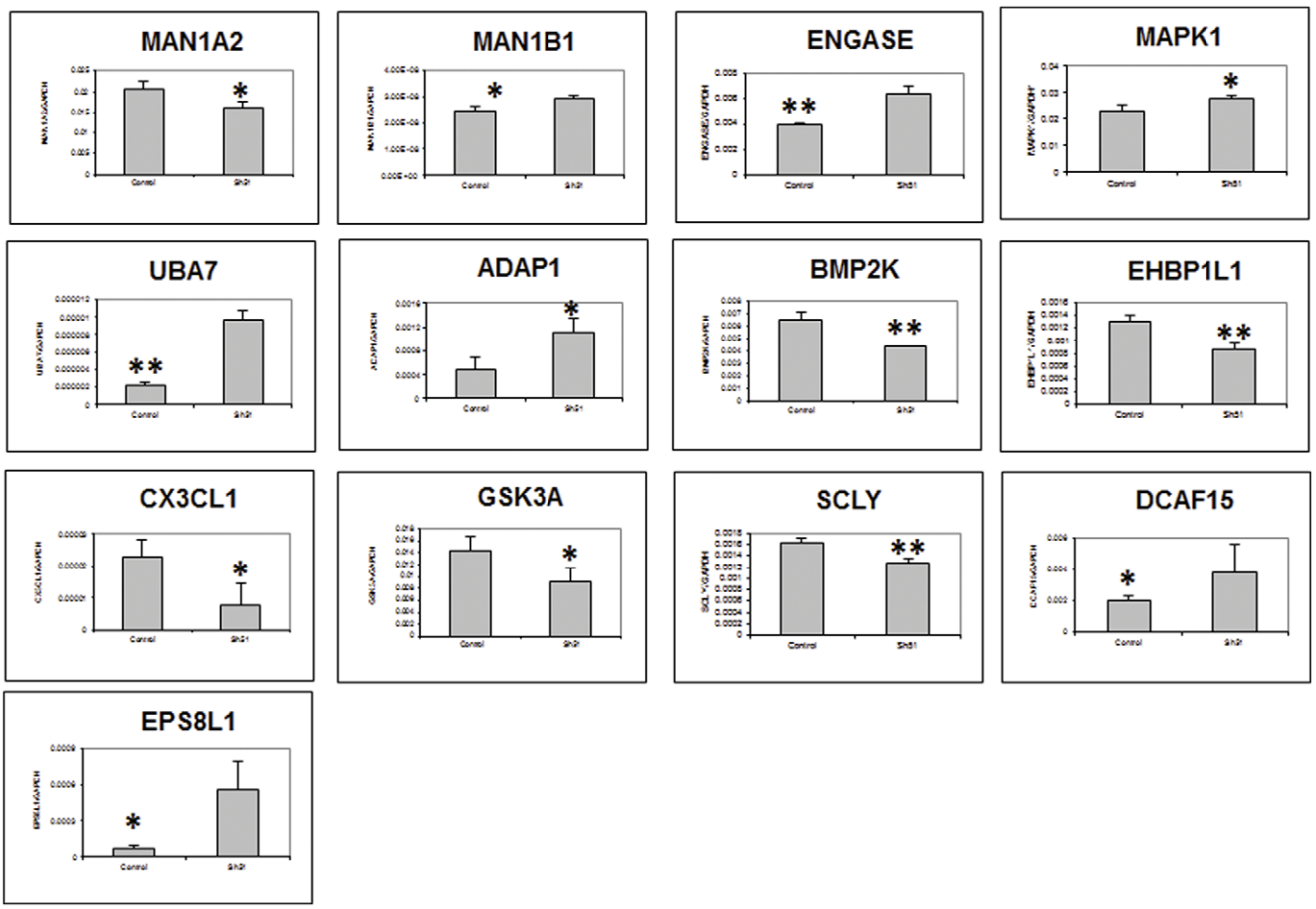

Figure 5. Validation of selected genes from stable transfectant by qRT-PCR. qRT-PCR validation of mRNA expression levels of individual genes was performed by two-step real-time RT-PCR analysis on Applied Biosystems 7900HT Prism instrument. *, P<.05; **, P<.01; ***, P<.001. Measurements were performed in triplicates and data presented as Mean ± SD.
doi:10.1371/journal.pone.0028837.g005

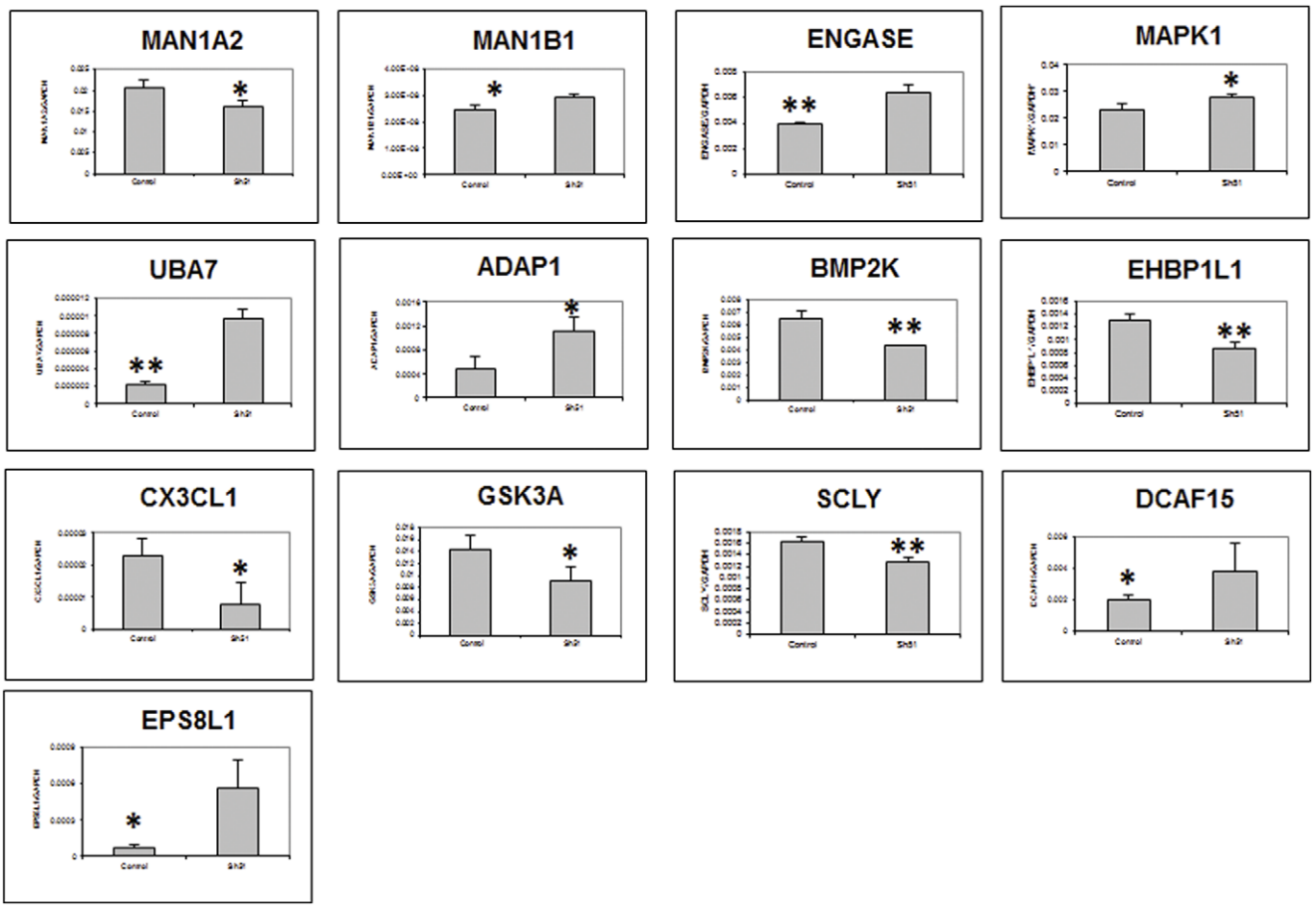

Figure 6. Validation of selected genes from transient transfectant by qRT-PCR. qRT-PCR validation of mRNA expression levels of individual genes was performed by two-step real-time RT-PCR analysis on Applied Biosystems 7900HT Prism instrument. *, P<.05; **, P<.01; ***, P<.001. Measurements were performed in triplicates and data presented as Mean ± SD.
doi:10.1371/journal.pone.0028837.g006

of gene expression [23]. We therefore examined the effects of downregulation of SIM2 in prostate cancer cells. To this end, the shRNA which yielded the highest silencing rate of SIM2, i.e. shRNA51, was selected. PC3 cells treated with shRNA51 were compared to a control shRNA (shRNAc).

Gene expression profiles of PC3 SIM2^{low} and control PC3 cell lines were evaluated using Affymetrix GeneChip U133 array (Plus 2.0 chip) consisting of >52,000 transcripts from whole human genome transcripts. Figure 1 is a heat map showing the gene dysregulation after knocking down the expression of SIM2 in PC3 cells. The expression of a large number of transcripts exhibited a change of at least 2-fold (Figure 3A and Table S4). Pathway analysis revealed that many highly differentially expressed transcripts represent genes that belong to known signaling pathways, such as the PTEN and PI3K/AKT signaling pathways (Figure 3B), whose involvement in tumorigenesis is well documented [24,25]. Specific genes involved in each signaling pathway are shown in Table S1. Among those genes, CCL5, MAPK1, P38, DDR1 and ERK played a central role in the pathway network (Figure 4). The genes in this network have been involved in cell death, metabolism, cellular development, and tumor antigen presentation. More genes involved in the highest score networks are shown in Table S2. Further analysis showed that a number of important biological functions are dysregulated following SIM2 silencing (Figure 3C). Interestingly, several cell functions related to metabolism, such as drug metabolism and metabolic disease, are among the top ranked functions.

Validation by RT-PCR of a group of differentially expressed genes (Table S3) partially confirmed our in silico analysis of stable and transient transfectant PC3 cells (Figures 5 & 6).

Table 2. Top dysregulated metabolic pathways in Sim2^{low} PC3 cells.

Pathway Name	Total number of Metabolites	Hits
Purine Metabolism	92	11
Pyrimidine metabolism	60	6
Glycolysis or Gluconeogenesis	31	3
Thiamine metabolism	24	2
Pyruvate metabolism	32	2

Metabolites were measured using mass spectrometry and data were analyzed using MetaboAnalyst software.
doi:10.1371/journal.pone.0028837.t002

PC3 SIM2^{low} cells showed major alterations in their metabolic profile

We sought to determine whether gene expression changes result in significant shifts in metabolic pathways in PC3 SIM2^{low} cells. This was addressed by measuring 255 polar metabolites using targeted mass spectrometry (LC/MS/MS). Comparison of the metabolic profile of control cells to shRNA-SIM2-treated cells showed significant changes in several metabolic pathways and the production of 39 metabolites (Tables 2&3). The purine metabolism pathway was the top one dysregulated pathway with 11 metabolites significantly up- or down-regulated levels out of total 92 metabolites in this pathway in SIM2 silencing PC3 cells. Pyrimidine metabolism pathway listed as the second dysregulated pathway with 6 out of total of 60 metabolites with significant changed levels (Table 2, Fig. 7). The significant alterations to the nucleic acid metabolism may indicate its important role in the prostate cancer development.

Discussion

In our previous biomarker identification efforts, we have identified SIM2 as a potential biomarker for PCa. Thanks to its overexpression in prostate tumors and its highly restricted expression in humans, we proposed to use SIM2 as an immunotherapy target and were able to identify 5 HLA-A2.1, SIM2-derived immunogenic epitopes [12]. In the present study we attempted to characterize the role of SIM2 in prostate cancer using a short hairpin RNA-induced gene silencing approach in PC3 cells as a model. We focused on profiling both the transcriptome and metabolome in SIM2^{low} and normal PC3 cells, and evaluated the impact of SIM2 silencing on cell signaling and function.

The SIM2s isoform has been reported to be expressed in colon, pancreas, and prostate tumors while absent in the corresponding benign tissues [8]. We found that SIM2 genes are detectable in all these prostate cancer cells by real time PCR. However the expression levels in DU145 and LNCaP are relatively lower than other prostate cancer cells while PC3 cells express moderate level of SIM2 genes which are consistent with other report [14].

The whole spectrum of regulation of gene expression by the transcription factor SIM2 is still poorly defined. The level of regulation could be reflected by the differential expression of about 200 genes as revealed through gene expression profiling of PC3 SIM2^{low} cells. Other groups have reported specific genes that are regulated by SIM2. The bHLH/PAS transcription factor single minded 2s was reported to promote mammary gland lactogenic differentiation by regulation of Csn2 expression [26]. SIM2 regulates the expression of MMP-2 and TIMP-2, which drive its role in glioblastoma cells [11]. SIM2s represses BNIP3, a pro-apoptotic gene, through its hypoxic response element in PC3 cells [14]. Our gene expression profile in PC3 SIM2^{low} cells showed significant change in PTEN, PI3K/AKT and Toll-like receptor (TLR) signaling pathways which are involved largely in the tumor progression. PTEN negatively controls the PI3K signaling pathway for cell growth and survival by dephosphorylating the 3 position of phosphoinositides [24,25]. TLR regulates cell proliferation and survival and central signaling molecules mitogen-activated protein kinase (MAPK) and PI3K play key roles [27]. Our data show that inhibition of Sim2 gene in PC3 cells affects expression of several genes encoding proteins that are organized in a network around p38MAPK. These proteins, which include CCL5, MAPKs, ERK and DDR1 (Figure 4), have been reported to be involved in tumor development. The chemokine CCL5 has been reported to be expressed by prostate cells and affect their growth and survival. Following activation of MAPKs p38 and ERK1/2 in LNCaP cells, the expression of CCL5 increases, resulting in enhanced cell proliferation [28,29]. PC3 cell proliferation and invasion were also significantly suppressed after DDR1 knockdown by siRNA [30,31].

Our RT-PCR data revealed discrepancies between transient and stable silencing of SIM2 in PC3 cells. This may be a result of 1) the presence of two isoforms of SIM2 that are silenced to

Table 3. List of dysregulated metabolites in Sim2^{low} PC3 cells.

Metabolite	P value*
UTP	0.00021736
CTP	0.000266674
Thiamine-phosphate	0.00027101
CDP	0.00027427
ATP	0.00032043
GDP	0.00047402
2-ketohaxanoic acid	0.00099085
dGTP	0.0011366
Adenosine	0.0025014
allantoate	0.0031712
4-Pyridoxic acid	0.0032341
Hydroxyphenylacetic acid	0.004154
IMP	0.0046357
Inosine	0.0052766
xanthosine	0.0056235
N-carbamoyl-L-aspartate	0.0057818
CDP-choline	0.0067616
lactate	0.007935
GTP	0.0084853
dCTP	0.011521
dATP	0.011737
Geranyl-PP	0.014616
Thiamine pyrophosphate	0.017058
dihydroxy-acetone-phosphate	0.017355
AMP	0.018114
Sn-glycerol-3-phosphate	0.019883
3-phosphoglycerate	0.021186
UDP	0.023169
dAMP	0.023309
Guanine	0.025068
Glucose-6-phosphate	0.027664
Fructose-6-phosphate	0.035608
Hexose-phosphate	0.036721
dTMP	0.044375
Guanosine 5-diphosphate, 3-diphosphate	0.046342
2-Isopropylmalic acid	0.047328
GMP	0.04827
hydroxyproline	0.049448

Metabolites were quantitated using mass spectrometry and data were analyzed using MetaboAnalyst software.
*$P<0.05$.
doi:10.1371/journal.pone.0028837.t003

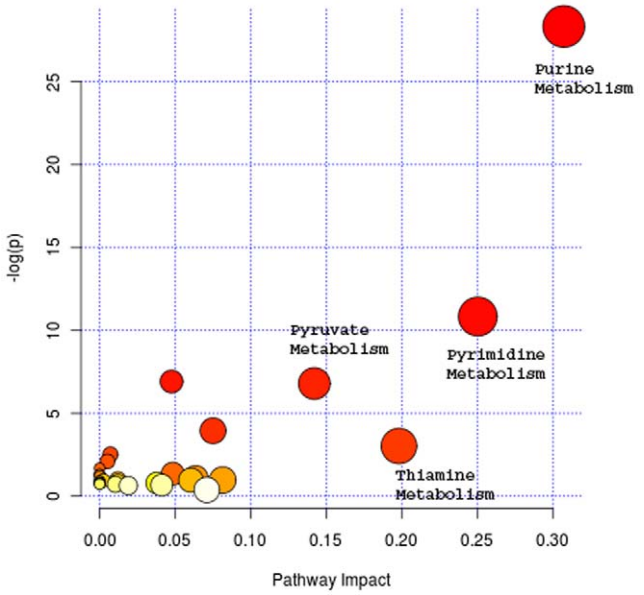

Figure 7. PC3 SIM2-shRNA cells showed major alterations in purine and pyrimidine metabolism pathways. Metabolites were extracted from SIM2^{low} and normal PC3 cells using methanol and the abundance of 239 metabolites were measured using targeted LC/MS/MS. Data were analyzed using MetaboAnalyst software. The metabolic pathways arranged according to the scores from enrichment analysis (y axis) and from topology analysis (x axis). Triplicate measurements were performed.
doi:10.1371/journal.pone.0028837.g007

different extents in both setups, or 2) SIM2 may regulate gene expression of other genes either directly or indirectly.

Function analysis also revealed that three functions related to cell metabolism had been dysregulated in the PC3 SIM2^{low} cells. This suggested that SIM2 might have metabolic consequences. We have evaluated the production by PC3 cells of 255 metabolites that encompass a large number of human metabolic pathways. Of these, data were obtained for 239 metabolites. Our analysis revealed significant changes in metabolites that constitute key pathways, such as the purine and pyrimidine pathways.

Suppression of SIM2 short isoform (SIM2s) by antisense oligonucleotides reduced tumor growth in colon cancer cells and induced CAPAN-1 pancreatic cell death through apoptosis [7,8,9]. SIM2s was also reported to be an aggressive prostate cancer biomarker since SIM2s protein was associated with increased preoperative serum prostate specific antigen (PSA), high histological grade, invasive tumor growth and increased tumor cell proliferation [13]. A recent study showed that SIIM2s may attenuate cell death processes through BNIP3 repression in PC3AR+ cells. However, knockdown of SIM2s in breast cancer MCF-7 cells increased tumorigenesis and thus showed tumor suppressor activity [32,33]. Most of the previous studies focused on the SIM2s by either intruding or knockdown of SIM2s, we are lacking of the data clarifying the functional role of SIM2 protein including both of its isoforms. Our study reported a combined role of both isoforms of the SIM2 implicated in the prostate cancer cell. Distinguishing the roles of SIM2s and SIM2L may have more profound meaning to understand the functional role of SIM2 in prostate cancer progression, which is our next step to uncover more significance of this gene.

Supporting Information

Figure S1 Transient silencing of SIM2s and SIM2L expression in PC3 cells. PC3 cells were transduced with either a control (Ctrl) or shRNA51 (sh51) and cultured in the presence of puromycin for 3 days. Real time RT-PCR was performed in triplicates to evaluate gene expression of SIM2 s (Upper Panel) and SIM2L (Lower Panel).
(TIF)

Table S1 The top Dysregulated Signaling Pathways in SIM2^{low} cells. Top dysregulated canonical pathways were identified through analysis of differentially expressed gene data, using Ingenuity Pathway Analysis package.
(DOC)

Table S2 The Molecules in the Highest Score Networks in SIM2^{low} cells. Data representing differentially expressed genes were submitted to Ingenuity Pathway Analysis package and high score networks were identified.
(DOC)

Table S3 List of primers used for RT-PCR quantitation of expression of of selected genes. The primers were designed using Pimer3 program: http://frodo.wi.mit.edu/primer3/.
(DOC)

Table S4 Gene expressions that were either up- or down-regulated greater than 2 fold in the SIM2^{low}.
(XLSX)

Author Contributions

Conceived and designed the experiments: BL JMA MGS MSA. Performed the experiments: BL JMA MSA. Analyzed the data: BL JMA MGS MSA. Contributed reagents/materials/analysis tools: MSA JMA. Wrote the paper: BL MGS MSA.

References

1. Chrast R, Scott HS, Chen H, Kudoh J, Rossier C, et al. (1997) Cloning of two human homologs of the Drosophila single-minded gene SIM1 on chromosome 6q and SIM2 on 21q within the Down syndrome chromosomal region. Genome Res 7: 615–624.
2. Moffett P, Reece M, Pelletier J (1997) The murine Sim-2 gene product inhibits transcription by active repression and functional interference. Mol Cell Biol 17: 4933–4947.
3. Ema M, Ikegami S, Hosoya T, Mimura J, Ohtani H, et al. (1999) Mild impairment of learning and memory in mice overexpressing the mSim2 gene located on chromosome 16: an animal model of Down's syndrome. Hum Mol Genet 8: 1409–1415.
4. Moffett P, Pelletier J (2000) Different transcriptional properties of mSim-1 and mSim-2. FEBS Lett 466: 80–86.
5. Yamaki A, Tochigi J, Kudoh J, Minoshima S, Shimizu N, et al. (2001) Molecular mechanisms of human single-minded 2 (SIM2) gene expression: identification of a promoter site in the SIM2 genomic sequence. Gene 270: 265–275.
6. Deyoung MP, Scheurle D, Damania H, Zylberberg C, Narayanan R (2002) Down's syndrome-associated single minded gene as a novel tumor marker. Anticancer Res 22: 3149–3157.
7. DeYoung MP, Tress M, Narayanan R (2003) Identification of Down's syndrome critical locus gene SIM2-s as a drug therapy target for solid tumors. Proc Natl Acad Sci U S A 100: 4760–4765.
8. DeYoung MP, Tress M, Narayanan R (2003) Down's syndrome-associated Single Minded 2 gene as a pancreatic cancer drug therapy target. Cancer Lett 200: 25–31.
9. Aleman MJ, DeYoung MP, Tress M, Keating P, Perry GW, et al. (2005) Inhibition of Single Minded 2 gene expression mediates tumor-selective apoptosis and differentiation in human colon cancer cells. Proc Natl Acad Sci U S A 102: 12765–12770.
10. Kwak HI, Gustafson T, Metz RP, Laffin B, Schedin P, et al. (2007) Inhibition of breast cancer growth and invasion by single-minded 2s. Carcinogenesis 28: 259–266.

11. He Q, Li G, Su Y, Shen J, Liu Q () Single minded 2-s (SIM2-s) gene is expressed in human GBM cells and involved in GBM invasion. Cancer Biol Ther 9: 430–436.
12. Arredouani MS, Lu B, Bhasin M, Eljanne M, Yue W, et al. (2009) Identification of the transcription factor single-minded homologue 2 as a potential biomarker and immunotherapy target in prostate cancer. Clin Cancer Res 15: 5794–5802.
13. Halvorsen OJ, Rostad K, Oyan AM, Puntervoll H, Bo TH, et al. (2007) Increased expression of SIM2-s protein is a novel marker of aggressive prostate cancer. Clin Cancer Res 13: 892–897.
14. Farrall AL, Whitelaw ML (2009) The HIF1alpha-inducible pro-cell death gene BNIP3 is a novel target of SIM2s repression through cross-talk on the hypoxia response element. Oncogene 28: 3671–3680.
15. Jones J, Otu H, Spentzos D, Kolia S, Inan M, et al. (2005) Gene signatures of progression and metastasis in renal cell cancer. Clin Cancer Res 11: 5730–5739.
16. Li C, Wong WH (2001) Model-based analysis of oligonucleotide arrays: expression index computation and outlier detection. Proc Natl Acad Sci U S A 98: 31–36.
17. Yuen T, Wurmbach E, Pfeffer RL, Ebersole BJ, Sealfon SC (2002) Accuracy and calibration of commercial oligonucleotide and custom cDNA microarrays. Nucleic Acids Res 30: e48.
18. Ramalho-Santos M, Yoon S, Matsuzaki Y, Mulligan RC, Melton DA (2002) "Stemness": transcriptional profiling of embryonic and adult stem cells. Science 298: 597–600.
19. Haram KM, Peltier HJ, Lu B, Bhasin M, Otu HH, et al. (2008) Gene expression profile of mouse prostate tumors reveals dysregulations in major biological processes and identifies potential murine targets for preclinical development of human prostate cancer therapy. Prostate 68: 1517–1530.
20. Livak KJ, Schmittgen TD (2001) Analysis of relative gene expression data using real-time quantitative PCR and the 2(-Delta Delta C(T)) Method. Methods 25: 402–408.
21. Xia J, Psychogios N, Young N, Wishart DS (2009) MetaboAnalyst: a web server for metabolomic data analysis and interpretation. Nucleic Acids Res 37: W652–660.
22. Xia J, Wishart DS Web-based inference of biological patterns, functions and pathways from metabolomic data using MetaboAnalyst. Nat Protoc 6: 743–760.
23. Metz RP, Kwak HI, Gustafson T, Laffin B, Porter WW (2006) Differential transcriptional regulation by mouse single-minded 2s. J Biol Chem 281: 10839–10848.
24. Cantley LC, Neel BG (1999) New insights into tumor suppression: PTEN suppresses tumor formation by restraining the phosphoinositide 3-kinase/AKT pathway. Proc Natl Acad Sci U S A 96: 4240–4245.
25. Yuan TL, Cantley LC (2008) PI3K pathway alterations in cancer: variations on a theme. Oncogene 27: 5497–5510.
26. Wellberg E, Metz RP, Parker C, Porter WW The bHLH/PAS transcription factor singleminded 2s promotes mammary gland lactogenic differentiation. Development 137: 945–952.
27. Li X, Jiang S, Tapping RI Toll-like receptor signaling in cell proliferation and survival. Cytokine 49: 1–9.
28. Colombatti M, Grasso S, Porzia A, Fracasso G, Scupoli MT, et al. (2009) The prostate specific membrane antigen regulates the expression of IL-6 and CCL5 in prostate tumour cells by activating the MAPK pathways. PLoS One 4: e4608.
29. Vaday GG, Peehl DM, Kadam PA, Lawrence DM (2006) Expression of CCL5 (RANTES) and CCR5 in prostate cancer. Prostate 66: 124–134.
30. Shimada K, Nakamura M, Ishida E, Higuchi T, Yamamoto H, et al. (2008) Prostate cancer antigen-1 contributes to cell survival and invasion though discoidin receptor 1 in human prostate cancer. Cancer Sci 99: 39–45.
31. Yamanaka R, Arao T, Yajima N, Tsuchiya N, Homma J, et al. (2006) Identification of expressed genes characterizing long-term survival in malignant glioma patients. Oncogene 25: 5994–6002.
32. Gustafson TL, Wellberg E, Laffin B, Schilling L, Metz RP, et al. (2009) Ha-Ras transformation of MCF10A cells leads to repression of Singleminded-2s through NOTCH and C/EBPbeta. Oncogene 28: 1561–1568.
33. Laffin B, Wellberg E, Kwak HI, Burghardt RC, Metz RP, et al. (2008) Loss of singleminded-2s in the mouse mammary gland induces an epithelial-mesenchymal transition associated with up-regulation of slug and matrix metalloprotease 2. Mol Cell Biol 28: 1936–1946.